Journal of Physics: Energy

ROADMAP

2021 roadmap for sodium-ion batteries

Nuria Tapia-Ruiz[1,2,*] ⓘ, A Robert Armstrong[2,3,*] ⓘ, Hande Alptekin[4] ⓘ, Marco A Amores[2,5], Heather Au[4] ⓘ, Jerry Barker[6] ⓘ, Rebecca Boston[2,7], William R Brant[8] ⓘ, Jake M Brittain[9,10], Yue Chen[2,11], Manish Chhowalla[2,12], Yong-Seok Choi[2,13,14] ⓘ, Sara I R Costa[1,2], Maria Crespo Ribadeneyra[4] ⓘ, Serena A Cussen[2,5,7] ⓘ, Edmund J Cussen[2,5,7], William I F David[9,10] ⓘ, Aamod V Desai[2,3] ⓘ, Stewart A M Dickson[2,15], Emmanuel I Eweka[16], Juan D Forero-Saboya[17] ⓘ, Clare P Grey[2,18], John M Griffin[1,2] ⓘ, Peter Gross[2,7], Xiao Hua[2,5], John T S Irvine[2,15], Patrik Johansson[19,20] ⓘ, Martin O Jones[2,21], Martin Karlsmo[19] ⓘ, Emma Kendrick[22] ⓘ, Eunjeong Kim[2,3], Oleg V Kolosov[2,11] ⓘ, Zhuangnan Li[2,12], Stijn F L Mertens[1,2] ⓘ, Ronnie Mogensen[8], Laure Monconduit[23,24] ⓘ, Russell E Morris[2,3,25], Andrew J Naylor[8] ⓘ, Shahin Nikman[1,2], Christopher A O'Keefe[2,18], Darren M C Ould[2,18], R G Palgrave[2,13], Philippe Poizot[26] ⓘ, Alexandre Ponrouch[17], Stéven Renault[26] ⓘ, Emily M Reynolds[2,21], Ashish Rudola[6], Ruth Sayers[6] ⓘ, David O Scanlon[2,13,14,27], S Sen[2,13], Valerie R Seymour[1,2] ⓘ, Begoña Silván[1,2] ⓘ, Moulay Tahar Sougrati[23,24] ⓘ, Lorenzo Stievano[23,24] ⓘ, Grant S Stone[28], Chris I Thomas[2,7] ⓘ, Maria-Magdalena Titirici[4] ⓘ, Jincheng Tong[2,12] ⓘ, Thomas J Wood[9] ⓘ, Dominic S Wright[2,18] and Reza Younesi[8] ⓘ

1 Department of Chemistry, Lancaster University, Lancaster LA1 4YB, United Kingdom
2 The Faraday Institution, Quad One, Harwell Science and Innovation Campus, OX11 0RA, United Kingdom
3 EastChem School of Chemistry, University of St. Andrews, St. Andrews KY16 9ST, United Kingdom
4 Department of Chemical Engineering, Imperial College London, London SW7 2AZ, United Kingdom
5 Department of Chemical and Biological Engineering, University of Sheffield, Sheffield S1 3JD, United Kingdom
6 Faradion Limited, The Innovation Centre, 217 Portobello, Sheffield S1 4DP, United Kingdom
7 Department of Materials Science and Engineering, University of Sheffield, Sheffield S1 3JD, United Kingdom
8 Department of Chemistry—Ångström Laboratory, Uppsala University, Box 538, SE-75121 Uppsala, Sweden
9 ISIS Neutron and Muon Spallation Source, STFC Rutherford Appleton Laboratory, Harwell, Oxford OX11 0QX, United Kingdom
10 Inorganic Chemistry Laboratory, University of Oxford, Oxford OX1 3QR, United Kingdom
11 Department of Physics, Lancaster University, Bailrigg, Lancaster LA1 4YB, United Kingdom
12 Department of Materials Science and Metallurgy, University of Cambridge, Cambridge CB3 0FS, United Kingdom
13 Department of Chemistry, University College London, 20 Gordon Street, London WC1H 0AJ, United Kingdom
14 Thomas Young Centre, University College London, Gower Street, London WC1E 6BT, United Kingdom
15 School of Chemistry, University of St. Andrews, St. Andrews KY16 9ST, United Kingdom
16 Amte Power Ltd, 153A Eastern Avenue, Milton Park, Oxford OX14 4SB, United Kingdom
17 Institut de Ciéncia de Materials de Barcelona (ICMAB-CSIC), Campus UAB, 08193 Bellaterra, Catalonia, Spain
18 Department of Chemistry, University of Cambridge, Lensfield Road, Cambridge CB2 1EW, United Kingdom
19 Department of Physics, Chalmers University of Technology, 412 96 Göteborg, Sweden
20 Alistore-ERI, CNRS FR 3104, 15 Rue Baudelocque, Amiens 80039, France
21 Science and Technology Facilities Council, North Star Avenue, Swindon SN2 1SZ, United Kingdom
22 School of Metallurgy and Materials, University of Birmingham, Edgbaston, Birmingham BT15 2TT, United Kingdom
23 ICGM, University Montpellier, CNRS, Montpellier, France
24 RS2E, CNRS, Amiens, France
25 Department of Physical and Macromolecular Chemistry, Charles University, Hlavova 8, Prague 128 43, Czech Republic
26 Université de Nantes, CNRS, Institut des Matériaux Jean Rouxel, IMN, F-44000 Nantes, France
27 Diamond Light Source Ltd, Diamond House, Harwell Science and Innovation Campus, Didcot, Oxfordshire OX11 0DE, United Kingdom
28 Amte Power Ltd, Denchi House, Thurso Business Park, Thurso, Caithness KW14 7XW, United Kingdom
* Authors to whom any correspondence should be addressed.

E-mail: n.tapiaruiz@lancaster.ac.uk and ara@st-andrews.ac.uk

Abstract

Increasing concerns regarding the sustainability of lithium sources, due to their limited availability and consequent expected price increase, have raised awareness of the importance of developing alternative energy-storage candidates that can sustain the ever-growing energy demand. Furthermore, limitations on the availability of the transition metals used in the manufacturing of cathode materials, together with questionable mining practices, are driving development towards more sustainable elements. Given the uniformly high abundance and cost-effectiveness of sodium,

as well as its very suitable redox potential (close to that of lithium), sodium-ion battery technology offers tremendous potential to be a counterpart to lithium-ion batteries (LIBs) in different application scenarios, such as stationary energy storage and low-cost vehicles. This potential is reflected by the major investments that are being made by industry in a wide variety of markets and in diverse material combinations. Despite the associated advantages of being a drop-in replacement for LIBs, there are remarkable differences in the physicochemical properties between sodium and lithium that give rise to different behaviours, for example, different coordination preferences in compounds, desolvation energies, or solubility of the solid–electrolyte interphase inorganic salt components. This demands a more detailed study of the underlying physical and chemical processes occurring in sodium-ion batteries and allows great scope for groundbreaking advances in the field, from lab-scale to scale-up. This roadmap provides an extensive review by experts in academia and industry of the current state of the art in 2021 and the different research directions and strategies currently underway to improve the performance of sodium-ion batteries. The aim is to provide an opinion with respect to the current challenges and opportunities, from the fundamental properties to the practical applications of this technology.

Contents

Introduction

Nuria Tapia-Ruiz
Department of Chemistry, Lancaster University, Lancaster LA1 4YB, United Kingdom
The Faraday Institution, Quad One, Harwell Science and Innovation Campus, OX11 0RA, United Kingdom

Na-ion batteries (NIBs) promise to revolutionise the area of low-cost, safe, and rapidly scalable energy-storage technologies. The use of raw elements, obtained ethically and sustainably from inexpensive and widely abundant sources, makes this technology extremely attractive, especially in applications where weight/volume are not of concern, such as off-grid energy storage, load levelling, and starting, lighting, and ignition batteries, which amount to a potential worldwide demand of $\approx$1 TWh.

Given the similarities between the fundamental working principles and materials used in NIBs and the well-known rechargeable lithium-ion batteries (LIBs), the swift appearance of this technology in the market is to be expected, based on the use of existing battery manufacturing lines. Furthermore, NIBs can be stored and transported at 0 V, reducing the costs associated with expensive shipping and safety risks, and thus, they can be commercialised worldwide.

Despite their tremendous potential, only a limited number of companies, such as Faradion (UK), Tiamat (Europe), Altris AB (Europe), HiNa (China), and Natron Energy (USA) are devoted to sodium battery development. These manufacturers do not follow a consensus on the choice of sodium chemistry (e.g., positive electrodes can be made from layered oxides, Prussian blue analogues, or vanadium-based polyanionic compounds, and used with aqueous and non-aqueous electrolytic solutions), allowing for market/application diversification, and importantly, highlighting the immense scope of NIB materials research by developing new chemistries for positive and negative electrodes and electrolytes.

The multiple research prospects of NIBs have been recognised by the Faraday Institution, the UK's independent institute for electrochemical energy storage research, which launched NEXt-GENeration NA-ion batteries (NEXGENNA) [1] in October 2019 as part of its research portfolio of post-lithium batteries. The NEXGENNA consortium combines a multidisciplinary and diverse team of academics at the forefront of research in their respective fields, and the chief players in the UK Na-ion battery industry, with the ambition to deliver a revolution in the development of high-performance, cost-competitive, safe, and long cycle-life Na-ion batteries for stationary and low-cost transportation applications.

This 2021 NIB roadmap contains contributions from the NEXGENNA consortium and external project partners, as well as other relevant academics in the NIB field. The various contributions to this roadmap are divided into eight main research themes, ranging from fundamental experimental and computational science to large-scale industrial processing and techno-economic metrics, i.e. (a) cathode materials; (b) anode materials; (c) computational discovery of materials; (d) electrolytes and the solid–electrolyte interphase layer; (e) testing protocols; (f) advanced characterisation techniques, (g) manufacturing and scale-up, and (h) industrial targets and technoeconomics, totalling eight sections.

Sections 1, 2 and 4 contain an overview of the most relevant to date inorganic and organic cathode, anode, and electrolyte materials in NIBs, with a focus, where possible, on industry-relevant families of electrodes and electrolyte materials, but without losing sight of novel emerging materials with enough potential to become the next generation of candidates. In parallel, supercomputing architectures and more accurate and cost-effective quantum chemistry approaches (covered in section 3) will undoubtedly help us to discover new materials in broad compositional ranges which otherwise would consume extensive research time.

We include a subsection on the not-so-well-known solid–electrolyte interphase (SEI) layer in section 4), given its critical but extremely challenging role (due to the soluble nature of its components) in the cycling stability and performance of NIBs. The unstable behaviour of the SEI may result in unreliable data interpretation and thus, electrochemical measurement protocols need to be established to avoid discarding potentially interesting candidate materials or making erroneous interpretations of results (section 5).

Furthermore, characterisation of the SEI under *operando* or *in-situ* conditions will be crucial to provide good insight into the behaviour of this layer, and to draw correlations between electrolyte and electrode formulations, the physicochemical properties of the SEI, and battery performance. Similarly, understanding the long- and short-range processes occurring in electrode materials during battery operation is vital to characterise the charge-compensation mechanisms that occur in the different families of NIB materials. A relevant assortment of advanced *in-situ*/*operando* characterisation techniques—all used in the NEXGENNA advanced characterisation platform, is described in section 6. Sections 7 and 8 cover relevant manufacturing aspects of NIBs. This brings into play the use of full cells, which requires additional features that are not well considered in half-cell studies, including a good synergy between the cathode, anode, and electrolyte components, optimal electrode formulation, and architecture, among others. Finally, we provide an overview

of the current UK and international industry targets for NIBs, with special emphasis on the future performance metrics targeted by Faradion in the next five years with their technology, followed by a technoeconomic analysis. To permit a comparison, the performance and economic targets of NIBs are presented alongside commercial Li-ion battery data.

We expect that this 2021 roadmap for NIBs will be reference reading material for researchers working in the areas of electrochemical science, battery chemistry, energy materials, advanced characterisation, manufacturing, and computational methods. We also recommend other recent reviews on the topic of NIBs to the readers of this roadmap (e.g. [2–4]). Furthermore, we hope to inform key industries about current trends to encourage further investment in this technology, and influence decision-making from funding agencies and private investors.

1. Cathode materials

1.1. Layered transition-metal oxides: P2 | O3 materials

Jake M Brittain[1,2], Thomas J Wood[1] and William I F David[1,2]
[1] ISIS Neutron and Muon Spallation Source, STFC Rutherford Appleton Laboratory, OX11 0QX, United Kingdom
[2] Inorganic Chemistry Laboratory, University of Oxford, Oxford OX1 3QR, United Kingdom

Status

LIBs have not only transformed our digital electronic world but have also enabled the future electrification of transport and domestic energy storage. NIBs can extend and expand these opportunities, offering safer and more environmentally sustainable options. Recent significant developments indicate that Na-ion batteries can achieve performances that are similar to their Li-ion counterparts.

The cathode materials in all the highest-performing LIBs have two-dimensional (2D) layered crystallographic structures that are based on the chemical substitutions of the prototypical Li-ion cathode, $LiCoO_2$. The most promising Na-ion battery cathode materials possess a similar but richer layered geometry. This additional structural richness is a consequence of the larger ionic radius of the sodium ion, which not only adopts the elongated octahedral geometry observed in Li-ion cathode materials, but also crystallises into a trigonal prismatic configuration. This added structural versatility not only offers the opportunity to optimise for power and energy applications but also provides research directions for improved NIB performance that include increased capacity, higher charge and discharge rates, superior cyclability, extended lifetimes, and improved recycling.

Many P2 and O3 layered materials have been investigated for their potential use as Na-ion cathodes. Figure 1 not only indicates the combinatorial opportunities for cation permutation but also highlights the substantial variations in electrochemical performance. The symbols P2, O3, and P3 in figure 1 follow the notation developed by Delmas *et al* [5] to describe the prototypical crystal structures that can be adopted by layered Na-ion cathode materials. P and O respectively denote the coordination of trigonal prismatic and elongated octahedral Na-ion sites between (MO_2) metal-oxide sheets.

Figure 2 illustrates the two principal structural types. Assuming the sheets are stacked perpendicular to the *z*-direction, the oxygen atoms in each layer within the *xy*-plane can occupy three possible positions, denoted A, B and C. Each MO_2 sheet contains two layers of oxygen atoms that are paired above and below the metal layer. The number of pairs required to describe the Na_xMO_2 layered structure completes Delmas' notation. An elongated octahedral Na-ion coordination is typically adopted for $x = 1$ materials. This, combined with three oxide pairs per unit cell (AB CA BC) gives the rhombohedral phase its O3 notation. The standard, single-metal O3 materials in the literature include $NaNiO_2$ [7], $NaFeO_2$ [8], and the nickel-manganese hybrid, $NaNi_{1/2}Mn_{1/2}O_2$ [9]. Trigonal prismatic Na-ion coordination is preferred for $0.6 < x < 0.7$ and these phases typically form, with a two-pair repeating unit (AB BA), leading to a P2 notation for the hexagonal phase. $Na_{2/3}MnO_2$ [10], $Na_{0.7}CoO_2$ [11], and $Na_{2/3}Ni_{1/3}Mn_{2/3}O_2$ are the standard undoped P2 materials described in the literature [12].

Current and future challenges

Many of the current and future challenges associated with layered Na-ion batteries are linked to the development of higher-performance cathode materials. However, the added opportunities afforded by the two distinct sodium environments within the P2 | O3 layered materials result in additional structural complexities upon battery cycling. The atomic, nano- and meso-structural progressions of these structural changes are not yet adequately characterised. A fundamental and comprehensive understanding of these structural evolutions over many thousands of cycles is necessary to improve cycling, mitigate degradation, and increase lifetime performance. Significant variations in performance, however, can result from subtle substitutions. The observation, for example, that the addition of small percentages of redox inactive ions, such as Mg^{2+} and Ti^{4+}, results in substantial changes in electrochemical performance, is today an unresolved issue, but looking forward, it will be both a combinatorial challenge and a commercial opportunity [13, 14].

A focus on power performance will best be met by P2-based systems because of the unique sodium-ion environment, which enables facile ionic mobility through rectangular faces between adjacent trigonal prismatic environments. This diffusion mechanism is not available to Li-ion batteries, suggesting that the optimisation of P2-based sodium batteries may lead to higher diffusion coefficients and consequently higher charge and discharge rates than for Li-ion batteries.

The best battery capacity performances will be associated with O3-based systems, which have the highest sodium stoichiometries. Mimicking the best over-lithiated Li-ion batteries by over-sodiation may lead to a further improvement in performance. The requirements of intermediate applications that involve both
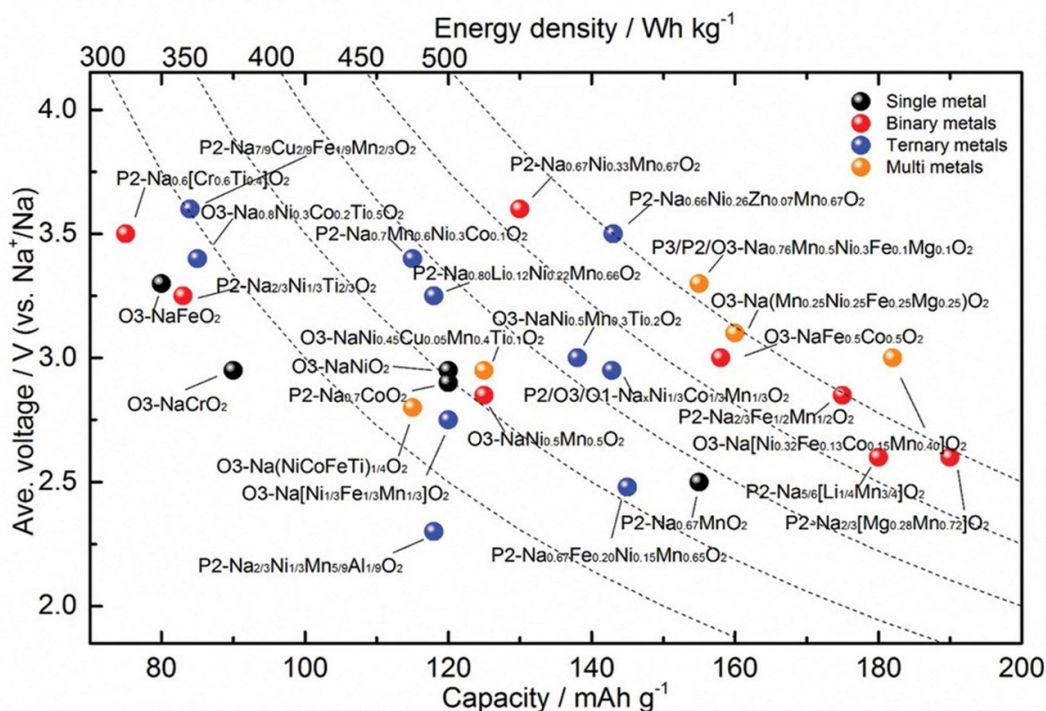
Figure 1. An electrochemical summary of various layered oxide sodium-ion cathode materials, comparing voltage, capacity and energy density. All measurements are in half-cell systems. [6] John Wiley & Sons.
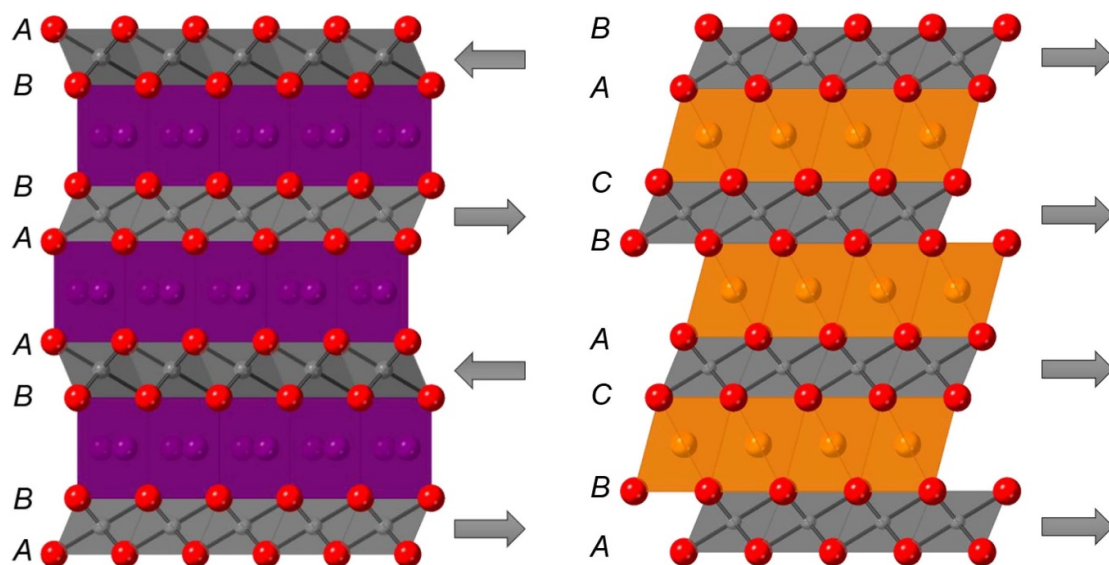
Figure 2. Crystal structures of P2 (left) and O3 (right) materials. Sodium ions are in trigonal prismatic (purple) and elongated octahedral (orange) geometries, respectively. The metal layers are shown in grey, with their directionality indicated by the grey arrows.

power and energy optimisation can be addressed by the development of hybrid P2 | O3 materials [15]. Figure 1 indicates that there is a large combinatorial space of cation permutations that can be explored to improve power and energy densities, cycle life, and recyclability to meet the optimisation requirements of different industrial applications.

Perhaps most significantly, layered P2 | O3 cathodes offer the opportunity to develop sustainable 'green' batteries that are only manufactured from earth-abundant materials. LIBs face ethical challenges associated with mining the metal-containing ores as well as economic issues related to material scarcity and the environmental impact of recycling toxic chemical constituents. Fabricating high-performance NIBs from safe, earth-abundant materials containing, for example, a combination of sodium, iron, manganese,

magnesium, and titanium ores mitigates environmental impacts and offers a global opportunity for the deployment of safe and affordable batteries to both the developing and the developed parts of the world.

Advances in science and technology to meet challenges

The principal research challenges facing the development of improved P2 | O3 Na-ion batteries are centred around the combinatorial chemical exploration of the fundamental angstrom- to micron-scale structures of layered transition-metal cathodes, and how these multiscale structures change throughout the battery lifetime. Synchrotron x-ray and neutron scattering facilities play a central role in determining the relationship between crystal structure and electrochemical performance. Addressing the combinatorial aspects of cation permutation along with point-by-point measurements of structural transitions over multiple charge and discharge cycles necessitates the development of, and access to, increasingly precise, rapid, high-resolution, *in-situ* and *operando* diffraction, spectroscopy, and thermodynamic and electrochemical experiments. For a detailed fundamental understanding of battery behaviour from fabrication to failure, these experimental measurements must be accompanied by rapid computational chemical calculations.

Concluding remarks

NIB performance has improved substantially over the past decade, and layered P2 | O3 cathode technologies are in leading positions in many of the battery metrics. The close structural similarities between P2 | O3 materials and layered lithium-ion cathodes have helped inform their scientific and commercial development. However, the increased structural complexity of P2 | O3 materials, resulting from the ability of sodium ions to adopt both trigonal prismatic and elongated octahedral coordination, creates many challenges but also offers significant opportunities. The challenges result from the combinatorial complexity of the cation permutations. The opportunities are to develop NIBs that are competitive with the best LIBs. One of the major goals is to 'go green' by producing high-performance NIBs, with a minimal carbon footprint, from sustainable and abundant resources.

1.2. Anion redox layered transition-metal oxides

Eunjeong Kim[1,3], *Begoña Silván*[2,3], *Nuria Tapia-Ruiz*[2,3] *and A Robert Armstrong*[1,3]
[1] EastChem School of Chemistry, University of St. Andrews, St. Andrews KY16 9ST, United Kingdom
[2] Chemistry Department, Lancaster University, Lancaster LA1 4YB, United Kingdom
[3] The Faraday Institution, Quad One, Harwell Science and Innovation Campus, OX11 0RA, United Kingdom
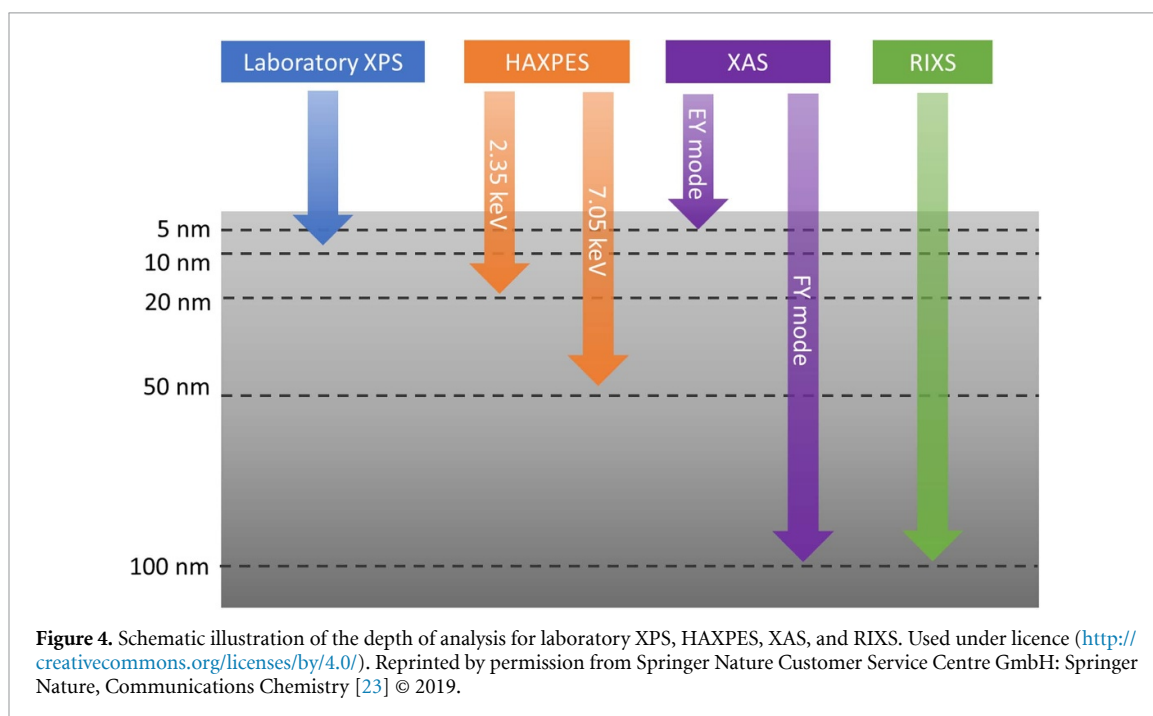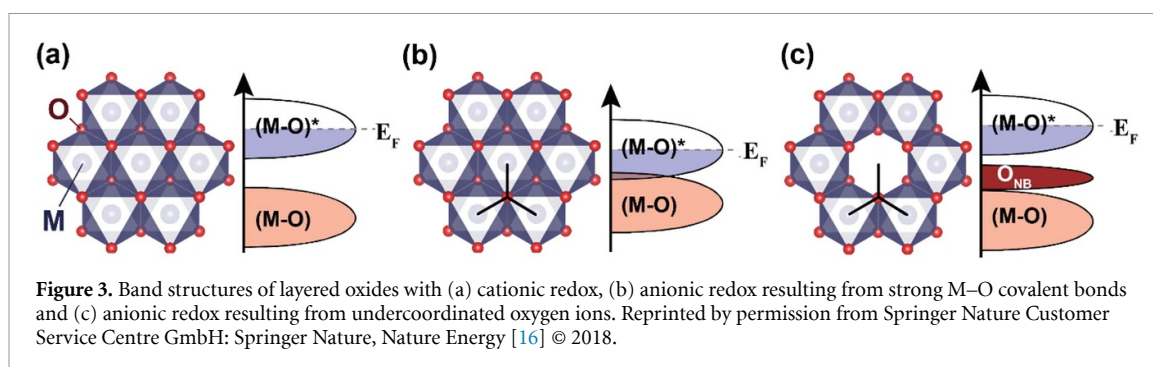
Status

Oxygen redox-based reactions have gained interest among NIB researchers, due to the prospect of obtaining extra capacity at high voltages beyond those available from conventional transition-metal redox reactions. The study of anionic redox reactions in sodium layered cathode materials is especially relevant, due to their intrinsically lower energy density when compared to their Li counterparts. As with oxygen reactions observed in Li-rich cathode materials for LIBs, these are typically kinetically limited, and thus, research efforts are devoted to improving their reversibility [16]. To date, most studies in this area have focussed on P2-type materials (where Na occupies trigonal prismatic sites), accounting for over 60% of the reported compounds.

Anionic redox reactions can be described in terms of band structure, where the overlap of bonding (M–O) and antibonding (M–O)* orbitals leads to a continuum band which enables the removal of electrons from oxygen ions (figure 3(b)). In contrast, separated M d and O p bands may be observed in pure cationic redox-driven compounds (figure 3(a)). From a proof-of-concept perspective, the formation of strong covalent bonds and consequently favourable M–O orbital overlap was first demonstrated with 4d (Ru) and 5d metals (Ir). However, for practical reasons, oxygen redox research has naturally shifted toward the use of low-cost and non-toxic 3d metals, such as manganese-rich compounds. When up to one third of the manganese is replaced by another more electronegative and active element (e.g., Ni^{2+}, Fe^{3+}, Co^{3+}), the strong overlap with the O 2p states favours electron transfer, often via a reductive coupling mechanism, while the substituted inactive elements (e.g., Li^+, Zn^{2+}, Mg^{2+}) allow O 2p states to be placed at the top of the valence band [17]. Furthermore, the more covalent Mn–O bonds tend to stabilise the crystal structure, thereby avoiding unwanted phase transitions while reducing the inherent structural instability caused by Jahn–Teller active Mn^{3+} ions and parasitic disproportionation reactions. A challenge encountered in these materials is their large hysteresis, typically explained by the irreversible migration of certain metals (including Mn) towards the Na layers or within the MO_2 planes [18]. This has been partially alleviated by designing materials with undercoordinated oxygen ions (i.e., with either 'direct' or 'indirect' vacancies – mobile Li dopants that leave the transition-metal layers upon charging), where the presence of non-bonding oxygen states translates into a new non-bonding O band (O_{NB}) above the (M–O) band, where extra electrons can be located (figure 3(c)). These vacancies need to be well dispersed and thus isolated from a nearby vacancy to avoid the formation and release of O_2 gas, which is favoured by the under-bonded O ions [19].

Current and future challenges

While oxygen redox represents an effective way of enhancing energy density in NIBs, limited reversibility on cycling needs to be overcome for most oxygen redox-active compounds. In general, the structural transformation from P-type to O-type structures is induced by gliding of the transition-metal layers upon excess deintercalation of Na ions [20]. The lattice stress caused by this phase transition as well as the partial irreversibility of the structural transition are often responsible for a reduction in oxygen redox activity. In addition, cation migration, either from transition-metal layers to Na layers, or within transition-metal layers, may lead to large voltage hysteresis. The local coordination around oxygen anions has a direct effect on the voltage at which the discharge plateau occurs [19]. Moreover, increasing the upper cutoff voltage beyond ~4.1 V accelerates the removal of cations from the transition-metal layers, which may result in lattice oxygen loss due to uncoordinated oxygen atoms [21]. Finally, since oxygen redox occurs in the high-voltage region where classical organic electrolytes are unstable, detrimental reactions associated with the decomposition of electrolytes are also a significant problem.

In order to gain deep insights into oxygen redox behaviour in cathode materials, spectroscopic techniques have been heavily used (figure 4). It is important to select appropriate techniques to distinguish bulk vs. surface phenomena, since cathode-electrolyte reactions tend to dominate the surface chemistry. Laboratory X-ray photoelectron spectroscopy (XPS) has been widely applied to probe chemical changes in oxygen anions, although the technique is limited to surface information. Furthermore, synchrotron X-ray techniques, such as hard and soft X-ray absorption spectroscopy (XAS), hard X-ray photoelectron spectroscopy (HAXPES), and resonant inelastic x-ray scattering (RIXS) have been exploited for bulk characterisation. In addition to the depth of analysis, the different techniques provide a range of information. In this regard, soft XAS and RIXS are promising tools for demonstrating oxygen redox, whilst hard XAS provides indirect evidence of the participation of oxygen anions in the charge-compensation mechanism. Additional laboratory-based characterisation techniques, such as differential electrochemical mass

Figure 3. Band structures of layered oxides with (a) cationic redox, (b) anionic redox resulting from strong M–O covalent bonds and (c) anionic redox resulting from undercoordinated oxygen ions. Reprinted by permission from Springer Nature Customer Service Centre GmbH: Springer Nature, Nature Energy [16] © 2018.

Figure 4. Schematic illustration of the depth of analysis for laboratory XPS, HAXPES, XAS, and RIXS. Used under licence (http://creativecommons.org/licenses/by/4.0/). Reprinted by permission from Springer Nature Customer Service Centre GmbH: Springer Nature, Communications Chemistry [23] © 2019.

spectrometry, Raman spectroscopy, electron paramagnetic resonance spectroscopy (EPR) and sequential cyclic voltammetry (CV) are often in demand to decouple oxygen redox from electrolyte decomposition. However, *ex situ* techniques may be unreliable due to the reactivity and instability of the phases formed at high states of charge. This has led to the recent suggestion that the behaviour of Li-rich layered materials may be derived from the $Mn^{4+} \rightarrow Mn^{7+} + 3e^-$ redox reaction, the resulting species being too unstable to be observed [22]. Nonetheless, there is a strong indication of oxygen redox activity, based on a combination of *ex-situ, in-situ* and *operando* techniques.

Advances in science and technology to meet challenges

As mentioned above, the biggest problems encountered in cathode materials exhibiting oxygen redox are capacity fade combined with large voltage hysteresis. Among the exceptional materials which exhibit suppressed voltage hysteresis are $Na_2Mn_3O_7$ [24], with ordering between Mn and intrinsic transition metal vacancies and $Na_xMn_{1-y}Li_yO_2$ [19], with a ribbon superstructure. These examples confirm that well-defined ordering in the transition-metal layers mitigates detrimental cation migration and phase changes. In the case of $Na_xMn_{1-y}Li_yO_2$, repopulation of mobile Li at the original site is critical to the retention of the superstructure. To exploit these advantages, the design of materials containing transition-metal vacancies and/or dopants that migrate reversibly represents a promising route towards reversible oxygen redox. This strategy should be coupled with an investigation of the mobility of transition-metal vacancies and the associated electronic structure changes. The development of ultra-high-resolution XAS and RIXS will be necessary to describe the complete mechanism of oxygen redox by distinguishing different oxidised oxygen species and to provide a detailed account of transition-metal charge transfer. As an alternative strategy, the activation of materials via partially reversible oxygen redox may be used to develop materials with enhanced cycling performance not accessible by direct synthesis. This approach may be considered analogous to the

activation of the Li_2MnO_3 component of Li-rich layered materials for LIBs [25]. To suppress oxygen release, surface engineering methods, such as the use of coatings, namely Al-based oxides and phosphates, may be implemented. Typically, these coatings react with the cathode material to stabilise the surface by creating a composite of the active material and the coating compounds [26]. Furthermore, electrolytes that are stable at very high potentials must be sought to enable an accurate study of the cathode material without interference from parasitic electrolyte reactions. To address this, several approaches can be adopted based on high-voltage LIBs, namely the use of electrolyte additives or super-concentrated commercial salts in organic solvents. On the other hand, organic solvents can be replaced by more stable ionic liquids or solid electrolytes, although these approaches are far from large-scale commercialisation [27].

Concluding remarks

The anion redox reaction represents a major challenge, in terms of both understanding and successful exploitation. However, the potential rewards in terms of increased energy density, together with the realisation that its occurrence is more widespread than hitherto believed, make it an important area for future development. This may take the form of materials that undergo irreversible changes as a result of oxygen redox and thereby generate phases with enhanced electrochemical performance. Alternatively, the developments outlined in the previous section could lead to the preparation of phases exhibiting truly reversible oxygen redox reactions stabilised by surface coatings and/or the availability of novel electrolytes. Progress will be assisted by the further development and increasing availability of advanced characterisation techniques, such as RIXS, which may be combined with HAXPES and XAS to obtain information at a range of depths.

Acknowledgment

1.3. Polyatomic anion-based materials

Xiao Hua[1,3], *Peter Gross*[2,3], *Edmund J Cussen*[1,2,3] *and Serena A Cussen*[1,2,3]

[1] Department of Chemical and Biological Engineering, University of Sheffield, Sheffield S1 3JD, United Kingdom
[2] Department of Materials Science and Engineering, The University of Sheffield, Sheffield S1 3JD, United Kingdom
[3] The Faraday Institution, Quad One, Harwell Campus, OX11 0RA, United Kingdom

Status

Na-ion battery cathodes based on polyatomic anion insertion compounds offer a rich structural chemistry and a variety of crystallographic architectures. This class of materials provides enhanced structural stability, improvements in safety, and the ability to tune the resulting redox potentials, offering opportunities to extend the operating voltages to above 3.5 V vs. Na^+/Na [28, 29]. In addition to single polyatomic anion species, a search is under way for mixed anion systems that can further extend redox potential improvements. This ability to increase the cell voltage is associated with a phenomenon known as the inductive effect, where a judicious choice of polyatomic anion species can influence the metal–oxygen bonding, thereby tuning the resulting operating voltage. This is illustrated in figure 5 for a series of polyatomic anion cathodes used in NIBs.

Vanadium-containing phosphates and fluoride phosphates are among the most promising Na-ion cathodes, owing to their structural stability and high ion mobility as well as the ability to tune the operating voltage by varying the electronegativity of the polyatomic anions. NASICON-type $Na_3V_2(PO_4)_3$, for example, can reversibly intercalate two Na ions at a potential of 3.4 V. The mixed fluoride phosphate species $Na_3V_2(PO_4)_2F_3$ displays a higher average operating voltage of 3.9 V, with a high theoretical capacity of 128 mAh g^{-1} (based again on a two-Na-ion exchange) [29]. Solving the crystal structures of these materials, which can display polymorphism, has presented an interesting challenge to the battery materials community; however, synchrotron x-ray diffraction studies have unveiled subtleties in polymorphic Na-ion ordering. These can potentially change materials' ionic conductivity, highlighting the critical need for in-depth structural analyses to rationalise the relationship between the crystal structure and the electrochemical properties of these materials [30, 31]. The move towards oxygen-substituted derivatives of $Na_3V_2(PO_4)_2F_3$ has led to improvements in energy density; for example, Ceder *et al* have demonstrated that $Na_3V_2(PO_4)_2FO_2$ can accommodate an additional fourth Na-ion at ∼1.6 V to become $Na_4V_2(PO_4)_2FO_2$ [32]. This exciting development, which is due to the strong screening effect of the O^{2-} ions, elevates the specific energy to ≈600 Wh kg^{-1} and presents an intriguing research challenge of increasing this redox potential.

Current and future challenges

A careful consideration of reaction conditions presents ongoing opportunities to arrive at a set of design principles that will enable the direct targeting of a desired polymorph or particle architecture. In a recent example, Yang *et al* discovered a new fluoride phosphate which crystallised in two forms, depending on the temperature chosen: a high-calcination-temperature *Pbca* phase and a lower-calcination *P*3 phase of $Na_5V(PO_4)_2F_2$ [33]. Both polymorphs exhibit high operating voltages (3.5 V and 3.4 V for the *Pbca* and *P*3 phases, respectively). In this context, a topic for future research is the exploration of dopants that could allow access to the V^{4+}/V^{5+} redox couple and further elevate the achievable capacity.

The replacement of vanadium by earth-abundant and cheaper alternatives remains an ongoing research challenge. In the work referenced earlier, Ceder *et al* also demonstrated that the replacement of vanadium by aluminium ($Na_3V_{2-z}Al_z(PO_4)_2F_3$, where $z \leqslant 0.3$) also permits additional Na insertion at low voltages of ∼1.3 V [32]. While this is impractically low, it does suggest that doping could provide a rational route to disrupting sodium ordering and improving ion mobility. The triplite phase $LiFeSO_4F$ (which also exists in the tavorite polymorph) has exhibited the highest redox potential for an Fe^{2+}/Fe^{3+} redox couple at 3.9 V. Interestingly, the synthesis of a sodium triplite-analogue, $NaFeSO_4F$, has been achieved through the chemical delithiation and subsequent chemical sodiation of the triplite phase $LiFeSO_4F$ [34]. The monoclinic *C*/2 symmetry, with a random distribution of Na and Fe across the two metal octahedral M1 and M2 sites enabled by the sodiation approach, provides a redox potential of 3.7 V and a capacity close to the theoretical limit (≈138 mAh g^{-1}) at 0.01 C. Sluggish diffusion kinetics and low coulombic efficiencies suggest that structural distortions are occurring; further research is required to overcome this.

Developments in synthetic control have also allowed access to high-quality, open framework alluaudite structures, which offer high potentials and energy densities, but are often difficult to achieve with stoichiometric control. Plewa *et al* have developed a new solution-based synthesis of $Na_2FeM(SO_4)_3$ (M = Fe, Mn, Ni) where the presence of impurity phases is reduced by the addition of excess sodium
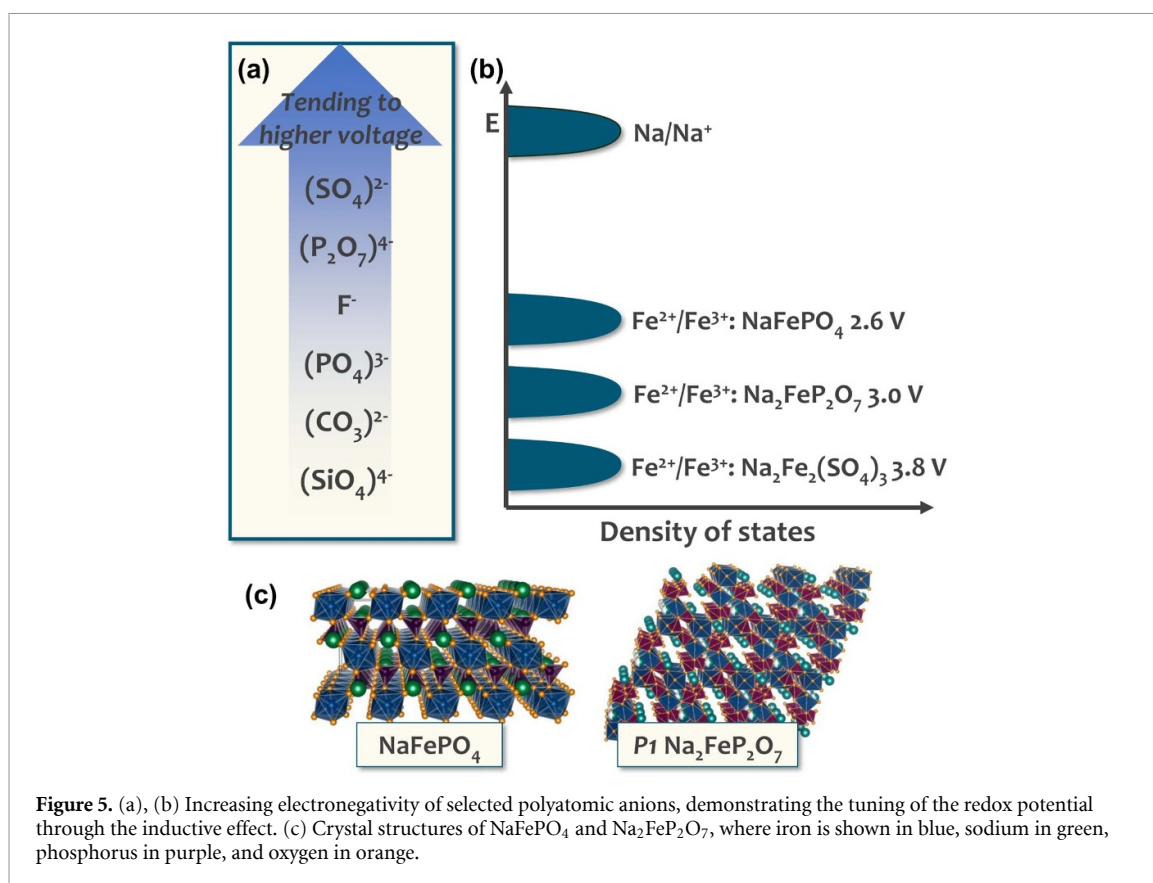
Figure 5. (a), (b) Increasing electronegativity of selected polyatomic anions, demonstrating the tuning of the redox potential through the inductive effect. (c) Crystal structures of $NaFePO_4$ and $Na_2FeP_2O_7$, where iron is shown in blue, sodium in green, phosphorus in purple, and oxygen in orange.

precursor and a glucose additive to preserve a reducing environment [35]. *In situ* XRD and thermogravimetric analysis monitoring provide effective optimisation guides during synthesis.

Investigations of mixed polyanionic materials continue to offer opportunities to tune the redox potential, as described by a recent report by Tang *et al* on the combined electronic inductive effect of oxalate and sulphate in the $Na_2Fe(C_2O_4)SO_4 \cdot H_2O$ phase [36]. Further investigations of dopant effects in this system could provide a pathway to improvements in electrochemical performance.

Advances in science and technology to meet challenges

Reliably determining the crystal structures of unknown phases remains a challenge. A recent development embracing a materials genomic approach was reported by Khalifah *et al*, who have focused on the unsolved structure of the low-temperature phase of $Na_3V_2(PO_4)_2F_3$ [37]. A plethora of enumerated plausible trial structures (of the order of 3000), informed by reasoned Na-ion ordering, were fitted to experimental data by Rietveld refinement, which enabled researchers to identify a set of closely related structural models that could reliably describe the experimental powder pattern. Subsequent density functional theory (DFT) and structural analyses then pointed to the $A2_1am$ space group as the proposed structure. This analytical approach represents an exciting development in the determination of structures, particularly for emerging cathode chemistries, where complex cation ordering exists.

Insights from *operando* investigations continue to shed light on the complex structural and redox processes ongoing in operating batteries. One recent report which exemplifies this is a study of vanadium oxyfluorides, $Na_3V_2(PO_4)_2F_{3-y}O_y$ ($0 \leqslant y \leqslant 2$), by Croguennec *et al* [38]. By following the desodiation process via *operando* x-ray absorption spectroscopy (XAS) and combining these observations with insights gleaned from DFT calculations, it is possible to examine the complex changes in the average local coordination environment of vanadium across a series of compositions where vanadium redox centres coexist. Ongoing upgrades to synchrotron beamline facilities will expand our ability to probe the highly complex and rapid processes that occur during charge and discharge, which will enable us to better understand materials' structure–performance relationship.

Concluding remarks

Polyatomic anion cathodes continue to provide a route to increase operating potential by capitalising on the inductive effect, as well as by conferring structural stability to the material. There is a trade-off in terms of the capacities that can be achieved with the heavier polyatomic anion component (in comparison to layered

oxides), but recent work to accommodate additional Na-ions through, for example, the application of suitable dopants, is intriguing. In addition to synthetic developments that allow access to high-quality samples and new polymorphs, particle size and shape tailoring will enable further improvements, such as higher power densities. In addition to a further examination of the effect of dopants, challenges remain in developing suitable coatings and additives that will bestow stability under ambient and high-voltage conditions.

Acknowledgments

1.4. Prussian blue and analogues
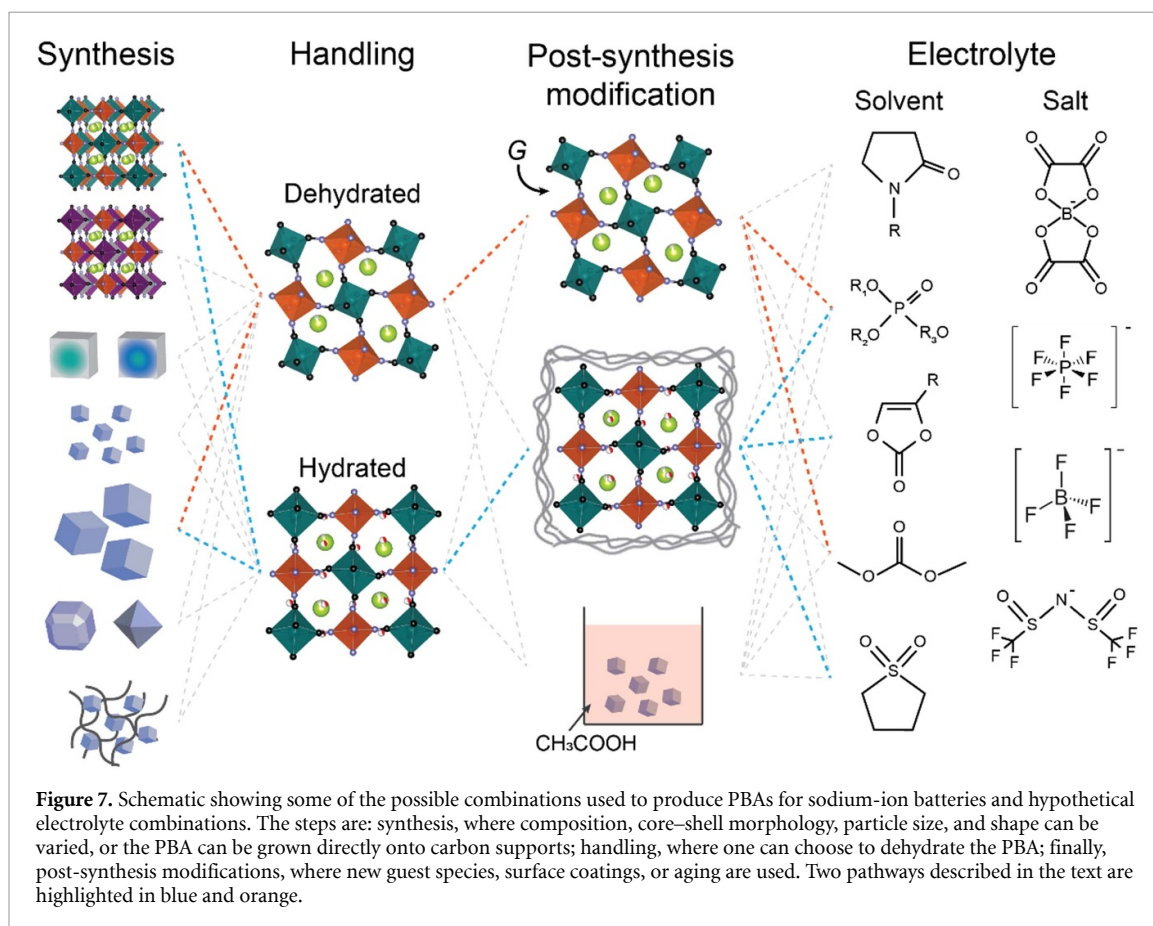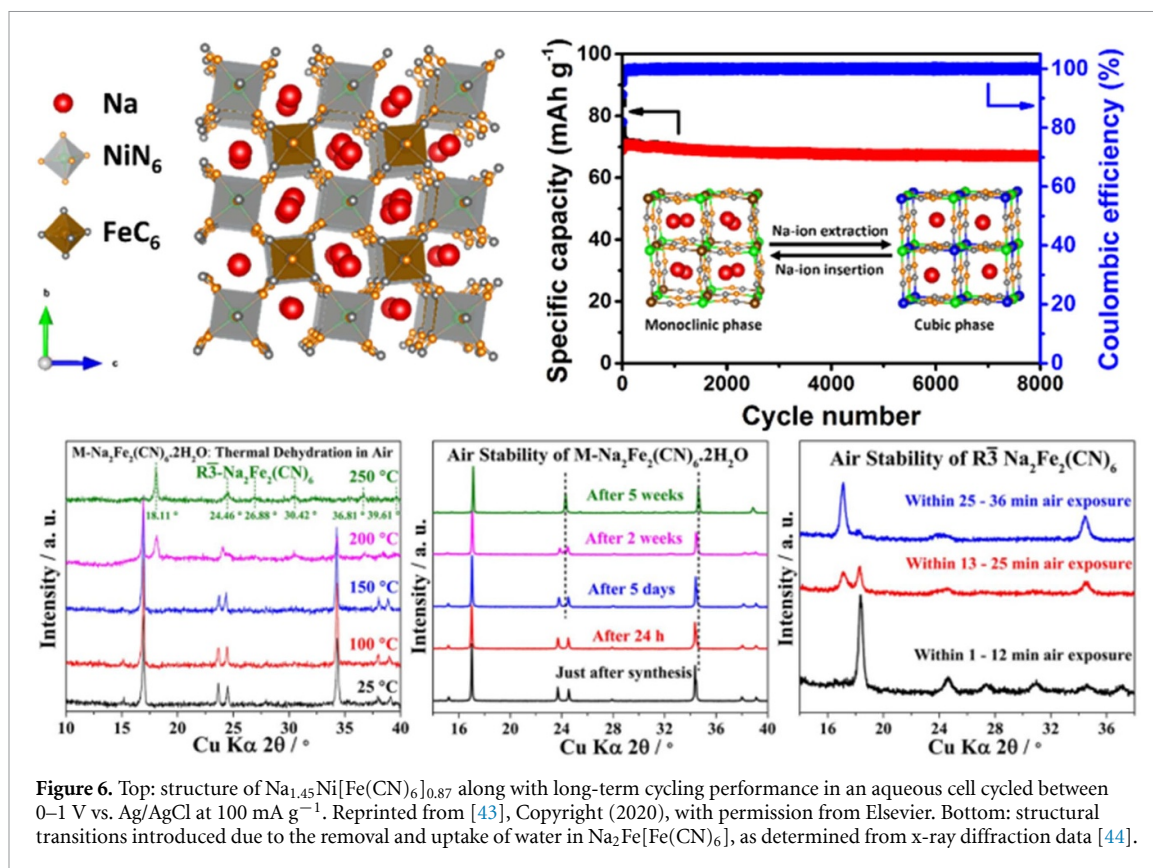
William R Brant and Ronnie Mogensen

Department of Chemistry—Ångström Laboratory, Uppsala University, SE-75121 Uppsala, Sweden

Status

Prussian blue analogues (PBAs), with the general formula $Na_xM[M'(CN)_6]_{1-y}.zG$ (where M and M' are transition metals, most commonly Mn, Fe, or Ni, y is the number of $[M'(CN)_6]^{n-}$ vacancies, and G is a neutral guest, such as H_2O), are highly porous positive-electrode materials for NIBs (top of figure 6). Since PBAs are comprised of abundant elements and can be produced at low cost, they provide the best price-to-performance ratio [39] for a positive electrode. Thus, PBAs capitalise on the key advantages of NIBs as cheap, sustainable, and safer alternatives to lithium-ion technology. They have become viable cathode materials for sodium batteries within the last decade. During this time, the greatest challenge facing the implementation of PBAs as positive electrodes has been the ability to produce highly-sodiated compounds that are structurally stable during cycling. The structural stability and maximum capacity of the material are severely reduced by the presence of the vacancies (y) introduced during synthesis. Due to the loss of a reducible cation (M') and the necessary charge compensation required to offset the negative charge of $[M'(CN)_6]^{n-}$, 1 mol% of vacancies can lead to a 3–4 mol% reduction in the maximum sodium content. Resolving this issue requires alternate synthetic approaches to the more traditionally applied co-precipitation reactions. For some M cations, in particular, Fe, co-precipitation results in a high vacancy concentration. In 2014, You *et al* reported a way of producing a low-vacancy PBA from a single precursor via an acid decomposition synthesis route for the first time [40]. This approach was subsequently used to produce the best-performing PBA to date, which delivered 120 mAh g^{-1} for over 800 cycles of charging at 0.5 C (75 mA g^{-1}) and discharging at 2 C (300 mA g^{-1}) [41]. Since then, extensive effort has been invested in the exploration of different M combinations, particle sizes, morphologies, and coatings, and improvements have been seen for either initial capacity or total cycling life, but not both [42]. Ultimately, the goal for PBAs is to achieve capacities of more than 160 mAh g^{-1} which are stable for up to 10 000 cycles. Eight thousand cycles have been demonstrated using aqueous electrolytes (figure 6 top) [43]; however, the resulting capacity is frequently limited to 60–80 mAh g^{-1}. Conversely, higher capacities (>80 mAh g^{-1}) can be achieved using non-aqueous electrolytes due to their wider potential stability window although, the number of cycles obtained is often an order of magnitude lower.

Current and future challenges

Two connected issues are plaguing the development of PBAs: moisture sensitivity and limited reversibility when cycling more than one atom of sodium per formula unit. Capacity fading in PBAs has generally been attributed to limited electronic conductivity, the presence of water, and phase transitions of the highly sodiated compounds. Several methods have been employed to overcome their limited electronic conductivities, such as growing PBAs directly on carbon nanotubes, enabling stable cycling down to −25 °C [45]. Structural stability has seemingly been a greater challenge to overcome, since phase transitions in sodium-rich PBAs are heavily influenced by their water content. Wang *et al* [41] first demonstrated that, when completely dehydrated, Fe-based PBAs adopt a rhombohedral structure with a unit cell volume that decreases by ≈18%. This work was followed up by Rudola *et al* [44], who demonstrated that obtaining a moisture-free PBA depends heavily on the temperature and pressure used for drying and that, if exposed to air, a hydrated structure forms within minutes (bottom of figure 6). Further, a 16% volume change between cubic $Fe[Fe(CN)_6]$ and rhombohedral $Na_2Fe[Fe(CN)_6]$ leads to a lower cycling stability compared to the hydrated compound, if the capacity and voltage window are limited in the hydrated case. Water also increases the average voltage output [46], which may be perceived as an advantage. However, the high voltage plateau may lie beyond the upper stability limit of water (3.9 V vs. Na^+/Na). Finally, it has been shown that desodiated PBAs have a lower affinity for water [47]. Consequently, charging the cell runs an additional risk of releasing water into the electrolyte. Thus, the influence of water on electrochemical performance is complicated. The presence of water is beneficial for ensuring structural stability by minimising volume contraction during cycling. However, it limits the maximum capacity that can be utilised, as water is either released from the structure and reacts with the electrolyte, or is oxidised inside the material at high potential. Solving this challenge will require further consideration of the role of the electrolyte. Electrolyte–PBA interactions will be the greatest hurdle to overcome in the future, as all synthetic design choices (figure 7) will have to determine the optimum electrolyte combination. The synthetic possibility space for PBAs is large, and so one must take a holistic view when designing a cell based on this material.

Figure 6. Top: structure of $Na_{1.45}Ni[Fe(CN)_6]_{0.87}$ along with long-term cycling performance in an aqueous cell cycled between 0–1 V vs. Ag/AgCl at 100 mA g^{-1}. Reprinted from [43], Copyright (2020), with permission from Elsevier. Bottom: structural transitions introduced due to the removal and uptake of water in $Na_2Fe[Fe(CN)_6]$, as determined from x-ray diffraction data [44].

Figure 7. Schematic showing some of the possible combinations used to produce PBAs for sodium-ion batteries and hypothetical electrolyte combinations. The steps are: synthesis, where composition, core–shell morphology, particle size, and shape can be varied, or the PBA can be grown directly onto carbon supports; handling, where one can choose to dehydrate the PBA; finally, post-synthesis modifications, where new guest species, surface coatings, or aging are used. Two pathways described in the text are highlighted in blue and orange.

Advances in science and technology to meet challenges

Optimal material design choices for PBAs are ones that address multiple issues while maintaining stable or synergetic interactions with the electrolyte. More advanced material modifications can be achieved, given a rigorous understanding of how a modification influences other synthetic steps and compatibility with other material features or the electrolyte. For example, if one elects to utilise the hydrated PBA material, a surface coating, such as reduced graphene oxide [48] might be designed. This could keep the water from leaving the structure and prevent soluble electrolyte decomposition products from entering the structure, while permitting the passage of sodium. Thus, structural integrity would be maintained while preventing side reactions with the electrolyte (figure 7, blue path). However, this solution will only function with M and M' cations for which the voltage remains below the stability limit of water [46]. Alternatively, the electrolyte may intentionally include small molecules, such as acetonitrile, which co-insert with sodium, fulfilling a similar role to water in aqueous-based electrolytes (figure 7, orange path). Any potential solution must be balanced against all other synthetic choices, such that the potential benefit that the modification brings is not offset by a lack of compatibility with either the electrode or the electrolyte. Thus, a paradigm shift in research mindset must be made, away from simply aiming to boost performance with a single modification, and towards deconstructing the fundamental interactions within the material and between the material and its environment.

Concluding remarks

PBAs are a challenging class of compounds to investigate for NIBs due to the highly tuneable nature of their synthesis and the tangled web of chemical interactions within the material and with its environment. However, their potential as positive electrodes in beyond lithium-ion systems is clear, in terms of both cost and performance. Thus, the grand challenge will be to build a robust fundamental understanding of these complex interactions, enabling material developments which foster synergies that can be established using new advanced electrolytes.

1.5. Organic materials
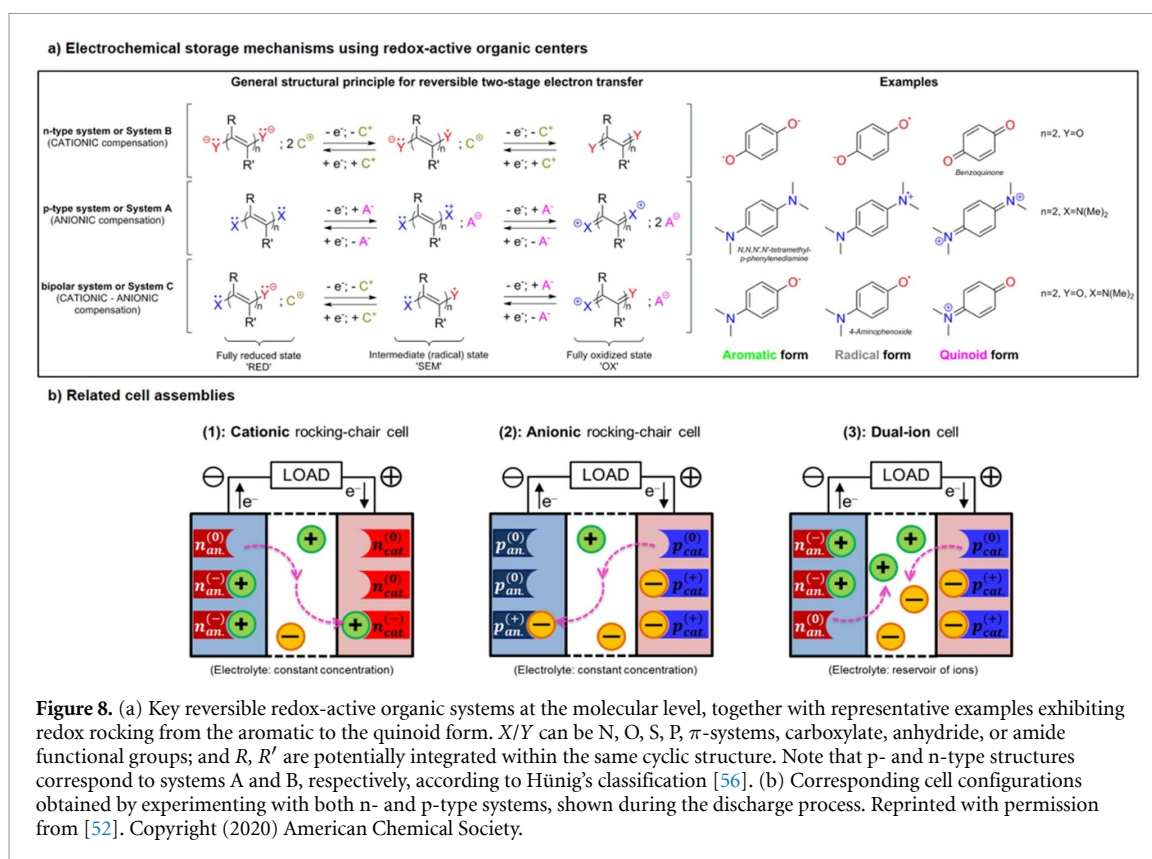
Philippe Poizot and Stéven Renault

Université de Nantes, CNRS, Institut des Matériaux Jean Rouxel, IMN, F-44000 Nantes, France

Status

Most of the materials studied for use in NIBs are typically inorganic, inherited from the abundant knowledge developed in the field of LIBs over the last four decades. Although sodium can indeed be considered to be highly abundant on Earth and related to low-pollution resources, that may not be the case for other elements comprising inorganic electrode materials (especially metals). It is now well documented that commercial (inorganic-based) batteries involve a large consumption of energy from 'cradle to grave' and generate environmental pollutants, including hazardous waste and greenhouse-gas emissions [49, 50]. Hence, the environmental impacts of large-scale battery use as well as recycling and re-use represent major challenges that will require further attention in the future. Organic electrode materials (OEMs) may offer novel and more sustainable storage solutions, allowing eco-design at the scale of the active material itself [51, 52]. As they are composed of naturally abundant elements (C, H, O, N, and even S) coupled with possible biosourcing, OEMs can be produced using low-energy and low-cost synthetic chemical routes. In addition, organic molecular engineering gives access to great structural diversity and easy control of functional groups. After use, OEMs can be thermally disposed of, with energy recovery, or eventually recycled [53]. In practice, two reversible electrochemical storage mechanisms can be used (alone or combined), which are characterised either by conventional cation charge compensation (in n-type systems) or anion charge compensation (p-type), as illustrated in figure 8. In principle, organic materials exhibit flexible crystal structures containing discrete entities, and bind to each other by weak interactions, such as van der Waals bonding, making the accommodation of large cations such as Na^+ or anions possible without much spatial hindrance. The first electrochemical assessments of OEMs for NIBs date from the 1980s, but occurred at a time when lithium chemistry quickly appeared superior, halting further development until recently. Despite their early stage of development, during the past few years, a considerable amount of effort has also been devoted to promoting organic NIBs alongside the development of inorganic electrode materials [54, 55]. Nevertheless, further improvements are necessary, especially in terms of organic cathode materials (i.e., positive electrodes), because most of the investigated compounds suffer from limited electrochemical performance.

Current and future challenges

In principle, n-type cathode materials are required to assemble NIBs, because the electrode reaction enables reversible cation uptake/removal. To date, the best reported electrode materials that can achieve excellent stability over thousands of cycles are based on polymerised perylene diimides (table 1, entry 1) [57, 58], because aromatic diimides are robust redox-active organic moieties. However, they suffer from limited working potential values which usually do not exceed 2.5 V vs. Na^+/Na. Moreover, they are usually prepared in their oxidised (desodiated) state (left-hand side of the half-reaction at the positive electrode in table 1, entries 1–3), which restricts their practical use in sodium half-cells or requires a pre-reduction (sodiation) step before full-cell assembly (table 1, entries 2 and 3) [59, 60]. One of the few examples of a sodiated cathode material is the tetrasodium salt of 2,5-dihydroxyterephthalic acid (Na_4DHTA), which has been successfully introduced in a symmetric Na-ion cell configuration [61]. Again, the output voltage of the cell was restricted to about 2 V due to the low working potential of the cathode side (2.3 V vs. Na^+/Na). This potential limitation for non-polymer n-type OEMs (such as Na_4DHTA salt) is notably related to the high electron density in the redox-active organic centre. The DHTA organic ligand exhibits at least two permanent negative charges through the two inactive carboxylate functional groups. The latter serve as a simple and effective way to prevent dissolution in aprotic electrolytes [51] but their electron-donating behaviour drags the average redox potential of the whole compound down. Although polymerisation is another excellent strategy for preventing dissolution in the electrolyte, the high-molecular-weight polymers are unlikely to be chemically prepared in their reduced (sodiated) state. It is worth noting that the low operating potential of n-type organic cathodes seems related to sodium chemistry itself. As first underlined by Song *et al* [62], the electrochemical uptake/removal of Na^+ in OEMs is negatively shifted (by several hundreds of mV) in comparison with its lithium counterpart beyond the expected standard potential gap between Na^+/Na and Li^+/Li redox couples. Moreover, the larger radius of Na^+ sometimes induces sluggish electrochemical kinetics as well as lowered utilisation of the available redox-active moieties, giving rise to diminished reversible capacity values. In short, there is currently a lack of efficient and robust sodiated organic cathodes with high working potential.

Figure 8. (a) Key reversible redox-active organic systems at the molecular level, together with representative examples exhibiting redox rocking from the aromatic to the quinoid form. X/Y can be N, O, S, P, π-systems, carboxylate, anhydride, or amide functional groups; and R, R' are potentially integrated within the same cyclic structure. Note that p- and n-type structures correspond to systems A and B, respectively, according to Hünig's classification [56]. (b) Corresponding cell configurations obtained by experimenting with both n- and p-type systems, shown during the discharge process. Reprinted with permission from [52]. Copyright (2020) American Chemical Society.

Advances in science and technology to meet challenges

Efforts must be focused on molecular design to obtain high-potential sodiated cathode materials. This would probably entail the identification of innovative n-type organic functional groups possibly guided by simulation and modelling. Furthermore, potential gain could still be possible by considering electronic effects acting on a redox centre of interest. Thus, the redox potential is classically increased at the molecular level (discrete entities) by introducing electron-withdrawing groups. More recently, it was demonstrated for a lithiated organic cathode that the electronic effects acting on a redox-active organic centre can be very efficiently mitigated in the solid state thanks to structural effects [66]. Alternatively, other OEMs can operate as cathodes thanks to p-type functionality with anionic compensation (figure 8). The latter, which is a redox system rarely encountered in inorganic materials, typically works at a higher potential than n-type redox centres, making these organic systems very appealing for Na-based batteries. For instance, several organic p-type polymer families are known to be stable in organic liquid electrolytes. Poly(2,2,6,6-tetramethylpiperidinyloxy methacrylate) or PTMA represents a relevant example in this field which exhibits bipolar (n/p) electroactivity. From its initial state (centre of the half-reaction at the positive electrode in table 1, entry 5), PTMA can electrochemically accommodate a cation at 2.3 V vs. Na^+/Na (in reduction) or an anion at 3.6 V vs. Na^+/Na (in oxidation) [63]. However, in the case of the closely related poly(2,2,6,6-tetramethylpiperidine-4-yl-1-oxyl vinyl ether) or PTVE, the cation insertion mechanism was shown to be unstable, and steady capacity was obtained with anion insertion alone (table 1, entry 6) [64]. Such p-type functionality gives access to high-potential materials which can be paired with n-type negative OEMs in a dual-ion cell configuration (table 1, entry 7) [65]. P-type OEMs are usually synthesised in their reduced state, making them suitable for a positive electrode without requiring an electrochemical pre-treatment. As monomers, they do not possess permanent negative charges to prevent dissolution in aprotic electrolytes, but polymeric p-type OEMs seem to be the most appropriate choice of positive electrode for Na-based batteries to achieve a combination of high potential and cycling stability. However, as underlined in figure 8(b), the electrolyte is a reservoir of ions for charge compensation within electrode materials which causes a depletion of ionic carriers during operation, requiring a larger volume of electrolyte. Strictly speaking, such a cell configuration cannot be considered to be a NIB, although promising electrochemical data upon cycling have been reported (table 1, entry 7).

Table 1. Selected organic positive electrode materials tested in non-aqueous electrolytes, either in Na half-cell or full-cell configurations. Note that specific capacity values are reported per mass of positive active material, except for entry #4, which is expressed per mass of negative active material. PTCDI: 3,4,9,10-perylenetetracarboxylic diimide; TPA: terephthalic acid; DHTPA: 2,5-dihydroxyterephthalic acid; PTMA: poly(2,2,6,6-tetramethylpiperidine-4-yl-1-oxyl methacrylate); PTVE: poly(2,2,6,6-tetramethylpiperidine-4-yl-1-oxyl vinyl ether); PTPAn: polytriphenylamine; PAQS: poly(anthraquinonyl sulphide); EC/DMC: ethylene carbonate/dimethyl carbonate; DME: 1,2-dimethoxyethane; PC: propylene carbonate; DEGDME: Diethylene glycol dimethyl ether; DEC: diethyl carbonate; DOL: 1,3-dioxolane.

#	Half-reaction at the positive electrode	Half-reaction at the negative electrode	Electrolyte	Output voltage (V)	Specific capacity (mAh g^{-1}), capacity retention, cycles, ref.
1	Poly(ethylene PTCDI)		1 M NaPF$_6$ in EC/DMC (w/w 1:1)	2.2	111, 88%, 5000 [57] /100, 100%, 1000 [58]
2	Poly/PTCDI	Na$_4$TPA	1 M NaPF$_6$ in PC	≈1.6	73, 70%, 20 [59]
3	Na$_4$rhodizonate	Na$_4$TPA	0.6 M NaPF$_6$ in DEGDME	≈1.25	137, 85%, 30 [60]
4	Na$_2$DHTPA	Na$_4$DHTPA	1 M NaClO$_4$ in EC/DMC (v/v 1:1)	≈2.0	204, 76%, 100 [61]
5	PTMA		1 M NaClO$_4$ in EC/DEC (v/v 1:1)	≈3.0	222, 92%, 100 [63]
6	PTVE		1.5 M NaClO$_4$ in EC/DEC (v/v 1:1)	≈3.45	127, 94%, 100 [64]
7	PTPAn	PAQS	Saturated NaPF$_6$ in DOL/DME (v/v 1:1)	≈1.8	180, 85%, 500 [65]

Concluding remarks

Further work is primarily required to develop high-potential and efficient sodiated organic cathode materials beyond p-type materials for NIB technology. A better understanding of the charge/discharge storage mechanisms is also crucial in order to design functional batteries, because each OEM seems to behave differently upon cycling. The use of computational techniques could be very useful in this quest. Organic compounds will not be able to supplement inorganic materials in terms of volumetric energy density, since their densities do not exceed $1.5\,\mathrm{g\,cm^{-3}}$, i.e. four to five times less than inorganic electrode materials. Furthermore, another drawback lies in their tendency to dissolve in liquid organic electrolytes, although the use of solid electrolytes could solve this limitation. Conversely, the implementation of soft organic polymer electrodes enables the fabrication of flexible and thin electrochemical devices which are potentially environmentally friendly. Finally, aqueous organic NIBs can be perceived as the ultimate solution for promoting non-flammable, cost-effective, and green batteries even if only hybrid systems are reported at the moment.

2. Anode materials

2.1. Hard carbon

Heather Au, Hande Alptekin, Maria Crespo Ribadeneyra and Maria-Magdalena Titirici
Department of Chemical Engineering, Imperial College London, London SW7 2AZ, United Kingdom

Status

Hard carbon materials are the most popular choice for NIB anodes. They are produced from oxygen-rich precursors which cannot be converted into graphite, no matter how high the carbonisation temperature. Hard carbons consist of randomly oriented graphitic domains possessing a higher interlayer spacing than graphite (i.e. >0.34 nm) connected by disordered carbon regions with different curvatures. In between these disordered and more ordered domains, hard carbons have 'closed' pores, meaning they cannot be probed by gas sorption. The larger the size of the graphitic crystallites, the larger the pore size in between. In addition to curvatures and edge sites, hard carbons also contain the remaining heteroatoms (mainly oxygenated groups). Such a complex mixture of crystalline and disordered domains with defects allows sodium diffusion pathways and sodium storage sites. The first structure of 'graphitisable' vs. 'non-graphitisable' carbons was described by Rosalind Franklin in a seminal paper entitled 'The interpretation of diffuse x-ray diagrams of carbon' published in Acta Crystallographica in 1950 (figure 9(a)) [67]. Interestingly, until today, the exact structure of hard carbon has remained unknown, as this depends on the precursor and carbonisation conditions, which result in materials with varying interlayer spacing, crystallite size, pore domains and edge termination. Such different structures store Na ions in very different ways. Hence, it is no surprise that there is much debate in the literature about the mechanism of Na insertion into hard carbons. Figure 9(b) provides a typical Na insertion load curve (sodiation curve in a half-cell built with hard carbon vs. metallic Na) showing a typical sloping region between 1 V and 0.1 V and a plateau region below 0.1 V. The first theory by Stevens and Dahn using the 'house of cards' model for hard carbon attributed the slope to Na insertion into expanded graphitic domains, and the plateau to pore filling by Na (figure 10) [68]. Yet the situation is more complex than this, as hard carbons can exhibit different features depending on the choice of precursor, pre-treatment, and carbonisation conditions and temperature.

Current and future challenges

The biggest challenge for hard carbons is to improve their storage capacity to match or even overtake that of graphite in LIBs (>372 mAh g^{-1}). The practical measured capacities for hard carbons today (mostly in coin cells vs. metallic Na) vary from 200 to 450 mAh g^{-1}; most of the values reported in the literature average around 300 mAh g^{-1}. While the theoretical energy density of the commercial graphite used in LIBs can be calculated using the LiC_6 formula, for Na in hard carbons, the situation is far more complicated, due to the heterogenous nature of hard carbons and the unknown storage mechanism, which depend on many structural parameters. Therefore, all the structural and morphological features of hard carbons must be clearly determined using multiple characterisation techniques applied in concert to accurately determine the exact features, such as the interlayer spacing (XRD), defects (Raman, positron annihilation spectroscopy), functional groups (XPS), the nature of ordered vs. disordered domains and the interconnectivity between the two (x-ray pair distribution function), opened vs. closed pores and pore sizes (SAXS, SANS, gas adsorption). All these features must be precisely correlated with the electrochemical performance, which should be accurately determined in half cells, but also using three-electrode configurations [71] to better understand the fundamental electrochemistry happening at the working anode. Finally, *operando* characterisation techniques should be employed to understand the structural and morphological changes occurring during the intercalation of Na ions into hard carbons. Some of these techniques involve the use of XRD/SAXS to determine the change in the interlayer spacing as proof of Na intercalation [68, 72, 73], *operando* XPS [74] to determine the interaction of Na with different functional groups, *in situ* electrochemical TEM to observe the interaction of Na with defects [75], *operando* Raman spectroscopy to understand the changes in graphitic/amorphous structure upon (de)sodiation [76], *operando* NMR [77–79], MRI [80] and EPR [81] to understand the Na chemical state/deposition inside pores at less than 0.1 V. Another major challenge in the development of high-performance hard carbon anodes is to understand the solid–electrolyte interface [82, 83] and how the anode's structural features, in combination with the electrolyte of choice, affect the thickness and, more importantly, the ionic conductivity of the SEI. To probe this, we recommend *operando* AFM [84] as well as electrochemical impedance spectroscopy coupled with quartz crystal microbalance measurements [85], corroborated by electrochemical mass spectroscopy [86] and *operando* FTIR [87]. To understand macroscale phenomena related to the anode volume change, *operando* x-ray computed tomography [88] and electrochemical dilatometry are good options [89, 90]. Once the fundamentals are understood, both in an individual electrode as well as during its operation, these could be used to build
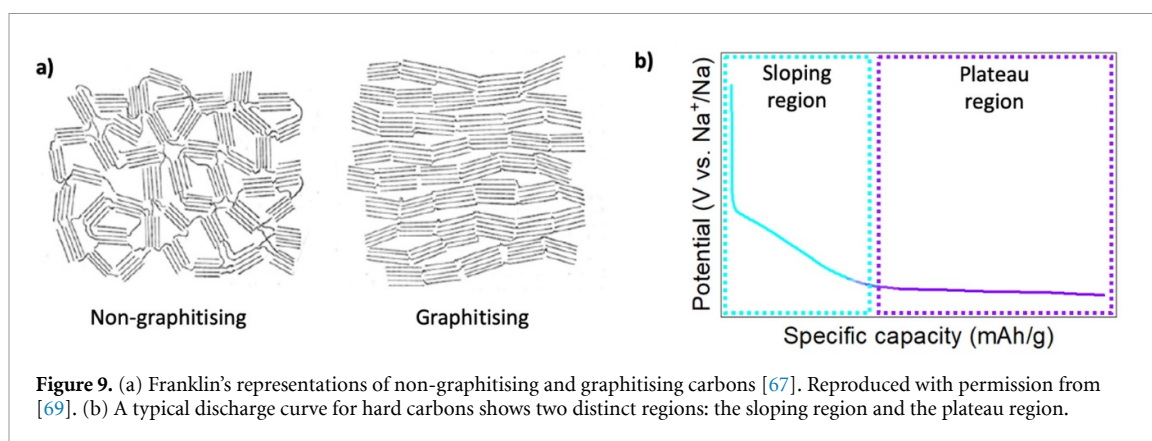
Figure 9. (a) Franklin's representations of non-graphitising and graphitising carbons [67]. Reproduced with permission from [69]. (b) A typical discharge curve for hard carbons shows two distinct regions: the sloping region and the plateau region.
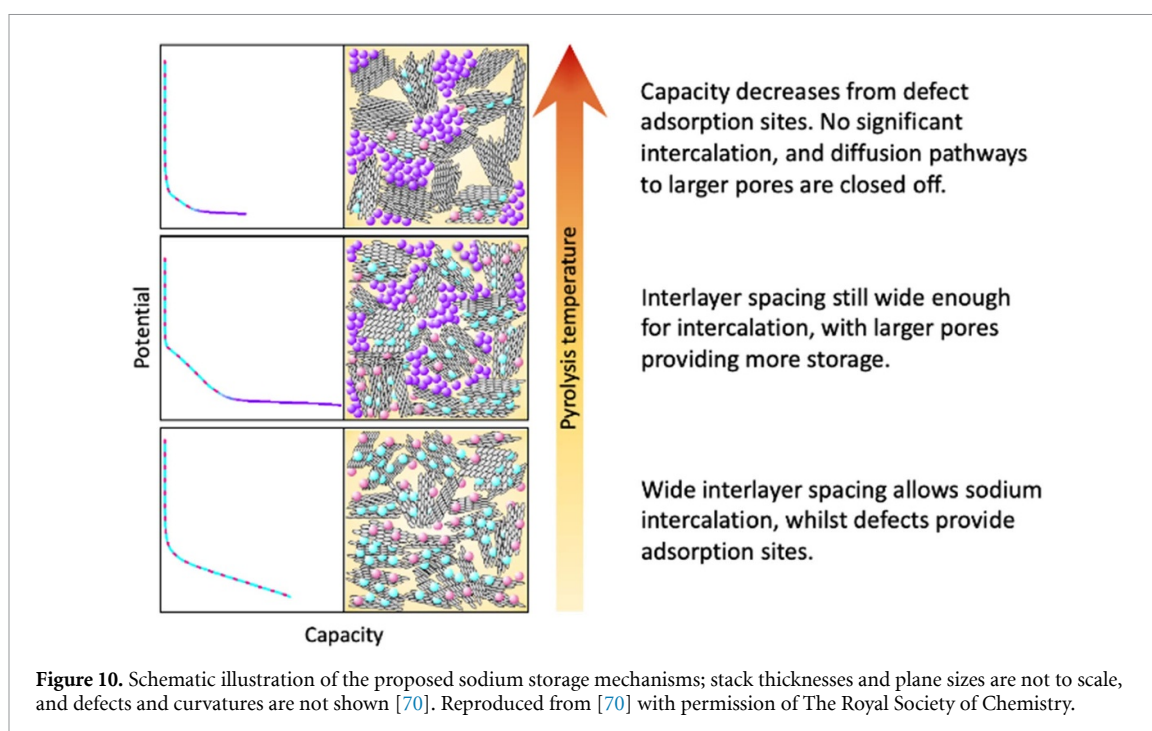

Figure 10. Schematic illustration of the proposed sodium storage mechanisms; stack thicknesses and plane sizes are not to scale, and defects and curvatures are not shown [70]. Reproduced from [70] with permission of The Royal Society of Chemistry.

models for further optimisation based on DFT [91, 92], molecular dynamics (MD) [93], and machine learning [94] to predict the optimal structural and morphological parameters.

Advances in science and technology to meet challenges

Several research groups have made great advances in developing hard carbon anodes with outstanding performance from low-cost precursors, based on a careful synthetic design combined with advanced *ex-situ* and *in situ* characterisation [95]. Most debates to date have arisen from contradictory Na storage mechanisms in such carbons. Currently, there are several published theories: (a) the 'intercalation-filling' model: Na$^+$ ions intercalate into graphitic layers in the sloping region, and insert themselves into nanopores in the plateau region [96]; (b) the adsorption-intercalation model: Na$^+$ ions adsorb at the surface or defect sites of the carbon electrodes within the sloping region and intercalate into the graphitic layers within the plateau region [97]; (c) the adsorption-filling model: in the sloping region, Na$^+$ ions adsorb at the defect sites while filling the nanopores in the plateau region [72], and (d) the 'three-stage' model: defect adsorption of Na$^+$ ions takes place in the sloping region, but in the plateau region, the Na$^+$ ions first intercalate into the graphitic layers and fill the nanopores at the end [98]. More recent investigations by my research team as well as other authors have gathered stronger evidence to propose an alternative model, with adsorption and intercalation occurring simultaneously during the sloping region, and pore filling during the plateau region, all the while keeping in mind the dependence on the structure and pore system of the respective carbons (figure 10). Great progress has been achieved in using *operando* characterisation techniques to probe the mechanisms of different carbon materials; in particular, *operando* NMR has been used to probe the metallic nature of Na in the pores [79, 80], SAXS/WAXS [100, 101] has been used to probe the Na interaction with

defects and the importance of interlayer spacing, and x-ray PDF [102] has been used to understand the connectivity between ordered and disordered domains and the way Na travels throughout the hard carbon from defects and graphitic domains into the pores. Finally, significant machine learning efforts have recently been dedicated to the 'in silico' design of optimised carbons based on experimental characterisation techniques [94]. At a commercial level, the Japanese company Kuraray sells KURANODE™ as a hard carbon for LIBs and NIBs, with good performance, but few structural details. This product is often used as a benchmark by many researchers developing optimisation strategies for NIBs at the cell level, as well as by some of the small and medium enterprises developing NIBs.

Concluding remarks
Much progress has been made in developing hard carbon anodes with outstanding performance for NIBs. Future optimisation could be possible via automation of the synthetic processes using robots coupled with machine learning. Benchmarking of the best-performing hard carbons would be ideal to unify the efforts of NIB developers and standardise protocols at an international level.

Acknowledgment

2.2. Titanium-based oxides

Sara I R Costa[1,3], *Rebecca R Boston*[2,3] *and Nuria Tapia-Ruiz*[1,3]

[1] Department of Chemistry, Lancaster University, Lancaster LA1 4YB, United Kingdom
[2] Department of Materials Science and Engineering, University of Sheffield, Sheffield S1 3JD, United Kingdom
[3] The Faraday Institution, Quad One, Harwell Science and Innovation Campus, OX11 0RA, United Kingdom

Status

Titanium-based oxides are among the most promising and versatile Na anode materials, due to their low cost, ease of processing, and non-toxicity. These materials are safer than carbon-based anodes given their higher operating voltage, which prevents metallic sodium plating. This occurs, however, at the cost of delivering lower energy density. In most cases, the storage of Na^+ ions occurs through a (de)insertion mechanism driven by the Ti^{4+}/Ti^{3+} redox couple. The most representative oxides include TiO_2, $Li_4Ti_5O_{12}$, $Na_2Ti_6O_{13}$, and $Na_2Ti_3O_7$, which will be briefly described herein.

TiO_2-based anodes are a promising avenue of research, due to their high structural stability and theoretical capacity (335 mAh g^{-1}). Microsized TiO_2 is inactive in NIBs; however, reducing the particle size to the nanoscale activates reversibility, achieving practical capacities of ca. 155 mAh g^{-1} [103]. The various TiO_2 polymorphs exhibit different electrochemical performances, with anatase (crystalline and amorphous) generally being the favoured form [104]. $Li_4Ti_5O_{12}$ (Fd-3m) has been widely studied as an anode in LIBs due to its zero-strain behaviour [105]. In NIBs, it delivers a reversible capacity of 155 mAh g^{-1} by inserting three Na^+ ions into the structure at a relatively low potential (0.9 V) [106]. Among the Na–Ti–O ternary compounds, $Na_2Ti_6O_{13}$ (*C2/m*) shows high Na^+ ion diffusion due to its tunnel structure and small volume change (<1%) upon Na^+ ion (de)insertion. However, it displays an impractical storage capacity of 49.5 mAh g^{-1} [107]. Control of the morphology, particle size, and exposed crystal facets has significantly increased the capacity to 109 mAh g^{-1} (at a rate of 1 A g^{-1}) after 2800 cycles [108]. On the other hand, $Na_2Ti_3O_7$ (*P2$_1$/m*) has been widely investigated in recent years due to its low working potential (0.3 V); it delivers the highest energy density among this family of compounds (figure 11). $Na_2Ti_3O_7$ exhibits a specific capacity of 177 mAh g^{-1} through the reversible insertion of two Na^+ ions per formula unit [109].
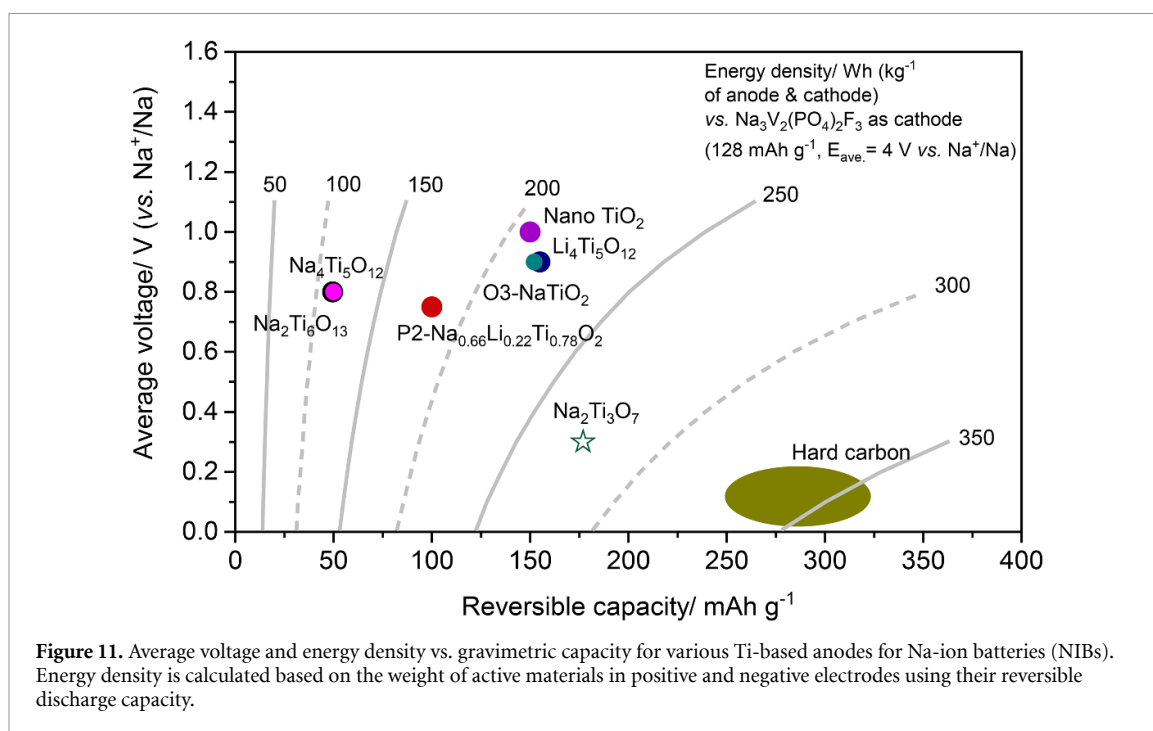
Current challenges to be overcome before this compound can be used in practical applications include poor electronic conductivity and sluggish Na^+ ion (de)insertion kinetics. These will be described in detail below. Recent advances in this area include the discovery of a new $Na_2Ti_3O_7$ triclinic phase (P-1) with a similar working potential to the monoclinic phase, but with an outstanding capacity retention of 94.7% (after 20 cycles at 20 mA g^{-1}) [110], and the development of $Na_2Ti_3O_7/Na_2Ti_6O_{13}$ hybrids, which combine the higher storage capacity and ionic conductivity of their respective phases, resulting in excellent cycling stability and superior rate performance [111].

Current and future challenges

The main factors limiting the commercialisation of $Na_2Ti_3O_7$ (NTO) in NIBs are the low electronic conductivity and sluggish Na^+ ion (de)intercalation kinetics, which result in poor rate performance and cycling stability.

The presence of Ti^{4+} ions (d^0) makes NTO an electrical insulator (bandgap energy ≈ 3.7 eV) [112], which hampers Na^+ ion diffusion within the crystal structure (D_{Na}^+ in NTO is ≈ 2–3 orders of magnitude lower than that in hard carbon). Thus, a major area of research encompasses the development of strategies to enhance long-term cycling stability, particularly at high current densities. These mainly involve: (a) bulk and surface structural control through doping and the introduction of defects; (b) nanostructuring; and (c) composite fabrication with carbon allotropes. Furthermore, the formation of an SEI layer on the surface of the electrode and the consumption of Na^+ ions by carbon additives below 1 V result in low initial coulombic efficiency (ICE) (40%–60%). These phenomena are particularly critical in full cells, where there is limited sodium available. Methodologies are therefore required to mitigate the initial capacity irreversibility, although, to date, such procedures are underdeveloped. Additionally, the high reactivity of Na metal when used in half cells contributes to the underperformance of NTO due to the formation of an unstable SEI layer, requiring the use of three-electrode cells and full cells to gain a better insight into the Na contribution to the overall performance.

Few studies have demonstrated the complex nature of the SEI composition. For example, Casas-Cabanas *et al* reported the formation of various SEI inorganic and organic species, such as Na_2CO_3, alkyl carbonates and PEO during discharge when using 1 M $NaClO_4$ in an EC:PC electrolyte [113]. Moreover, NaCl and NaF products have been observed before cycling, as a result of the decomposition of the $NaClO_4$ inorganic electrolyte salt and the Polyvinylidene fluoride (PVDF) binder, respectively. Alternative inorganic salts, such

Figure 11. Average voltage and energy density vs. gravimetric capacity for various Ti-based anodes for Na-ion batteries (NIBs). Energy density is calculated based on the weight of active materials in positive and negative electrodes using their reversible discharge capacity.

as $NaBF_4$ or NaFSI and binders, such as sodium alginate or sodium carboxymethylcellulose have shown superior cycling stability, although their performance still lags behind those of their Li analogues [114].

Therefore, the development of next-generation electrolytes and binders is crucial to further improve battery efficiency. Another issue is the structural relaxation of the fully sodiated phase ($Na_4Ti_3O_7$), attributed to the large electrostatic repulsion in the crystal structure [115]. This phenomenon may lead to self-discharge in full cells containing NTO, compromising cycling stability.
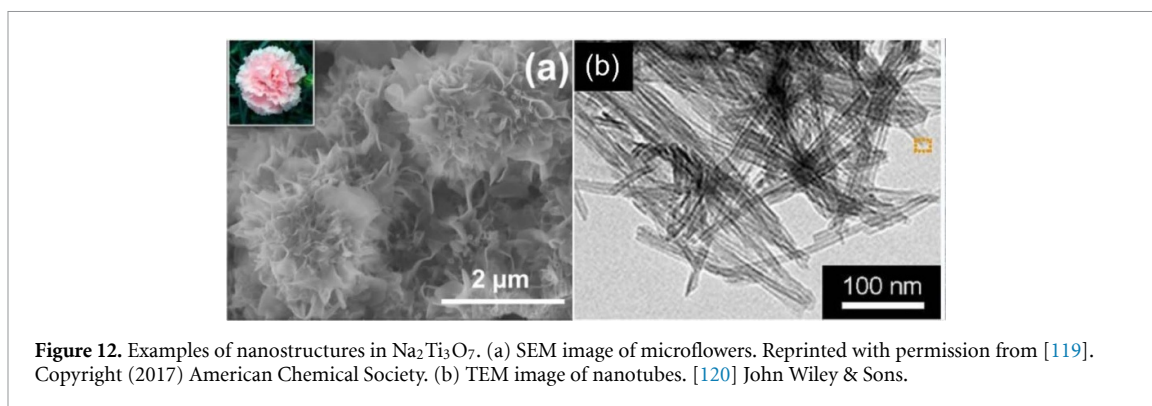
Advances in science and technology to meet challenges

To address the poor electronic conductivity and high Na^+ ion migration barriers in NTO, different approaches, including bulk and surface (micro)structure design and carbon composite fabrication have been considered.

Elemental doping using small concentrations (<5 at.%) of Nb [116] and elements from the lanthanide series (e.g. Yb) [117] has been shown to decrease the bandgap energy, enabling superior high-rate performance in NTO. For example, Nb-doped NTO demonstrated a 0.3 eV reduction in bandgap energy with respect to pristine NTO [116]. The enhanced electrochemical performance was attributed to doping-induced crystal structure distortions, together with the formation of Ti^{3+} ions. Furthermore, oxygen vacancies, which act as n-type defects, were claimed to contribute to the higher electrical conductivity observed in Yb-doped NTO [117]. Similarly, surface treatments involving the direct or indirect use of hydrogen have been used to create oxygen vacancies, conferring high capacities at fast rates [118].

Besides changes in the crystal structure, nanostructuring strategies have been extensively developed, showing an improved electrochemical performance through more efficient Na^+ ion (de)intercalation, exploiting larger surface areas which can be further enhanced by creating continuous networks of material to improve electronic conductivity. For instance, Anwer *et al* used solvothermal synthesis to create 3D networks of 2D NTO nanosheets [119], generating *microflowers* (figure 12(a)) with a stable capacity of 108 mAh g^{-1} (200 mA g^{-1}) over 1000 cycles, while NTO nanotubes 10–20 nm in diameter (figure 12(b)) have shown a high stable capacity of 100 mAh g^{-1} [120] (100 mA g^{-1}) over 2000 cycles. Moreover, the use of carbon coatings [115] and carbon composite mixtures [121] is a common strategy to improve the electronic conductivity and pseudocapacitive contribution during Na^+ ion storage. For instance, nanosheet-coated carbon shell particles delivered a capacity of 110 mAh g^{-1} (885 mA g^{-1}) over 1000 cycles [122].

Finally, understanding the impact of electrolyte composition on interfacial electrochemistry is crucial for developing approaches to further prolong the cycle life of NIBs. Although this area is still in its infancy, preliminary work has been developed to mitigate SEI film instability by improving electrolyte formulations (e.g., by the incorporation of fluoroethylene carbonate (FEC) additives) and through surface engineering, among others.

Figure 12. Examples of nanostructures in $Na_2Ti_3O_7$. (a) SEM image of microflowers. Reprinted with permission from [119]. Copyright (2017) American Chemical Society. (b) TEM image of nanotubes. [120] John Wiley & Sons.

Concluding remarks

Titanium-based oxides represent a very exciting class of anode materials due to their safety, stability, low-cost, non-toxicity, and ease of processing. While progress has been made in terms of understanding the factors limiting the rate performance and cycling stability, much work is still required to realise these concepts in terms of delivering high energy and power densities in NIBs. We anticipate that the greatest advances will arise from further enhancements in electronic conductivity (by combining several of the strategies described here) and further exploration within this family of compounds, including composites. Designing more stable anode/electrolyte interfaces will also be crucial to advance this area of research. This will require a better fundamental understanding of the physicochemical properties at the interface, the behaviour and stability of the fully sodiated phase, and the driving factors behind the poor initial coulombic efficiency.

Acknowledgments

2.3. Alloy and conversion materials

Lorenzo Stievano[1,2], Moulay Tahar Sougrati[1,2] and Laure Monconduit[1,2]
[1] ICGM, Univ. Montpellier, CNRS, Montpellier, France
[2] RS2E, CNRS, Amiens, France

Status

The development of alloy and conversion negative electrode materials for NIBs (which characteristics are resumed in figure 13) represent a substantial fraction of the work carried out to develop a suitable anode for application in commercial systems. While, on the one hand, the high reactivity of sodium and its low melting point (98 °C), as well as the formation of dendrites during its electrodeposition, make it significantly less safe than Li, on the other hand, in contrast to the case of LIBs, graphite does not intercalate Na$^+$ in conventional electrolytes, and thus alternative anodes have to be found.

Several families of materials capable of reacting electrochemically with sodium have been studied and can be classified, as for LIBs, according to their reaction mechanism, as either insertion, alloy, or conversion materials [123]. However, the mechanism and performance of such materials in NIBs cannot be directly extrapolated from those observed in LIBs.

The alloying reaction is usually observed with *p*-block elements (Ge, Sn, Pb, P, Sb, Bi, etc) and some transition metals (e.g., Ag, Zn and Au) which form stable alloys with Na [124]. Alloy materials (AM) usually involve a multiple-electron exchange, thus leading to very high capacities. However, the formation of the sodiated alloy causes a strong expansion of volume, even worse than that of LIBs, which represents a real limitation on their application. The most interesting AMs are surely phosphorus and antimony, which lead to the formation of Na$_3$P (2596 mAh g^{-1}) and Na$_3$Sb (660 mAh g^{-1}), respectively. Interestingly, silicon, while very promising in LIBs, is practically inactive in NIBs. While phosphorus delivers a very high theoretical capacity, antimony has shown the greatest affinity for sodium [125].

The family of conversion materials (CM) mainly includes metal oxides and sulphides, even though other families, such as metal selenides, carbodiimides, halides, and phosphides have been explored [126], all of which underwent the so-called conversion reaction [127] with Na. CMs can deliver high specific and gravimetric capacities with excellent cycling stability, but they also face at least one critical issue related to their low initial coulombic efficiency or high volume expansion.

The study of the electrochemical and aging mechanisms in both AMs and CMs has been rather challenging, given that multi-phase systems are often obtained during cycling, and many of the species formed are amorphous, nanosized, and especially metastable. The development of specific *operando* tools is therefore mandatory for the study of these materials [128, 129].

Current and future challenges

The main challenges for AMs and CMs in NIBs are related to volume expansion and both the ionic and electronic conductivities of these materials. The large reversible volume exchange during charge/discharge cycles produces mechanical stress, which, on the one hand, rapidly leads to the electrochemical pulverisation of the electrode material, and, on the other hand, exposes new portions of the metal surface to the electrolyte at each cycle, leading to continuous electrolyte degradation and thus difficult stabilisation of the SEI. Moreover, in some cases, such as that of phosphorus, the active material is intrinsically insulating, hindering electronic percolation in the electrode. Control of these phenomena is necessary for practical applications, and several strategies have been proposed to reduce the consequences of drastic volume changes and to boost electronic conduction.

The simplest approach is to optimise the electrode formulation using conducting additives, electrolytes, and binders. In the case of phosphorus, for instance, the addition of 1D (carbon nanotubes) or 2D (graphene) nanomaterials to the electrode formulation has been shown to improve the conductivity of C/P composites, leading to an outstanding capacity retention of 80% over 2000 cycles [130], despite noticeably impacting capacity and energy performance. Nanostructuring is also a common approach to accommodate the stress and strain in AMs and CMs without pulverising the electrode, and to improve the ionic and electronic transport pathways. For instance, tin particles smaller than 10 nm allow a decrease in the strain, effectively mitigate pulverisation, and also limit their aggregation during cycling. Such nanoparticles, homogeneously embedded in a carbon matrix, deliver a stable capacity of 415 mAh g^{-1} after 500 cycles at 1 A g^{-1} [131]. Even tuning the morphology and porosity of the materials may allow an improvement in the performance. An interesting way to do so is to transform bulk materials into 2D materials which can buffer volume expansion during alkali insertion [132]. For instance, phosphorene synthesised by exfoliating phosphorus shows a rapid charge transfer between less-conductive phosphorene interlayers. In the same spirit, layered graphene/phosphorene electrodes achieved a reversible capacity of 2440 mAh g^{-1} (per gram of P) over 100 cycles [133].
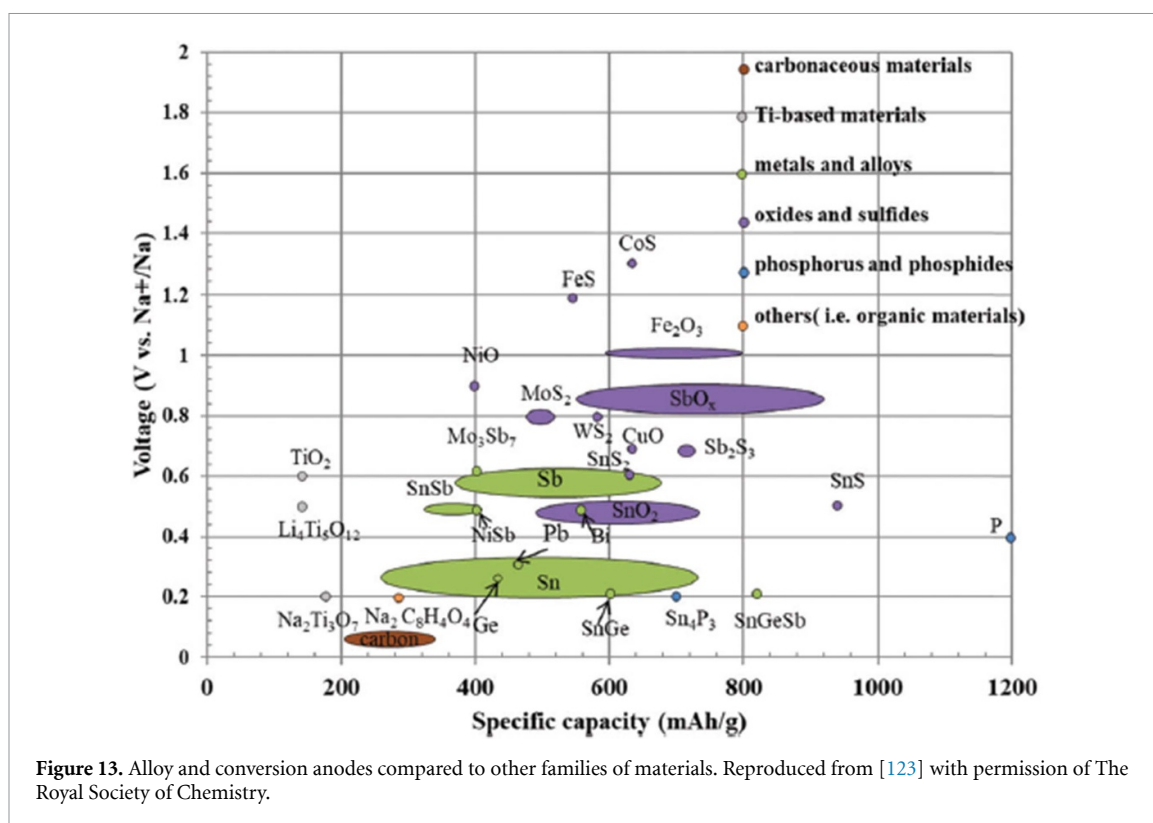
Figure 13. Alloy and conversion anodes compared to other families of materials. Reproduced from [123] with permission of The Royal Society of Chemistry.

Advances in science and technology to meet challenges

As described above, the main challenge for AMs and CMs is related to volume expansion, which results in the continuous pulverisation of electrode materials and leads to a steep deterioration in electrochemical performance. The consequences of the large volume expansion are worsened by continuous electrolyte reduction, which affects both the coulombic efficiency and the cycle life.

The different strategies presented in the previous section have led to great progress in electrochemical performance in terms of cycle life, even though a substantial decrease in volumetric energy density cannot be avoided, especially when composites with inactive materials are prepared. Moreover, if in the early papers, the effective behaviour of the presented materials was mainly tested in half-cells vs. Na metal, the more recent study of these materials in realistic full cells against a real cathode material has increased, and is now rather common (for CM, see [132]). These studies are necessary to correctly evaluate the viability of these materials, which still cause non-negligible electrolyte decomposition and irreversible sodium trapping, and thus, low coulombic efficiencies in both the first and the following cycles.

When compared with other types of anode material, up until now, the performance of AMs and CMs has not beaten that of hard carbon. This is partially due to the large amount of cathode excess required to compensate for the large initial irreversible capacity and the low coulombic efficiency in cycling. Therefore, one can conclude that the primary challenge for AMs and CMs has still to be solved [134].

Up until now, hard carbon has remained the most relevant candidate, even though its cost is significantly higher than that of graphite; in fact, the cost of graphite ranges between 500 and 2000 \$/ton, which is similar to the cost of some of the common precursors of hard carbon (e.g. cellulose or sucrose). Among AMs, antimony is probably the most promising material, since it possesses a large gravimetric charge storage capacity (660 mAh g^{-1}) associated with an excellent rate capability and cycle life. Such excellent performance, exceeding that of Sb in LIBs, should give it good prospects when used in composites with hard carbon. Indeed, a good compromise between energy and lifetime cost can, in principle, be attained for such composites.

Concluding remarks

Many studies of many AMs and CMs in NIBs have shown that most of them form Na-rich phases, and thus produce high specific capacities and energy densities. While volume expansion is often invoked as a possible limitation of the life span of such electrodes, several studies have shown impressively long cyclabilities, especially for antimony-based systems. Their durability lies in the elastic softening of the sodiated antimony phases, which enhances the ability of the electrode to absorb and mitigate the strong volume changes upon

(de)sodiation [135]. The development of composites of antimony with hard carbon seems, therefore, a viable alternative. Even though such composites might still not allow NIBs to reach the performance of current LIBs, their application is still suited to applications where the energy performance is not critical, such as in stationary energy storage.

2.4. 2D transition-metal dichalcogenides

Jincheng Tong[1,2], *Zhuangnan Li*[1,2] *and Manish Chhowalla*[1,2]
[1] Department of Materials Science and Metallurgy, University of Cambridge, Cambridge CB3 0FS, United Kingdom
[2] The Faraday Institution, Quad One, Harwell Science and Innovation Campus, Didcot OX11 0RA, United Kingdom

Status

The relatively large radius and heavy mass of sodium ions require NIB anode materials with large interlayer spacings. The large volume expansion and pulverisation of some anode materials during cycling also pose significant challenges for the development of high-performance NIB anodes. The rational stacking of various 2D nanosheets could allow electrode designs that would be mechanically stable over a large number of cycles.
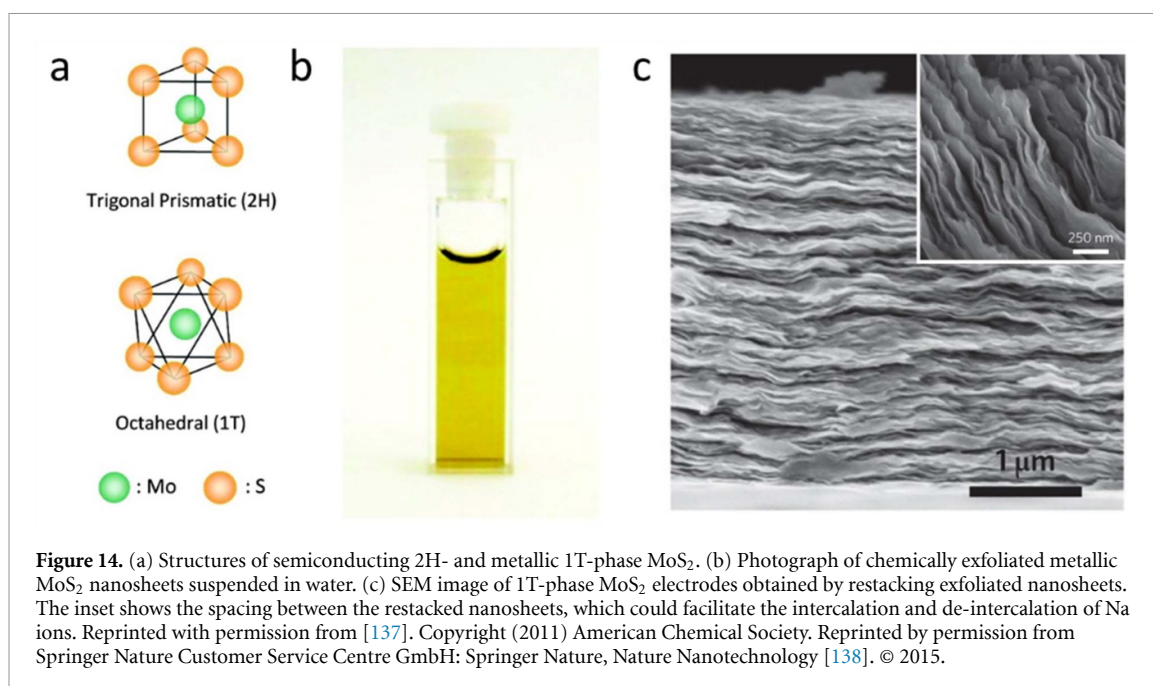
2D materials possess attributes that may help to address these challenges. In particular, metallic 2D materials with high conductivity may improve the reaction efficiency, and weak van der Waals bonding between planar layers may allow the fast diffusion of Na^+. Furthermore, the interlayer spacing between nanosheets can increase the contact area with the electrolyte and shorten the Na^+ diffusion length. Electrodes fabricated by the restacking of exfoliated 2D nanosheets are mechanically flexible and can accommodate large expansions in volume [136]. Among such electrodes, the metallic phases of 2D transition-metal dichalcogenides (TMDs) MX_2 (M = Mo, W, Ti *et al*; X = S, Se, Te) such as molybdenum disulphide (MoS_2) [137, 138] provide large channels (6.15 Å) for Na^+ intercalation and possess a high theoretical capacity of 670 mAh g^{-1}, which makes them promising for use in NIB anodes [139]. The unit cells of the semiconducting 2H phase and the metallic 1T phase of MoS_2, along with an image of a uniform solution of chemically exfoliated nanosheets are shown in figures 14(a) and (b). A cross-sectional scanning electron microscope (SEM) image of the restacked 1T phase MoS_2 nanosheets is shown in figure 14(c). Individual nanosheets can be seen, with intercalation sites between them.

Current and future challenges

2D TMDs are promising anode materials for Na-ion batteries, but several challenges hinder their performance. One challenge is the lack of understanding of the charge-storage mechanism. Broadly speaking, TMD-based NIB anodes work via the intercalation/extraction of sodium ions in the layered structure. Unlike storage mechanisms in conventional 2D materials (graphene, MXenes), a phase transition occurs in TMD-based electrodes, accompanied by electrochemical intercalation of sodium ions into the structure [140]. For example, in MoS_2 anodes, the intercalation of ions leads to a transformation from the semiconducting 2H phase to the metallic 1T phase [141]. This transition from 2H-MoS_2 to 1T-MoS_2 involves a slippage of the intralayer atomic planes, and thus largely influences the intrinsic properties of the material, as well as its electrochemical performance. A series of other structural features in MoS_2—such as lattice distortion, structural modulation, and irreversible decomposition—are also observed during sodium ion intercalation. Furthermore, information regarding the formation of the SEI layer on the MoS_2 anode is not well elucidated. Therefore, a better understanding of the working mechanism and intercalation chemistry of MX_2 compounds is required for better NIB design.

Advances in science and technology to meet NIB anode challenges

In-situ/operando characterisation techniques are being developed to understand the mechanisms at work in these materials and improve their electrochemical performance. *In-situ* atomic force microscopy (AFM) using a microcell has been used to study the evolution of structural changes and formation of an SEI on MoS_2. It was observed that mechanically exfoliated MoS_2 wrinkles upon sodiation at 0.4 V, and that the SEI layer forms quickly, before the intercalation of sodium ions. This measurement also showed that the SEI layer thickness on the MoS_2 electrode is ≈20.4 nm ± 10.9 nm [142]. In addition, aberration-corrected scanning transmission electron microscopy (STEM) was used together with *in-situ* x-ray diffraction (XRD) to track the phase transition in MoS_2 [141]. It has been demonstrated that in Na_xMoS_2, x = 1.5 is a critical point for reversible structural evolution. This critical point indicates that the structure of MoS_2 can be partially recovered if the concentration of intercalated sodium ions is less than 1.5 per formula unit of MoS_2. However, its structure cannot be restored once it is decomposed into Na_xS and metallic Mo. *In-situ* spectroscopy has been used to study the growth of Na dendrites and SEI formation on TMD-based anodes. Synchrotron-based soft XAS has been used to investigate discharge products by probing states near the Fermi level [143]. XAS has also been used to reveal the the local electronic and chemical structure of surfaces and interfaces. These types of analysis could be extended to 2D TMD electrodes to study local changes in their atomic and electronic structures during charging and discharging. Similarly, the Rutherford backscattering

Figure 14. (a) Structures of semiconducting 2H- and metallic 1T-phase MoS_2. (b) Photograph of chemically exfoliated metallic MoS_2 nanosheets suspended in water. (c) SEM image of 1T-phase MoS_2 electrodes obtained by restacking exfoliated nanosheets. The inset shows the spacing between the restacked nanosheets, which could facilitate the intercalation and de-intercalation of Na ions. Reprinted with permission from [137]. Copyright (2011) American Chemical Society. Reprinted by permission from Springer Nature Customer Service Centre GmbH: Springer Nature, Nature Nanotechnology [138]. © 2015.

spectrometry (RBS) technique can be employed to determine the composition and thickness of the SEI that forms on anodes during electrochemical cycling [143].

Concluding remarks

In summary, the field of 2D TMDs is in a nascent phase. While 2D TMDs are interesting, several key challenges remain. Furthermore, much of the work on Na-ion batteries has been done on the semiconducting 2H phase of TMDs. This phase is hydrophobic and lacks conductivity, resulting in sluggish ionic diffusion. In contrast, the metastable metallic phase of TMDs has been less studied. The exfoliation of metallic TMDs and the restacking of 2D nanosheets into electrodes are likely to provide electrodes with better intercalation efficiency and faster kinetics.

Acknowledgment

2.5. Organic materials

Aamod V Desai[1,2], *Russell E Morris*[1,2,3] *and A Robert Armstrong*[1,2]
[1] EastChem School of Chemistry, University of St. Andrews, KY16 9ST, United Kingdom
[2] The Faraday Institution, Quad One, Harwell Science and Innovation Campus, OX11 0RA, United Kingdom
[3] Department of Physical and Macromolecular Chemistry, Charles University, Hlavova 8, Prague 128 43, Czech Republic
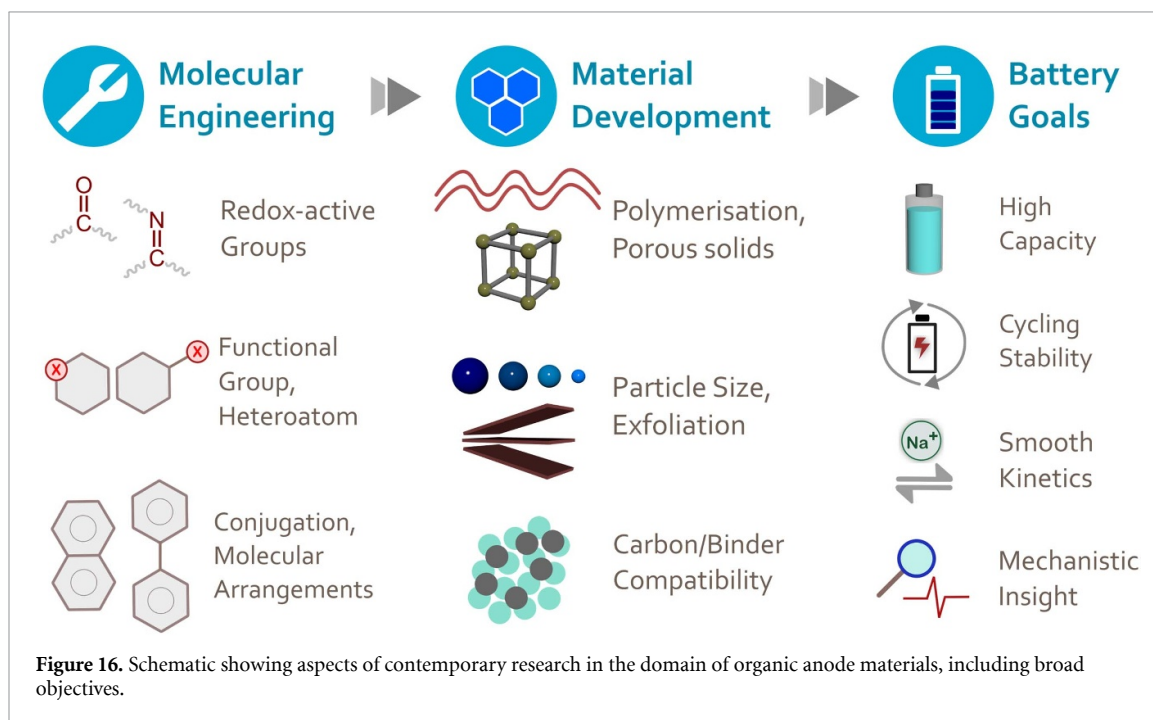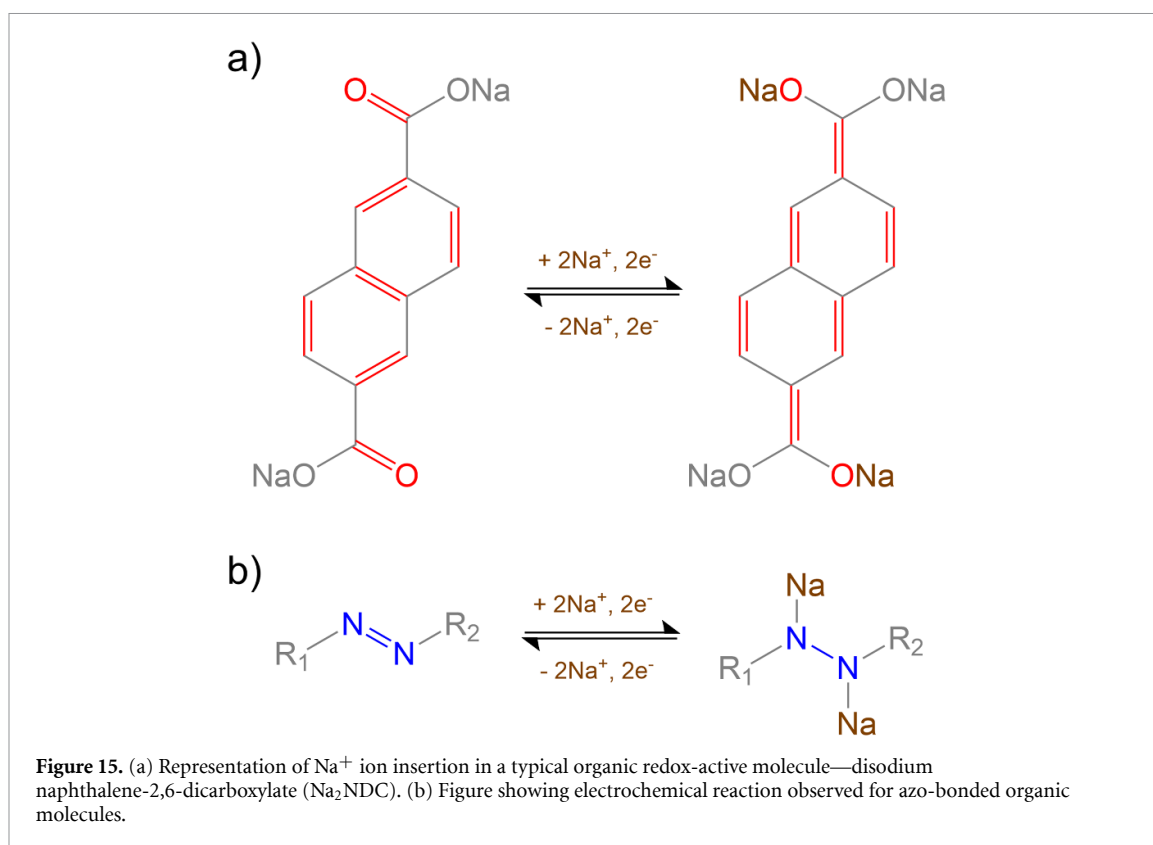
Status

OEMs currently lie at the periphery of rechargeable battery technology. However, with the increased emphasis on sustainability, electrochemically active organic molecules, which, in principle, can be derived from biomass or recycled from commercial waste, are the subject of increased interest [144]. Although the suitability of organic polymers as electrodes for alkaline metal-ion batteries was reported in the early years of secondary battery development, it is only during the last decade that research in this area has witnessed a resurgence, with the successful application of small redox-active organic molecules for reversible ion insertion in LIBs and subsequently NIBs, for example, disodium terephthalate ($Na_2C_8O_4H_4$) and its analogues [145]. This recent progress has coincided with the growing applications of small organic molecules in the preparation of several classes of solid-state materials. The features of structural diversity and the ability to modulate their electronic properties on demand, make organic systems attractive candidates to explore for battery applications.

Redox reactions in these materials typically involve molecules that have an initial neutral electronic state, but then acquire a net charge [146]. This is either accompanied by the rearrangement of π-bonds in the backbone, or other mechanisms that stabilise the redox state. Moieties such as carboxylates are well suited for anodes, on account of their low-voltage redox reaction (figure 15(a)) [147]. Since bare organic molecules have high solubility in polar solvents, usually, such active molecules are considered for use in coordination compounds, which are relatively stable solid-state materials. Organic chemistry permits the tailoring of the the local molecular environment to alter electrochemical features, such as the working voltage of the material and the density of active sites. Also, over the last few years, new redox chemistries and active moieties, such as azo (figure 15(b)) and imine have been identified and tested for charge storage at lower voltages. Although their working principle is similar to that of carboxylates, these groups are usually the central part of the molecule, unlike carboxylates, which tend to be terminal groups. Apart from these well-studied mechanisms, a few organic systems have shown reversible ion insertion using different pathways [147]. In addition to the goal of practical implementation, there is an interest in developing a fundamental understanding of the unexplored active groups.

Current and future challenges

Organic anode materials have considerable room for improvement, in terms of bothelectrochemical properties and material development (figure 16). Organic molecules show redox activity at specific active sites, which leaves a significant portion of the molecule unused. This directly contributes to lower theoretical capacities. An important aspect of the study of these materials is the improvement of cycling stability. The use of organic electrolytes in non-aqueous batteries leads to the formation of inactive side products or the solubility of small, active organic molecules for long-term cycling. The formation of a solid–electrolyte interphase (SEI) gives notably low coulombic efficiencies for the initial cycles, which is particularly relevant for practical applications [148]. Another feature of OEMs is their low density, resulting in significantly lower volumetric energy density. However, making their structures compact may result in an increase of volume expansion during (de)insertion of bulkier species, such as Na^+ ions. Most organic materials have poor electronic conductivity, requiring significant amounts of conductive carbon either as physical mixtures or as composites with the active solid, which directly adds to the non-contributing weight of the electrode. Although there is immense scope to modulate structural features, the carbonyl and imine groups only accommodate one Na^+ ion per site, and the stabilisation of the redox state requires a conjugated backbone (figure 15(a)). On the other hand, azo bonds can insert two Na^+ ions (figure 15(b)), but their working potential is seen to be much higher, which reduces the overall energy density of the battery.

Apart from electrochemical performance, an in-depth understanding of the activity and the factors that influence that activity are yet to be fully realised. These are crucial to meet the upcoming targets for the applications of rechargeable batteries. In this context, the production costs and scalability of this class of materials also have room for more research. In addition, the thermal and chemical stability of organic molecules is limited and requires more development to support practical implementation.

Figure 15. (a) Representation of Na$^+$ ion insertion in a typical organic redox-active molecule—disodium naphthalene-2,6-dicarboxylate (Na$_2$NDC). (b) Figure showing electrochemical reaction observed for azo-bonded organic molecules.

Figure 16. Schematic showing aspects of contemporary research in the domain of organic anode materials, including broad objectives.

Advances in science and technology to meet challenges

A major theme of research in this area has been to leverage the versatility of organic chemistry for molecular engineering and examine new molecules by varying their atomic or structural properties (figure 16). Among various molecules, carboxylates bonded to aromatic systems are the most popular moieties. Strategies to extend π-conjugation or vary the secondary functional groups have shown the potential to both improve cycling performance and stabilise redox states. In certain cases, upon careful design, the extended π-conjugation has participated in the electrochemical reaction, leading to the insertion of excess charges [149]. The role of secondary functional groups is to modulate the electronic properties of the molecule and provide additional interaction sites for Na$^+$ ions. It is observed that in structurally similar molecules,

electron donor groups lower the working voltages, while electron-withdrawing groups tend to increase the redox potentials [150]. Heteroatom (N-atom) substitution in the backbone has resulted in higher capacities and smoother kinetics by virtue of favourable interactions with Na^+ ions. In systems with sulphur (S) atoms, the capacity is seen to increase on account of the additional interaction sites, and the electronic conduction is also improved [151]. Apart from molecular features, bulk properties are known to affect the cycling performance of electrode materials. The morphology and particle size of the active organic material are seen to play significant roles in the practical capacities and kinetics of ion insertion [152].

Although atomic features lead to the modulation of electrochemical properties, even the conventionally studied molecules still show issues of cycling stability and volume expansion. In recent years, various porous materials displaying long-range order based on redox-active small organic molecules have been tested with the aim of circumventing the issues of solubility and stability. These include metal–organic frameworks (MOFs) and covalent organic frameworks (COFs), which are seen to be stable to cycling and can accommodate bulky Na^+ ions [153]. However, research into porous materials has largely been confined to the preparation of electrochemically active hierarchical carbonaceous matter; and very few examples have used the pristine materials.

Concluding remarks

Organic battery materials are likely to contribute significantly to the pursuit of sustainable technologies. As anodes in NIBs, small organic molecules with redox-active groups such as carboxylate, azo, and imine have shown much promise. Several aspects of these compounds, such as their cycling stability, volumetric densities, and poor electronic conductivity, require more research to compete with benchmark materials. Much progress is anticipated through the incorporation of the knowledge gained and the extensive testing of novel solid-state materials based on the use of organic molecules as battery electrodes. The rich diversity of organic chemistry presents an opportunity to explore untapped redox-active groups and expand our understanding of molecular engineering to support the delivery of high-performance materials. In addition to fundamental objectives, practical parameters such as scalability and production costs also need to be addressed.

3. Computational discovery of materials

Yong-Seok Choi[1,2,3] *and David O Scanlon*[1,2,3,4]

[1] Department of Chemistry, University College London, 20 Gordon Street, London WC1H 0AJ, United Kingdom
[2] Thomas Young Centre, University College London, Gower Street, London WC1E 6BT, United Kingdom
[3] The Faraday Institution, Harwell Campus, Didcot OX11 0RA, United Kingdom
[4] Diamond Light Source Ltd, Diamond House, Harwell Science and Innovation Campus, Didcot, Oxfordshire OX11 0DE, United Kingdom

Status

In the last two decades, advances in supercomputing architectures and the development of more accurate and cost-effective quantum chemistry approaches have enabled the computational exploration of new materials to take place in a more rapid and rigorous manner. DFT calculations have emerged as a key component in the computational discovery of materials. To accelerate the discovery of materials in such a vast chemical compositional space, numerous DFT-based approaches have been reported and can be classified into three types [154]: (a) chemical substitution, (b) crystal-structure prediction, and (c) data mining.

Most new materials have been discovered by chemical substitution, i.e., a simple element replacement in known structural prototypes. This is particularly effective for Na-ion battery (NIB) materials, as these materials share similar atomic structures with their LIB counterparts. Representative examples include layered oxide cathodes of Na_xTMO_2 (TM = transition metals) and solid electrolytes of $Na_{10}MP_2S_{12}$ (M = Si, Ge, Sn). In contrast, crystal-structure prediction, e.g., random structure prediction and evolutionary algorithms, begin with random atomic configurations within sensible constraints on bond lengths, followed by local optimisations that find the lowest-energy structures. In general, evolutionary algorithms should offer better efficiency, as they improve candidate guesses over time by comparing the lowest-energy solutions found at every iteration. These two methods have proven to be effective in predicting the intermediate phases of alloying electrodes of NIBs, such as Sn and Sb [155].

Data mining has now emerged as a promising method for facilitating materials discovery, as it can establish criteria for new material formations and construct quantitative structure–property relationships for predicting their properties. In conjunction with high-throughput algorithms, this approach has recently been applied to predict new potential cathodes and solid electrolytes for NIBs [156]. However, due to the high dimensionality of the problem and the relatively small number of known battery materials in databases, the predictive ability of the results obtained remains controversial. Continuous research effort has been devoted to improving the accuracy of models [156]. All the structure-prediction methods mentioned above can be supported by various open-source structure-prediction tools (figure 17).

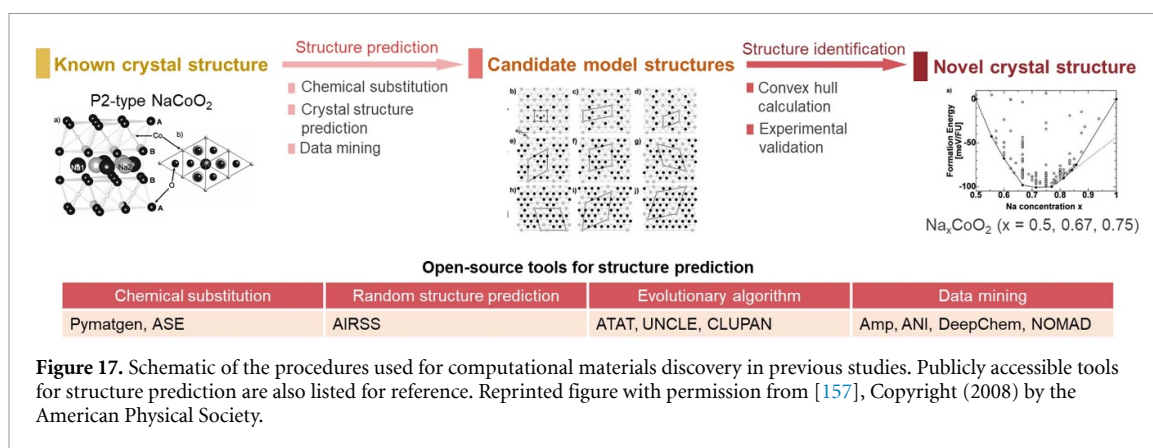### Current and future challenges

While various structure-prediction methods exist, the exploration of NIB materials has mostly been limited to structures with existing prototypes reported in LIBs. This is because of the difficulties involved in predicting previously unknown structures, which is especially tough for NIB materials that have characteristic features, including:

Large elemental phase space
The exploration of potential NIB materials often faces increased complexity necessitated by the large number of elemental combinations, which are sometimes even more numerous than their LIB counterparts. For instance, Na_xTMO_2 can feature a plethora of redox-active transition metals (TMs) (Ti, V, Cr, Mn, Fe, Co, Ni, and Cu) compared to Li_xTMO_2 where only Co-, Ni-, and Mn-redox are available [158]. Furthermore, continuous efforts to optimise their stacking sequence (e.g., P2- and O3-type) have introduced various dopants (e.g., Ni, Cu, Mg, Zn) [158], making the compositional space much more complicated. Such broad elemental combinations lead to a significant number of candidate chemical formulae that need to be considered for the prediction of high-performance cathodes.

Materials stable only at elevated temperatures
Among the various synthesis routes reported to date, high-temperature sintering has become one of the most common ways to fabricate electrodes and solid electrolytes with high Na^+ conductivities. The resultant structures are often only stable at elevated temperatures. The discovery of high-temperature metastable materials is challenging with standard DFT calculations alone, as they do not include the vibrational entropic contributions or the associated temperature effects. To predict materials at a finite temperature, it is therefore

Figure 17. Schematic of the procedures used for computational materials discovery in previous studies. Publicly accessible tools for structure prediction are also listed for reference. Reprinted figure with permission from [157], Copyright (2008) by the American Physical Society.

necessary to perform additional phonon calculations that can describe atomic vibrations, which carries a significant computational cost.

Strong self-interaction errors in correlated TM oxides
Anionic redox in *TM* oxides has emerged as a new paradigm to increase the energy density of NIB cathodes. However, accurate prediction of the redox activity of TM oxides has been challenging for standard DFT calculations. This is because conventional generalised gradient approximations of DFT cannot correct the self-interaction error in O and, in particular, in TM*s* with highly correlated *d*-orbitals [159]. To counteract the self-interaction error inherent in DFT, the use of computationally intensive methods, such as the DFT + U approach or hybrid density functionals, is essential.

**Advances in science and technology to meet these challenges**
Advances in computational resources and theoretical methods have progressed greatly recently, such that the difficult challenges of discovering novel NIB materials are now becoming tractable. There have been important developments in the consideration of temperature effects, such as the quasi-harmonic approximation and the highly efficient *ab initio* molecular dynamics [160]. Another recent direction in the study of temperature effects has targeted many-body approaches, such as the path-integral Monte Carlo and self-consistent harmonic approximations. The application of these methods provides a route for evaluating the thermal properties of materials, allowing the prediction of potential NIB materials that are stable at high temperatures. In order to accurately describe strongly localised *d*-orbitals, various novel functionals (e.g., the DFT + U approach and hybrid density functionals) have been suggested. To fully remove the self-interaction errors, many-body approaches, such as quantum Monte Carlo and random-phase approximation, are becoming achievable using today's supercomputing architectures.

Challenges remain, however, in exploring the potential phase space of multicomponent Na-ion systems, which is still prohibitively large to search fully. Therefore, to provide accurate descriptions of materials and at the same time maintain a competitive computational cost, researchers should take inspiration from the generations of chemical knowledge in the battery arena. The use of chemical heuristics has been shown to have great potential for narrowing down phase space. For example, the constraints of charge neutrality and electronegativity balance can significantly reduce the total number of candidate materials by two orders of magnitude [161]. Recent efforts to reduce the number of candidates have developed several less expensive and less accurate ways to estimate the properties of NIB materials: Mulliken electronegativity and the solid-state energy scale were used to estimate the electrochemical stability window (ESW) [161], Voronoi–Dirichlet partitioning and the bond valence sum were used to estimate the ionic conductivity [162], and 'cationic potential' was used to estimate the stacking sequence of cathodes [163].

Another persistent issue in battery materials is the environmental sustainability of the constituent elements, of which the drive to reduce expensive and toxic Co in LIBs is the prime example. Therefore, further improvements in the NIB arena should also be driven by using only earth-abundant and non-toxic elements, with an eye to our responsibility to be environmentally friendly.

Concluding remarks
Recent advances in computational methods and increasing computational power have provided researchers with a new toolkit with which to explore a vast chemical space for targeted materials discovery. The systematic integration of these tools can pave the way for the discovery of future NIB materials (figure 18). Major challenges remain, however, in the assessment of the properties of NIB materials. Despite the various

Figure 18. Integration of structure-prediction methods into the discovery of materials for future NIBs.
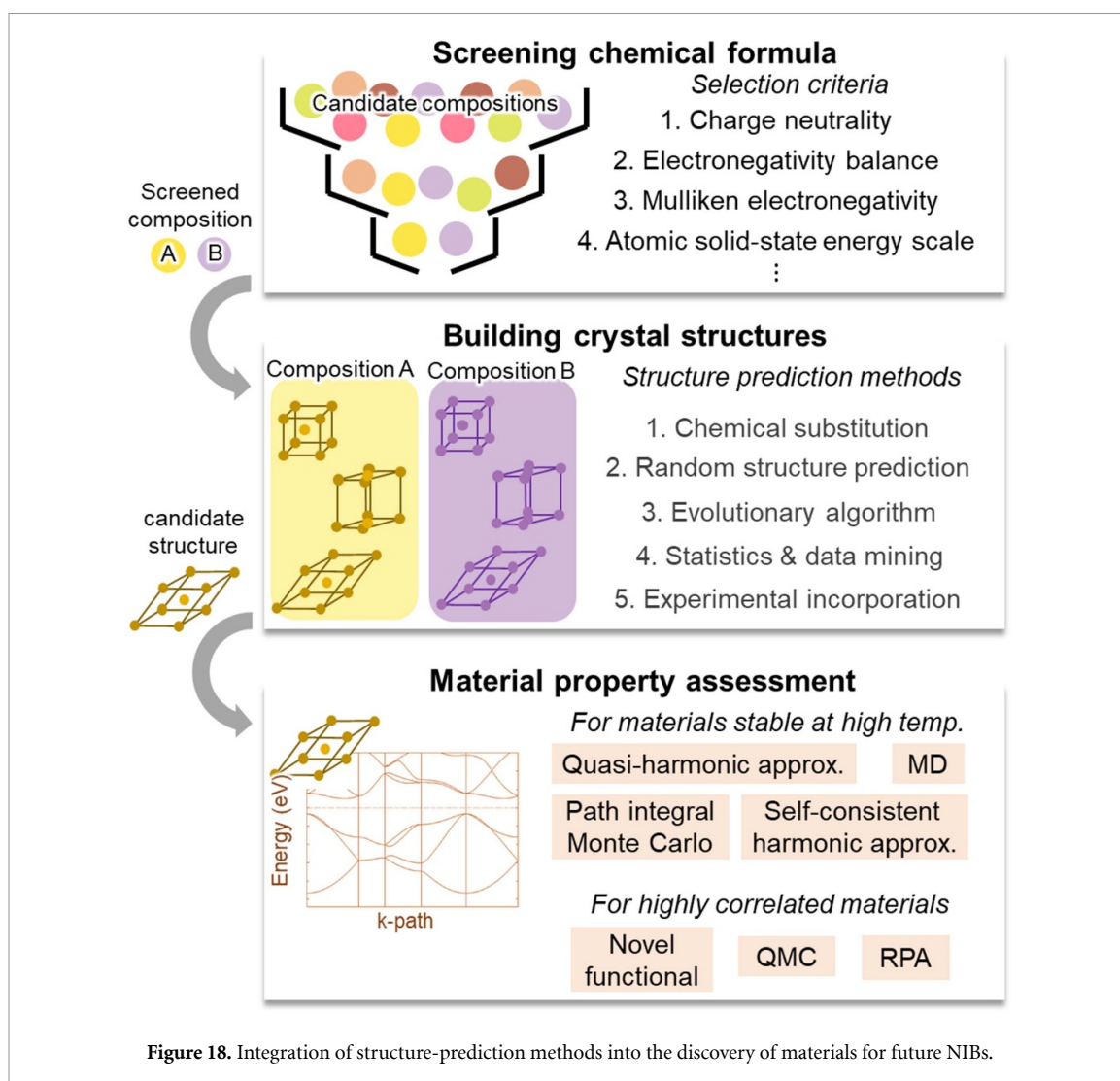
computational approaches developed to date, calculations for structures that can only form at high temperatures or strongly correlated NIB materials are still cost intensive. This severely slows down the exploration of chemical space, which hampers the prediction of new game-changing NIB materials. The development of new strategies to circumvent this bottleneck will thus be critical.

4. Electrolytes and SEI engineering

4.1. Organic electrolytes: salts

Darren M C Ould[1,2], *Christopher A O'Keefe*[1,2], *Clare P Grey*[1,2] *and Dominic S Wright*[1,2]
[1] Department of Chemistry, Lensfield Road, Cambridge CB2 1EW, United Kingdom
[2] The Faraday Institution, Quad One, Harwell Science and Innovation Campus, OX11 0RA, United Kingdom

Status

NIBs offer a cheaper and more sustainable large-scale energy storage solution, compared to well-established LIBs. However, contrary to the latter, which primarily use 1 M $LiPF_6$ in ethylene carbonate/dimethyl carbonate (EC/DMC) as a standard electrolyte solution, a leading electrolyte is yet to be established for NIBs [165–168]. This can be explained in part by the infancy of the field as well as the fact that electrolyte development is overlooked in favour of electrode research. Nevertheless, there is an urgent need to find high-performance electrolytes for NIBs, since they play a leading role in the overall lifetime, rate capability, and safety of the battery. Principally, this is due to the formation of a solid–electrolyte interphase (SEI) at the anode, which results from the degradation of the electrolyte and/or solvent during the charging/discharging process. Although well characterised for LIBs [168], the SEI composition for NIBs is poorly understood and remains one of the most critical areas for future research efforts.

To be an effective organic electrolyte, the sodium salt must adhere to a number of criteria: (a) chemical, electrochemical, and thermal stability; (b) high ionic conductivity; (c) low cost; (d) low toxicity/environmental benignity, and (e) simple, scalable synthesis. High ionic conductivity promotes facile, rapid exchange of sodium ions between the two electrodes, whereas a large highest occupied molecular orbital (HOMO) energy level ensures the stability of the salt. Such strict requirements naturally limit the possible choices of salts available; the most widely used anions are shown below, in figure 19. Traditionally, these anions have strong electron-withdrawing groups surrounding the central atom, which create a delocalised negative charge, and they are weakly coordinated to the Na^+ cation. Generally, sodium salts have higher melting points than their lithium counterparts, which is advantageous not only for easier drying but also safety, since the former have greater thermal stability.
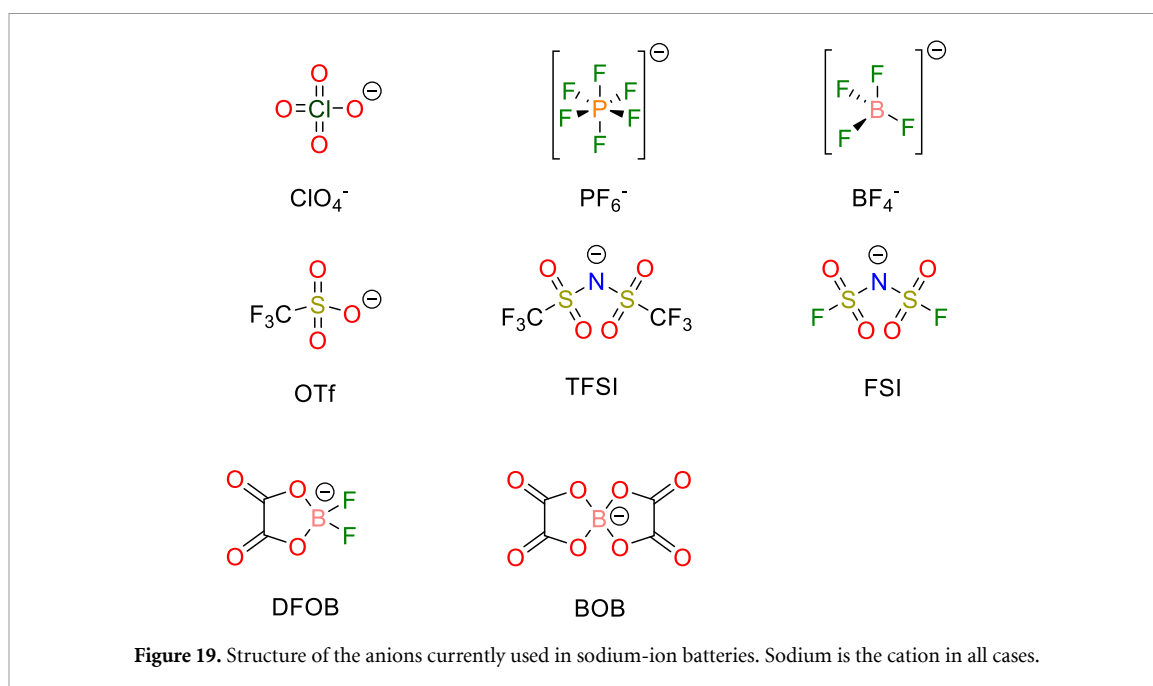
Current and future challenges

Among the electrolytes shown in figure 19, the most-studied electrolyte in NIBs is $NaClO_4$ [167] although its strong oxidising nature prohibits its commercial use due to safety concerns. In addition, $NaClO_4$ is known to be difficult to dry. Similarly to LIBs, the most promising salt to date for NIBs is $NaPF_6$; however, its high moisture sensitivity can promote the formation of HF via hydrolysis, leading to further electrolyte degradation and major safety concerns. As a result of this moisture sensitivity, the quality of commercially purchased $NaPF_6$ is problematic, and NaF formation occurs. $NaBF_4$ and NaOTf (OTf = trifluoromethanesulfonate) are poor choices, as they have strong cation–anion interactions, and it has been shown that NaOTf has reduced conductivity and electrochemical stability compared to $NaClO_4$ and $NaPF_6$ [164].

An interesting emerging class of electrolytes which has previously been used in ionic liquids contains NaTFSI (TFSI = bis(trifluoromethane)sulfonimide) and NaFSI (FSI = bis(fluorosulfonyl)imide), which are attractive due to their reduced toxicity and high thermal stabilities. However, these cannot be used as single salts, as they induce corrosion on the Al current collector, as well as incurring high cost. It is rare for new electrolytes to enter the field, but the DFOB (DFOB = difluoro(oxalato)borate) and BOB (bis(oxalato)borate) anions have recently both shown promising results in terms of reduced toxicity and low cost of synthesis [169]. Additionally, NaBOB has proved to be a non-flammable electrolyte when used in trimethyl phosphate (TMP) solvent; but in both cases, more work is required to optimise their performance [170]. Clearly, developing a salt that meets all the requirements outlined above is challenging, and future research efforts should focus on anions that have easily tuneable groups, which would allow for the fundamental properties of the salt to be simply modified.

Another challenge is to characterise the SEI. Few studies exist to address this, but x-ray photoelectron spectroscopy (XPS) and time-of-flight secondary-ion mass spectrometry (ToF-SIMS) analysis have confirmed the presence of Na_2CO_3 and $ROCO_2Na$ species [171]. These degradation salts are often more soluble than their lithium counterparts, and the Na^+ inductive effect on the solvents/anions should be weaker than for Li^+. This could, in turn, affect the reduction products formed at the anode.

Advances in science and technology to meet challenges

In recent times, the use of computational modelling and simulation has become a much more powerful method for the development of high-performance electrolytes. The early modelling of organic liquid

Figure 19. Structure of the anions currently used in sodium-ion batteries. Sodium is the cation in all cases.

electrolytes often focussed on the conduction mechanism, with little investigation into how the bulk ions themselves interacted. However, with advances in modern computer power, more recent studies have now started to quantitatively address the role of ion pairs, although currently, the high-level theory is too demanding for this to be a feasible method for the fast screening of electrolytes. In addition, computational methods can assist in better understanding the mechanism of SEI formation, where calculations have indicated that sodium electrolytes have faster desolvation of the cation at the electrolyte/electrode interface than that of Li^+ in analogous systems. DFT may also be used to simulate spectra (such as IR and Raman) of the degradation products in the SEI to aid the identification of the species present [172].

In addition to computational developments, there have been spectroscopic advances which may be utilised to address the challenges described above. Modern advances in dynamic nuclear polarisation-enhanced NMR spectroscopy (DNP-NMR) have recently been used as a method to aid characterisation of the SEI in LIBs. By using lithium metal as the polarisation source, selective observation of the low-concentration SEI components was possible. An intimate knowledge of the SEI composition and distribution is crucial in understanding how dendrites form, and is critical for preventing short circuits and improving the overall safety of the battery. A major advantage of this technique is that it allows for the direct probing of interfaces to reveal structural information, and it can be envisioned that this DNP-NMR spectroscopy technique can readily be applied to NIBs to provide further insights into SEI formation and composition [173]. While there have been several investigations into the structure of the SEI for NIBs, more work is necessary to understand the interplay between electrolyte chemistry, SEI composition, and stability.

Concluding remarks

In contrast to LIBs, which are a mature technology, much work is still required to unleash the full potential of NIBs. Electrolytes play a key role, as unwanted side reactions and degradation products significantly affect the overall performance and lifetime of the battery. The current range of sodium electrolytes has significant drawbacks, such as oxidising potential, moisture sensitivity, cost, and toxicity, meaning there is an urgent need to develop novel electrolytes to overcome these shortcomings. With increased research into, and development of, novel electrolytes, these challenges can be addressed, and this roadmap highlights key areas where focus should be applied. Principally, this is in characterising the degraded salts in the SEI as well as producing electrolytes which can easily be chemically modified to tune their fundamental properties. With this increased focus, NIBs undoubtedly have a prosperous future, rivaling that of their lithium counterparts.

Acknowledgment

4.2. Organic electrolytes: solvents

Martin Karlsmo[1] *and Patrik Johansson*[1,2]
[1] Department of Physics, Chalmers University of Technology, 412 96 Göteborg, Sweden
[2] Alistore-ERI, CNRS FR 3104, 15 Rue Baudelocque, 80039 Amiens, France

Status

In many ways, both R&D and the practical deployment of NIB organic electrolytes follow the development of LIB electrolytes [175–177]. This is logical, as the operating conditions and application areas are more or less the same, and thus, similar properties are needed; i.e., readily dissolved salts to create a large concentration of charge carriers offering fast ion transport with high fluidity and low viscosity. The latter also assists in the proper wetting of the separator and the porous electrodes. Additionally, high thermal and chemical stabilities are a must, to allow for usage in various climates and vs. different electrodes, as are wide ESWs matching the electrodes. Finally, all must be available at a low cost. As of today, this means linear and cyclic carbonates, such as DMC, EC and PC [174], or ethers, such as glymes, in particular, diglyme [174, 175].
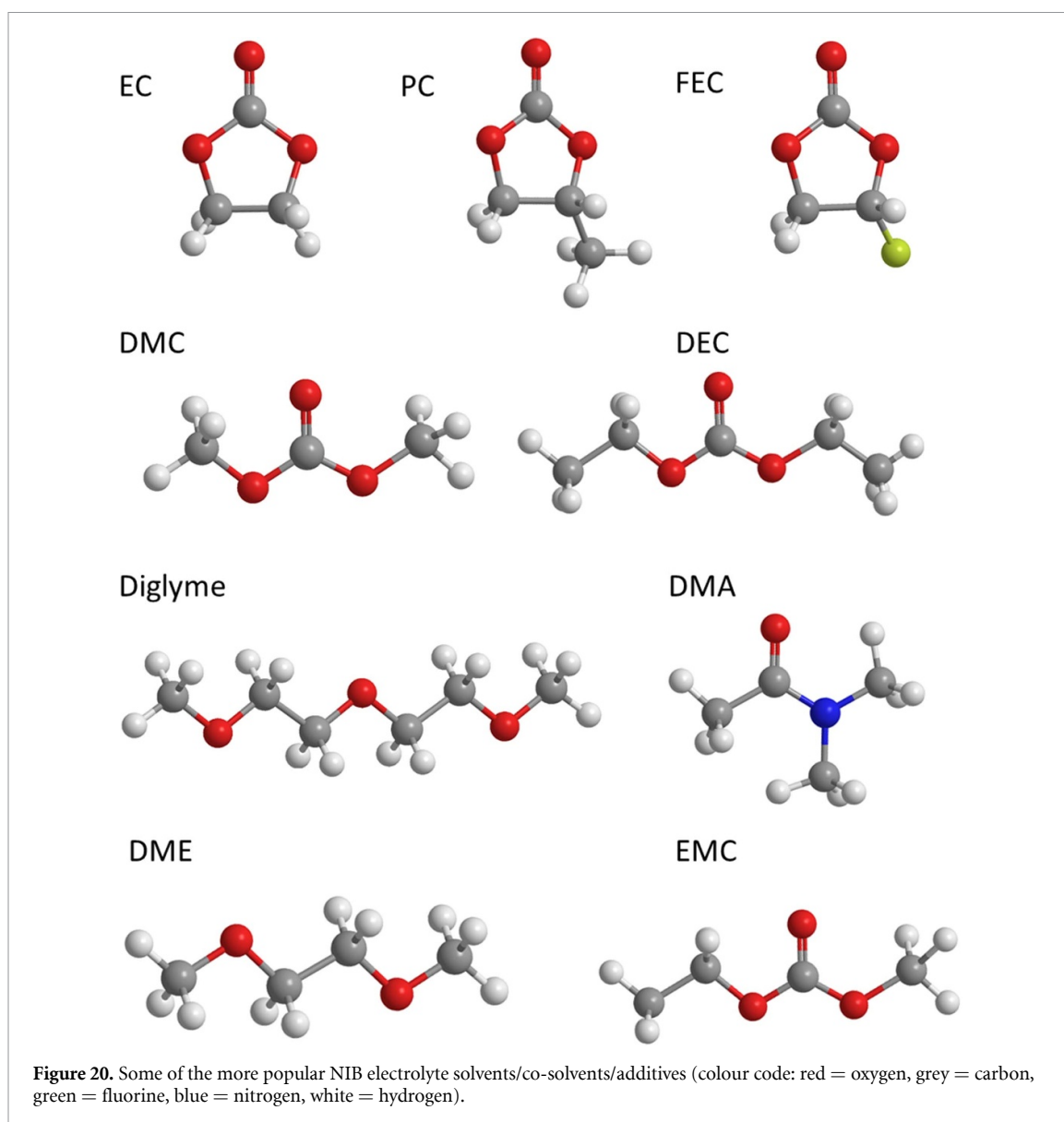
While much of NIB R&D follows from earlier LIB developments, there are some distinct practical differences to be found. One is that linear carbonates, such as DMC, used to lower the melting point and viscosity of LIB electrolytes, create soluble products upon reduction in a NIB, and hence, unstable SEIs at the anode, a problem that can be overcome by smart additive usage [176]. Another is that graphite is not capable of intercalating naked Na^+ ions and thus, it is not commonly used for NIBs. Therefore, PC, one of the original LIB electrolyte solvents, is frequently used for NIBs (as opposed to LIBs, as it exfoliates graphite) [174, 176, 177]. There is also a fundamental difference between the use of Na salts and Li salt: for the former, both the ion–ion and ion–solvent interactions are reduced to *ca.* 80% of the latter [178]—which paves the way for faster desolvation dynamics [179] which, at the cell level, manifests as improved power rates [174, 176, 177]. As with any other battery technology based on organic electrolytes, improved safety without making any departure from performance is key—and here, new NIB electrolytes, in particularm solvents, should evolve out of the LIB shadow. Another driving force should be to simplify recycling—and this, for example, means the use of F-free solvents/electrolytes [170].

Current and future challenges

Even if challenged by both solid-state electrolytes (SSEs) offering performance and safety advantages and aqueous electrolytes offering lower cost and better overall sustainability, organic solvent-based electrolytes are still likely to be the main route for years to come. They can be used in their own right and/or in hybrid electrolytes, with polymers or ionic liquids, to improve performance and safety [180] or to facilitate better SSE/electrode contact. A major challenge is to create a holistic and Na^+-centred (and not Li^+-derived) approach to the salt(s)–solvent(s)–additive(s) recipe for a standard functional NIB electrolyte [181]. This could also reduce the complexity and offer better control and understanding of e.g., solubility issues and ion-transport advantages. Today, the latter is, at the phenomenon level, a power performance advantage compared to LIBs, which is coupled to lower solvent desolvation energies [179] and the presence of fewer contact ion-pairs [178]. However, the reduction in strong interactions renders the organic products from solvent reduction more soluble and thus less stable, and creates/results in additional inorganic SEIs. Another large challenge comes directly from the +0.3 V shift in E_{red} of Na^+/Na vs. Li^+/Li. For the same final cell voltage, there is a corresponding more stringent demand on the electrolyte/solvent E_{ox} limit—which is not a minor issue, given the interest in high-voltage cathodes. The fact that the electrolyte must be developed not only in terms of ESW, but also to match both positive and negative electrodes, is a large challenge, as there is not yet a dominant electrochemical couple for NIBs. Improved fluidity, important for low-temperature performance as well as for the proper wetting of electrodes, must be achieved without compromising safety by using volatile solvents. Another path of research is highly concentrated electrolytes (HCEs), which improve safety, widen the ESWs, and utilise non-vehicular ion transport, which leads to improved cation transference numbers. For HCEs, Na-based systems have an earlier onset of some of these properties, compared to Li-based systems [179], which is cost-saving, as less salt is needed. However, the high viscosities of the highest concentrations of salt-based HCEs, i.e., those of very low solvent content, are a challenge for manufacturing and the cell formation stages.

Advances in science and technology to meet challenges

When the key performance indicators (KPIs) and the targets to be reached for NIBs by e.g., 2030 are listed, few are directly dependent on the solvent used, but very many are indirectly limited by the electrolyte. The first, most obvious KPI is the ionic conductivity, but the target, 1 mS cm^{-1}, has already been reached. The next is the cell voltage—intimately coupled to the electrolyte/solvent E_{ox} limit, as outlined above, while the less obviously connected KPIs are cycle-life and cost. However, for the NIB cycle life, the stability of the

Figure 20. Some of the more popular NIB electrolyte solvents/co-solvents/additives (colour code: red = oxygen, grey = carbon, green = fluorine, blue = nitrogen, white = hydrogen).

electrolyte/solvent, both in bulk and at the interfaces/interphases, is key. This is why different *operando* techniques enabling the study of NIB cells represent the most important technological advances needed. One such technology is based on embedding optical fibre sensors into the jelly-roll and, while it does not affect cell performance, it enables the monitoring of not only pressure and temperature changes as a function of the state-of-charge but also the origin of heat contributions and how different additives affect these properties, as elegantly demonstrated for a HC//NVPF NIB i.e. based on hard carbon as anode and $Na_3V_2(PO_4)_2F_3$ as cathode [182]. As a baseline electrolyte, this study used commercially available NP30 (1 M $NaPF_6$ in EC:DMC 50:50), a direct analogue to the LP30 electrolyte, and standard 18 650 cells and protocols. This points to several things that are needed to advance the science and technology of NIBs; commercially available electrolytes of high purity at a cost meeting KPI targets; standardised cells and protocols, both for electrolyte and electrode studies (at present, a chicken-and-egg problem, as no fixed-star materials exist, and different aspects are in focus using different setups), and understanding the roles/actions of additives in NIBs, as these may not be the same as those in LIBs—the differences in SEI formation being the most obvious. If a proper understanding of the limitations imposed by electrolytes, test protocols, and the actions of the additives is pursued, the growing community of NIB researchers should soon have a wealth of unambiguous data. While there is room for rethinking and emphasising the differences rather than the similarities between Na^+/NIBs and Li^+/ LIBs, NIBs should be using the field of LIB development to the maximum extent possible for real NIB leapfrogging.

Concluding remarks

While the R&D directions of NIBs have largely followed those of LIBs, they are slowly finding their own path, including applications where the emphasis is on complementarity rather than replacement. The somewhat overemphasised similarity of Na^+ and Li^+ dissolved in solvent(s) has, until today, promoted evolution, leaving NIBs always trailing behind LIBs. However, as an example, it should be possible to use the weaker solvent interactions and generally larger first solvation shells of Na^+ as design criteria for novel NIB electrolytes. Likewise, the problematic large solubility in the electrolyte of solvent reduction compounds should be a proper R&D target, similarly to e.g., the polysulphide issue in Li-S batteries. As we are seeing various *operando*, high-throughput, and robotic screening technologies starting to be applied for battery research, these could all be used to evaluate NIB electrolyte solvents and perhaps also enable the tailoring of the electrolyte to different operating conditions and applications.

4.3. Ionic liquid electrolytes

S Sen[1,2] and R G Palgrave[1,2]

[1] Department of Chemistry, University College London, 20 Gordon Street, London WC1H 0AJ, United Kingdom

[2] The Faraday Institution, Quad One, Harwell Science and Innovation Campus, OX11 0RA, United Kingdom
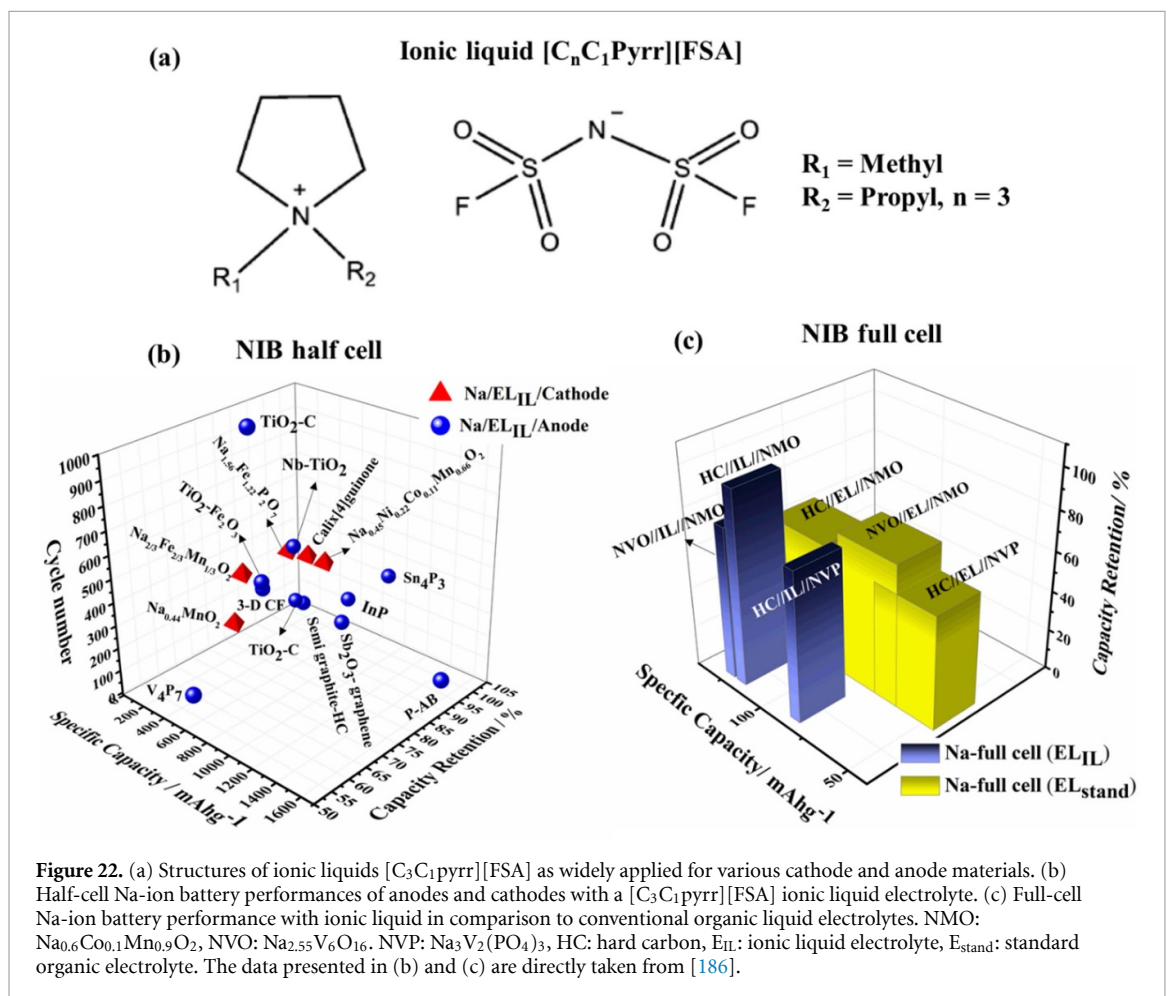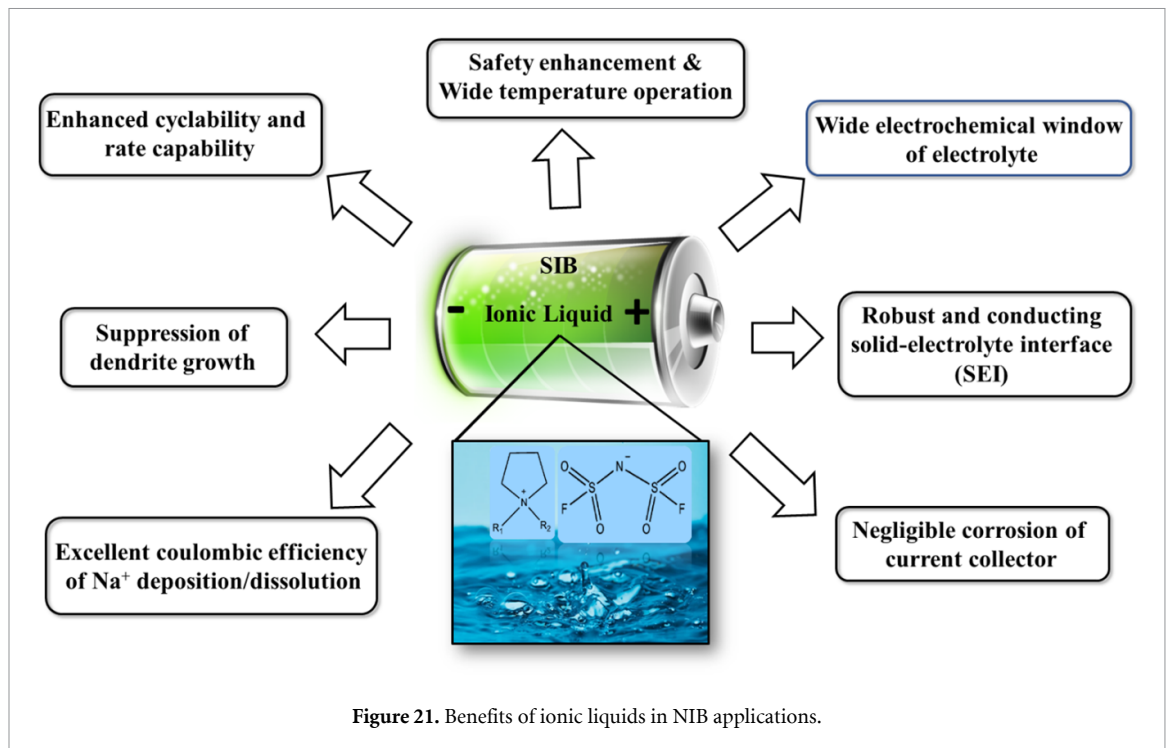
Status

NIBs have attracted attention in parallel to Li-ion technology due to their cost-effectiveness and the high earth abundance of sodium [71, 183, 184]. Despite the commercialisation of NIBs by several companies (Faradion [185], Tiamat [185, 186], SHARP labs [185, 186]), thermal runaway with volatile electrolytes and insufficient cyclability at room temperature demand more serious electrolyte research.

Ionic liquids (ILs) are promising alternative electrolytes due to their non-flammability and wide operating electrochemical window. They are glass-forming molten salts, consisting of versatile combinations of aromatic cations and weakly coordinating anions. The structures of the ions and their interactions (hydrogen bond, electrostatic, and Van der Waals) [187] govern their physicochemical properties, (phase transitions, viscosities, thermal stability, and HOMO-LUMO (lowest unoccupied molecular orbital) gap) [187] and electrochemistry (electrochemical window, ionicity, ionic conductivity, ionic association/dissociation, and the double-layer structure at the electrode–electrolyte interface) [187, 188]. In the realm of NIBs, ILs offer specific additional advantages, such as reduced corrosion of the Al current collector, a wide range of operating temperatures, and suitable electrode–electrolyte interface processes (homogeneous SEI formation, a conductive interface, and a dendrite-free anode–electrolyte interface) [185] (figure 21). The wider electrochemical window of ILs permits a wide variety of cathode materials for NIBs. Only anion decomposition defines oxidative stability and SEI composition. ILs offer a less resistive, more uniform, and consistent SEI throughout the battery cycle with hard carbon and alloy-based anodes [186]. The composition of an IL-derived SEI (with an HC anode) (SEIs formed with polyolefin, SCO) is distinctly different from those formed in organic electrolytes (SEIs formed with organic and inorganic sodium carbonates) [186]. Reduced aluminium corrosion in ILs is notable, even with salts that corrode the Al current collector in organic solvents [186]. Several imidazolium-, pyrrolidinium-, phosphonium-, and ammonium-cation-based ionic liquids have been explored in NIBs (e.g., $[C_2C_1Im][FSA]$, $[C_2C_1Im][BF_4]$, $[C_3C_1Pyrr][FSA]$, $[C_3C_1Pyrr][TFSI]$, $N_{2(20201)3}[FSA]$, $[P_{111i4}][FSA]$, $[C_4C_1pyrr][DCN]$, $[C_4C_1Im][SO_3CF_3]$. $C_nC_1im^+$: 1-alkyl-3-methylimidazolium, $C_nC_1pyrr^+$: N-alkyl-N-methylpyrrolidinium, $C_nC_1pip^+$: N-alkyl-N-methylpiperidinium, and N_{nnnn}^+: tetraalkylammonium) [186].

Current and future challenges

Despite several advantages, NIB research is falling behind the current state of the art of LIB technology. Safety and the battery cycle life are significantly influenced by the electrolyte formulation and various interfacial issues, including uncontrolled dendrite formation due to the use of sodium metal, unstable and increasingly resistive electrolyte interface SEI formation due to electrolyte decomposition, cracked and thicker SEIs, pronounced dissolution of SEIs, and the significant reactivity of sodium metal in the majority of volatile organic electrolytes.

Ionic liquids serve as green solvents. They mitigate safety issues and offer wider oxidative stability and relatively lower solvent degradation at the electrodes. However, the major challenges of ionic liquids are their relatively high cost, tedious purification methods, and the hygroscopic nature of widely used imidazolium- and pyrrolidinium-based ionic liquids. This is despite their excellent stability and wider temperature operability. Their relatively high viscosity and inferior ionic conductivity limit their battery cycling performance at room temperature, as compared to conventional organic electrolytes. The ionic liquids offer larger interfacial resistance and slower Na^+ transfer at the sodium metal anode, compared to organic electrolytes. In NIBs, the advantages of ionic liquids are only fully utilised at elevated temperatures ($\sim$90 °C) in half cells. Another important challenge with ionic liquids is to achieve a unity sodium transference number and reduce concentration polarisation. The majority of ionic liquid electrolytes are made at a maximum of 1 M concentration, a concentration at which unity transference numbers are difficult to achieve. Recently, super-concentrated ionic liquid-salt systems have been shown to offer relatively stable SEI properties and near-unity transference numbers. However, the availability of a wider range of IL structures with high salt dissolution capability is still limited. Designing electrolytes to achieve high transference numbers and reasonably good ionic conductivity is an unavoidable challenge for ILs in NIBs. Although minimal, the current-collector corrosion is not fully mitigated by the widely used fluorinated anion-based ionic liquids.

Figure 21. Benefits of ionic liquids in NIB applications.

Figure 22. (a) Structures of ionic liquids [C$_3$C$_1$pyrr][FSA] as widely applied for various cathode and anode materials. (b) Half-cell Na-ion battery performances of anodes and cathodes with a [C$_3$C$_1$pyrr][FSA] ionic liquid electrolyte. (c) Full-cell Na-ion battery performance with ionic liquid in comparison to conventional organic liquid electrolytes. NMO: Na$_{0.6}$Co$_{0.1}$Mn$_{0.9}$O$_2$, NVO: Na$_{2.55}$V$_6$O$_{16}$. NVP: Na$_3$V$_2$(PO$_4$)$_3$, HC: hard carbon, E$_{IL}$: ionic liquid electrolyte, E$_{stand}$: standard organic electrolyte. The data presented in (b) and (c) are directly taken from [186].

Advances in science and technology to meet challenges

ILs consisting of various combinations of ammonium and phosphonium-based cations and fluorinated and non-fluorinated anions have been explored in NIB applications (see figure 22(a) for structures).

Figures 22(b) and (c) present a survey of the battery performance of half cell (with sodium metal as the anode) and full cell (with a sodium intercalation compound as the anode) NIBs, respectively, employing pyrrolidinium-based IL electrolytes with a wide range of cathodes and anodes. Impressively, ionic liquids offer superior cyclability, rate capability, and powder density, compared to organic electrolytes. Despite the higher viscosity and inferior transference number, these results strongly encourage the investigation of IL chemistry in NIBs. The reasons for such exciting performance improvements are: the enhanced Na^+ diffusion at the interface, a compact SEI, dendrite-free sodium deposition/dissolution, the lower reactivity of ionic liquids with sodium metal, and reduced Al corrosion at elevated temperatures (figure 21). For example, highly conducting and stable SEI layers have been reported for an HC anode with an IL electrolyte, Na[FSA]-[C_3C_1Pyrr][FSA] [186], compared to $NaClO_4$-EC/DEC. The homogeneity and stability of the SEI of Na[FSA]-[C_3C_1pyrr][FSA] improves the cyclability of several anodes, such as Sn_4P_3 [a cyclability of 112% at 200 cycles] [190]. Full cells employing an IL electrolyte display similar benefits (figure 22(c)). A very energy-dense (368 Wh kg^{-1}) prismatic full cell has been developed using a Na[FSA]-[C_3C_1pyrr][FSA] electrolyte, a $Na_3V_2(PO_4)_3$ cathode, and an HC anode to deliver better capacity retention (75%) than that of a Na[ClO_4]-EC/PC electrolyte (figure 22(c)) [191]. A highly stable passivation layer with negligible dendrite formation was observed when a vinyl substituted imidazolium IL was used as electrolyte additive [192]. Super-concentrated 50 mol% NA[FSA]-[C_3C_1pyrr][FSA] exhibited dendrite-free sodium deposition/dissolution onto the SEI with a nanoengineered Na^+ conducting interface made from $(Na)_x(FSA)_y$ components [187].

Concluding remarks

In conclusion, ionic liquid electrolytes significantly improveme the safety of sodium ion batteries, widen the operating temperature and electrochemical window, and offer impressive cyclability and interface chemistry. However, insufficient literature is available to report the applicability of a wider range of electrodes in a wider range of ILs. Fine correlations between structure and critical interface electrochemistry are still under-represented in NIB research. Some additional concerns include cost, recyclability, tedious purification methods, and the high viscosities of ILs. Binary IL-organic/aqueous solvents (IL–water) and non-fluorinated cheap anion-based ILs could improve cost-effectiveness and decrease viscosity if they could be developed without sacrificing safety aspects. Interestingly, NIBs with ILs still exhibit good specific energy (near to that of LIBs) and better power than supercapacitors at elevated temperatures, which are difficult to achieve with organic solvents. The possibility of tuning the molecular structure of ionic liquids and a detailed understanding of the mechanical properties and solubility of SEIs with ILs are to be explored to enhance the performance of NIBs with ILs.

4.4. The SEI in Na-ion batteries

Andrew J Naylor and Reza Younesi

Department of Chemistry—Ångström Laboratory, Uppsala University, Box 538, SE-75121 Uppsala, Sweden

Status

An SEI may be formed through the decomposition reactions of an electrolyte at the interface with the anode of a battery [193]. The low electrode potential experienced by the anode causes the polar aprotic non-aqueous electrolytes employed to be thermodynamically unstable. The formation of a durable SEI is, however, essential for a kinetically stable battery and to obtain a long cycle life. This nm-scale interphase layer often has the characteristics of a solid electrolyte and can comprise both organic and inorganic, amorphous, and crystalline products derived from the electrolyte components. Ideally, it passivates the surface of the anode, being highly electronically insulating, impermeable to solvent molecules, insoluble, and inert, but offers ionic conductivity to allow the diffusion of cations (Na$^+$ ions in an NIB) between the electrode material and the electrolyte. The SEI should preferably be formed only within the initial cycles to prevent capacity losses and electrolyte depletion.

It has been shown through photoelectron spectroscopy (PES) measurements that the SEI in NIBs can vary in thickness and composition, depending on the state of charge [113]. The composition of the electrolyte is the main factor that influences the SEI composition and properties (figure 23), though other parameters including electrode-surface composition, current density, temperature, and potential limits can have an impact. The typical decomposition species formed from carbonate-based electrolytes in NIBs can be divided into inorganic species (mainly NaF and Na$_2$CO$_3$ but also Na$_2$O and NaOH in the presence of oxygen and water contamination) and organic species (sodium alkyl carbonates (ROCO$_2$Na) and polyethylene oxide oligomers) [194, 195].

Despite the fact that the SEI has been extensively studied in LIBs, resulting in the tuning of electrolyte formulations to provide maximum performance, it is still thought to be one of the major contributors to battery ageing [168]. However, while the concept of the SEI and its characteristics are largely similar for Na-ion batteries, many notable differences exist between the two technologies, even though they often use highly analogous materials [166]. A fundamental understanding of SEI formation mechanisms and properties is required to design an electrolyte that will lead to the commercialisation of NIBs. Here, we address the challenges of the SEI in NIBs, which can have such an important impact on their performance and ageing.

Current and future challenges

In NIBs, the main challenge that needs to be to overcome to stabilise the SEI is its *solubility* [197, 198]. While SEI *dissolution* has not been studied in great detail for LIBs, it is now a major focus of NIB research. The continuous dissolution of the SEI leads to its reformation in subsequent cycles with excessive irreversible capacity losses, poor coulombic efficiencies, and eventual failure. Because the charge density and hence the dissociation energy of sodium salts is lower than that of lithium salts, the solubility of SEI components (e.g., NaF vs. LiF) formed in NIBs is generally greater compared to that in LIBs, and this holds especially true for aqueous solutions [196]. Extensive SEI dissolution has been demonstrated for carbonate-based electrolytes and carbonaceous electrodes [197]. It has been determined that capacity loss through such dissolution is dependent on electrolyte composition and electrode surface area. It has even been debated whether the most soluble organic species can be considered to be SEI components at all [194, 195].

Additional challenges in *characterising* the SEI arise due to its high solubility. Most commonly, spectroscopic and imaging analyses are performed *ex situ* on electrodes after the drying/washing of samples. Such practices may inadvertently alter the composition of the SEI. The reports of an overall more inorganic SEI for NIBs compared to LIBs [199] could also be caused either by the leaching of organic species in the cells or their dissolution during the washing step.

The formation of high-resistance carbonates on the surface of sodium metal in half cells with continuous stripping/deposition can lead to a complex evolution of resistance. The lack of a reliable reference electrode and the consequential use of sodium metal in half cells results in poor SEI formation at the working electrode, and hence, inferior performance. The diffusion of decomposition products from the sodium electrode via the electrolyte to the working electrode ('crosstalk') is probably responsible. These issues prevent the extrapolation of performance from half cell to full cell; however, no such problems have been reported for full-cell configurations [196]. Nevertheless, information from studies published using half cells can still provide valuable insights and lead to a greater understanding of the challenges at hand.

Advances in science and technology to meet challenges

The low thickness and chemical complexity of the SEI in any battery system make it particularly difficult to characterise. Numerous techniques have been used, including PES, electron microscopy, electrochemical
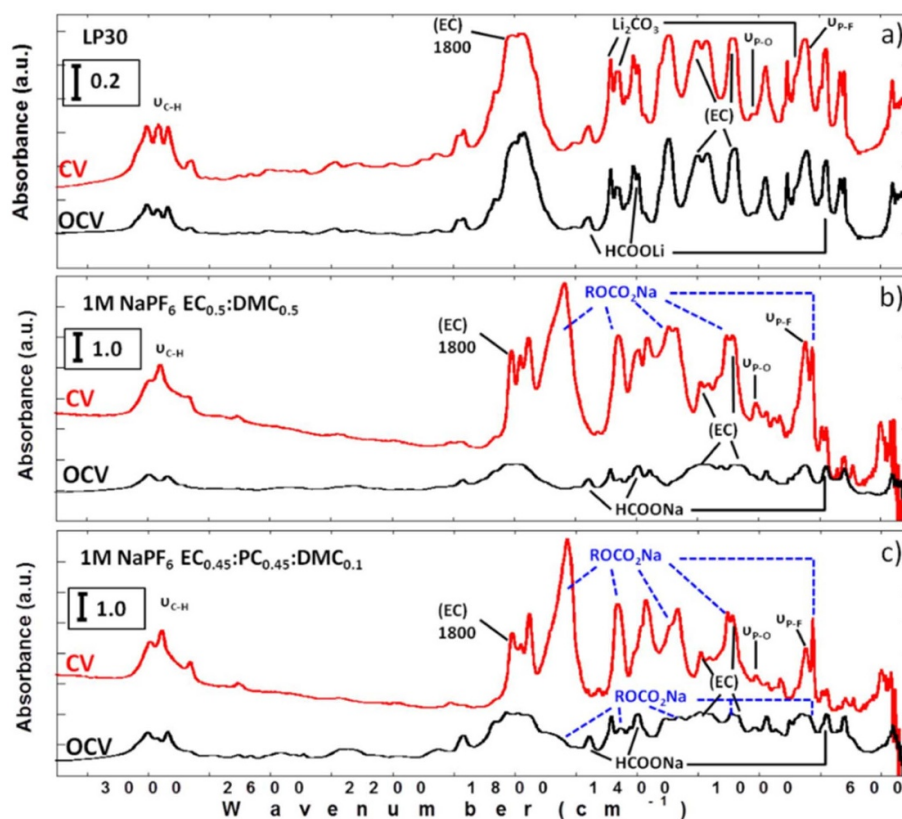
Figure 23. FTIR spectra obtained from Li or Na metal electrodes freshly prepared and stored for 24 h (OCV) or after cyclic voltammetry at 25 °C in (a) LP30 (1 M LiPF$_6$ in EC:DMC 1:1 wt. ratio), (b) 1 M NaPF$_6$ in EC:DMC 1:1 wt. ratio, and (c) 1 M NaPF$_6$ in EC:PC:DMC 45:45:10 wt.% [196]. Reproduced from [196]. CC BY-NC-SA 3.0.
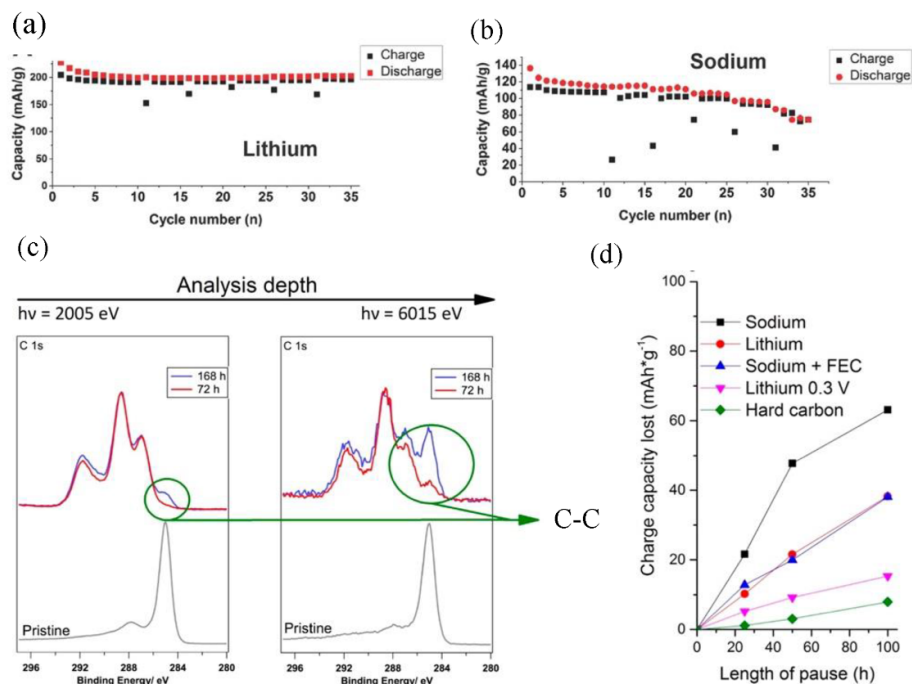
Figure 24. (a), (b) Galvanostatic cycling combined with pause testing of carbon electrodes in lithium and sodium half cells with 1 M (Li/Na)PF$_6$ in EC:DEC (1:1) electrolyte. (c) C 1s HAXPES spectra (two photon energies) of sodiated electrodes from sodium half cells after 72 and 168 h pauses. (d) Percentage charge capacity loss for different systems and pause lengths. Reprinted with permission from [198]. Copyright (2016) American Chemical Society.

quartz-crystal microbalances (EQCMs), electrochemical impedance spectroscopy (EIS), time-of-flight secondary-ion mass spectrometry (ToF-SIMS), and vibrational spectroscopies. However, innovative methods and advanced characterisation techniques are required to gain a deep understanding of the highly soluble SEI in NIBs.

Electrochemical 'pausing testing' can be used to investigate dissolution [197, 198], whereby a cell is switched to its open-circuit voltage (OCV) for a fixed duration after a period of cycling to determine how much capacity is lost through self-discharge (figure 24). Such experiments have shown that the capacity loss is higher in NIBs than in LIBs.

PES is very sensitive to surfaces and chemicals and is one of the techniques most commonly used to study SEI layers in all kinds of battery systems. Synchrotron hard x-ray photoelectron spectroscopy (HAXPES) measurements can be used to probe to a depth of 50 nm and have shown that the SEI thickness decreases with increasing pause durations (figure 24) [197, 198]. HAXPES measurements with large probing depths may allow for the elimination of electrode washing, an issue already discussed, although other parameters, including the pre-disassembly relaxation time, should also be considered. The future development of *in situ* and *operando* PES techniques may enable the direct measurement of SEI layer formation at an electrode during cycling.

While infrared spectroscopic (FT-IR) analysis of the electrolyte composition from cycled cells has already been demonstrated [195], it is underutilised for detecting soluble SEI species. Complementary techniques, such as gas chromatography mass spectrometry (GC-MS) and inductively coupled plasma (ICP) methods may also provide valuable insights. However, the extraction of electrolytes from cycled cells and data interpretation can present challenges.

The development of novel electrolyte components (salts and solvents) will almost certainly result in the formation of more stable SEIs and improved battery performance. However, given such development, one must bear in mind that cost-effective, non-toxic, and safe electrolytes will be required for the commercialisation of NIBs.

Concluding remarks

While relatively little is known about SEIs in NIBs and their formation mechanisms, particularly compared to their lithium counterparts, there is a growing body of knowledge on the topic as a result of increasing interest over recent years. Progress is inhibited, though, by the challenges posed by their complex nature. Their high solubility compared to the SEIs in LIBs causes difficulties in determining their composition and in preparing samples for *ex situ* characterisation. Furthermore, the lack of a suitably stable reference electrode and the issues of high resistance and crosstalk when employing sodium metal in half cells lead to complications in assessing the performance of materials. Novel electrolyte formulations will advance NIB technology towards commercialisation. However, a robust comprehension of the SEI achieved through the use of advanced characterisation techniques and innovative electrochemical testing methods will allow for the targeted design of electrolytes and a stable SEI.

Acknowledgments

4.5. SSEs for Na-ion batteries

Chris I Thomas[1,3], *Peter Gross*[1,3], *Marco A Amores*[2,3], *Serena A Cussen*[1,2,3] *and Edmund J Cussen*[1,2,3]

[1] Department of Materials Science and Engineering, The University of Sheffield, Sheffield S1 3JD, United Kingdom

[2] Department of Chemical and Biological Engineering, University of Sheffield, Sheffield S1 3JD, United Kingdom

[3] The Faraday Institution, Quad One, Harwell Campus, OX11 0RA, United Kingdom

Status

An ideal solid-state sodium electrolyte should deliver minimal ohmic losses and (electro)chemical stability with respect to both anode and cathode materials. Both of these parameters must be retained throughout the cycling processes and lifetime of the battery. Delivering such performance requires a combination of transport properties, chemical passivity, and processability, which represent a major challenge for materials science.

Sodium electrolytes have been a long-standing challenge, and Na^+ mobility is generally less facile than for Li^+ analogues. Conduction through solid polymers, such as Na salts in polyethylene oxide [200], can realise around 10^{-4} S cm^{-1} at room temperature and the relatively low melting point of Na makes operation above ambient temperature more fraught than in analogous Li batteries. The increased size and mass of Na^+ compared to Li^+ are both implicated in the more sluggish kinetics of the heavier group 1 metal, but it should be recalled that the heavier Ag^+ ion shows superionic conduction in a range of materials. Here, the polarisability of Ag^+ offers an advantage over the harder Na^+ cation. This points towards the potential of using polarisable anions, such as sulphide, in building a lattice for fast Na^+ conduction.

SSEs based on the material Na_3PS_4 have shown that the replacement of P^{5+} by Ge^{4+}, Ti^{4+}, or Sn^{4+} ions enables an increase in carrier concentration in the phases $Na_{3+x}M_xP_{1-x}S_4$. The introduction of dopants causes a tetragonal distortion away from the body-centred cubic parent phase, Na_3PS_4, leading to ordering of the Na ions. Unlike other ionic conducting systems, such as Li-stuffed garnets, this is not associated with a large decrease in Na^+ conduction, and computational simulations indicate that vacancy generation can be realised in the tetragonal phase, and that the conductivity of $Na_{3.1}Sn_{0.1}P_{0.9}S_4$ is similar to that realised in solid salt:polymer composites [201]. The efficacy of the approach is further demonstrated by the room-temperature Na^+ conductivity of 4 cm^{-1} afforded in the related phase, $Na_{11}Sn_2PS_{12}$, where a higher concentration of SnS_4 tetrahedral units delivers a complex three-dimensional pathway for Na^+ conduction involving all five crystallographic Na positions, and additionally, two low-energy interstices [202].

Similar conductivities have been realised in the NASICON structural family of oxide-based materials shown in figure 25, exemplified by series such as $Na_{1+x}Zr_2Si_xP_{3-x}O_{12}$, where the carrier concentration is adjusted by the classic approach of using an aliovalent chemical substitution, in this case, replacing P^{5+} with M^{4+} ions. In $Na_3Zr_2Si_2PO_{12}$ [203], the conductivity can be increased towards 4 mS cm^{-1} through control of the material's microstructure and densification processes.

Current and future challenges

The deployment of these materials into battery technologies faces the great challenge of interface management. Addressing this requires a better understanding of the role of electrolytes in interfacial processes. The minimisation of interfacial resistance is vital to avoid ohmic losses, which both reduce the energy storage capacity and lead to potentially hazardous heating. The challenge is to develop an interface which shows low resistance whilst retaining (electro)chemical stability during the multiple processes of battery cycling involving a change in potential and the (de-)swelling of electrodes. Meeting these challenges requires moving beyond the scale of material manipulation via crystal chemistry.

The NASICON phase has been explored via different synthetic routes, and these lead to variations in conductivity spanning an order of magnitude. An interesting development is the use of a 'fluoride-assisted' route to deliver a multi-phase sample with the composition $Na_3Zr_2Si_2PO_{12+x}$ NaF [204]. The presence of NaF leads to an increased grain size, which reaches a maximum for $x = 0.7$. As the grain size increases, the conductivity is enhanced from 0.23×10^{-3} to 1.4×10^{-3} S cm^{-1} as shown in figure 26. This is accompanied by a negligible change in the activation energy, indicating that the increase in grain size and the associated reduction in grain boundary volume is the likely cause for this enhancement in conductivity. Similar enhancements of conductivity up to 10^{-3} S cm^{-1} have been achieved using liquid-phase sintering [205] to aid the densification of $Na_3Zr_2Si_2PO_{12}$ at 900 °C rather than the 1200 °C necessary for conventional ceramic synthesis.

Many solid electrolytes have limited thermodynamic stability and react with metallic sodium. An examination of the interface between $Na_3Zr_2Si_2PO_{12}$ and a metallic Na anode has shown that the reduction of the electrolyte is kinetically limited; the initial reduction of Zr and Si is self-limiting and the electrolyte can
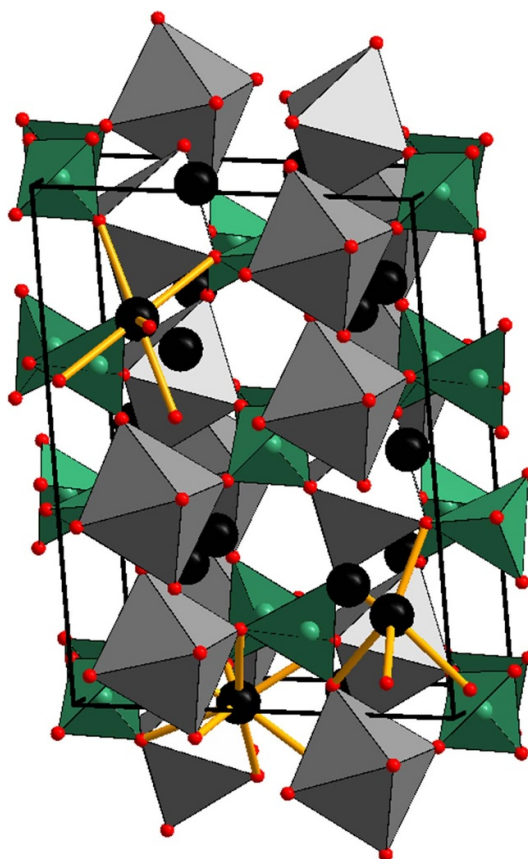
Figure 25. The fast Na^+ conducting material $Na_3Zr_3Si_2PO_{12}$ contains Na^+ (black spheres) in the three coordination environments indicated by orange Na–O bonds. The ZrO_6 and PO_4 units are represented by grey octahedra and green tetrahedra, respectively.
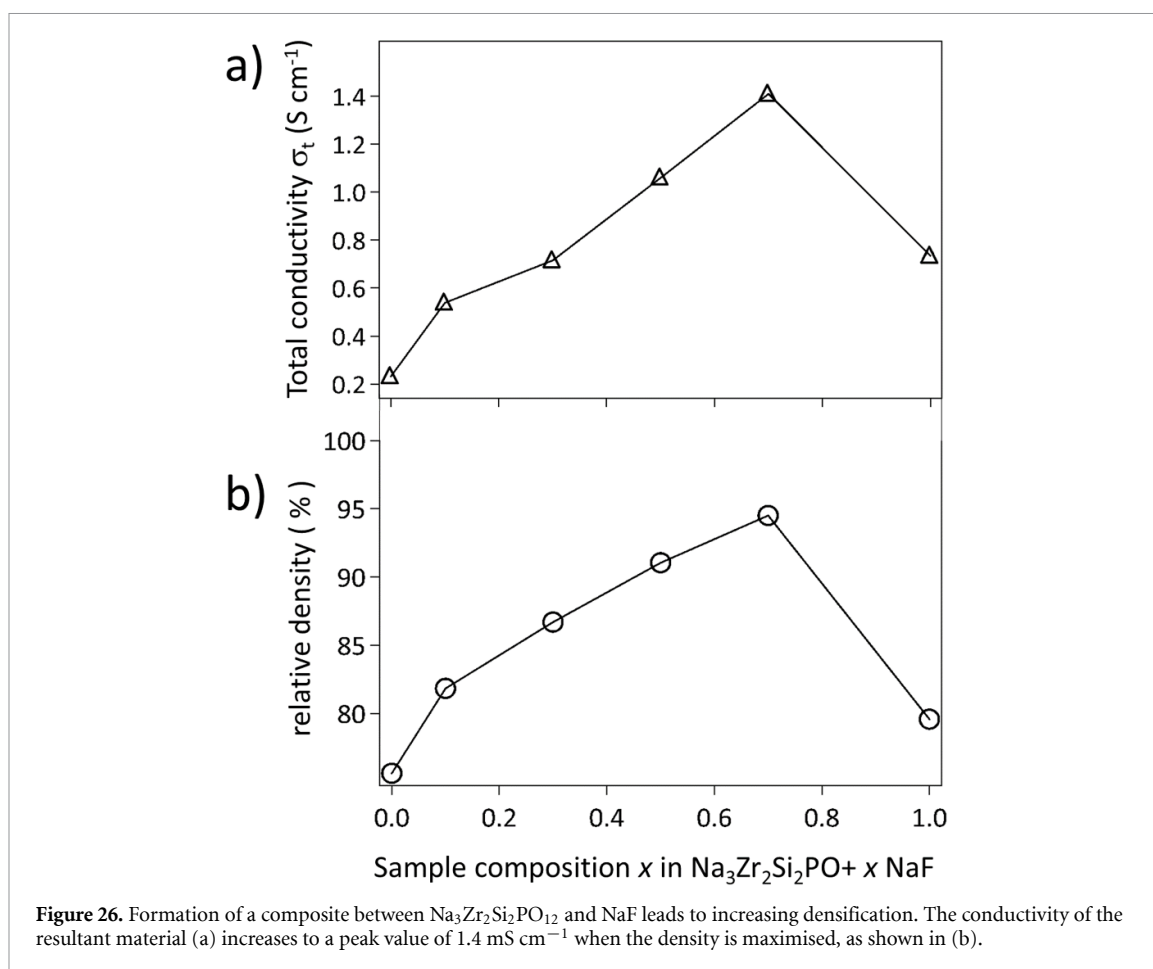
be plated and stripped with Na in a symmetric cell as long as the current density is kept below the 0.2 mA cm^{-2} limit for Na dendrite growth [203]. A relatively high charge rate of 2 C has been demonstrated using sulphide-based electrolytes $Na_{3+x}M_xP_{1-x}S_4$ ($M =$ Ge, Ti, Sn), although this was achieved using a $Na_2Ti_3O_7$ anode to avoid the problem of Na dendrite growth.

Advances in science and technology to meet challenges

The enhancement of electrolyte performance requires an intimate understanding of the mechanisms of Na^+ migration. A recent analysis of the effect of varying the Na content in the NASICON phases, $Na_{1+x}Zr_2Si_xP_{3-x}PO_{12}$, has indicated a more complex distribution of Na than expected, which implies that ionic conduction must proceed via a correlated mechanism with an organised movement of multiple ions, rather than the more widely anticipated hopping of individual ions onto vacant sites [206]. These insights arise from combining computational simulations of molecular dynamics and advanced analysis of neutron scattering data to deliver insights that could not come from either computation or experiment alone. Similar complementarity is seen in the characterisation of the lattice dynamics of the novel perovskite-phase $Na_{1.5}La_{1.5}TeO_6$ via both impedance and muon spin relaxation [207]. This combination of bulk and local probes shows how the local barrier for Na^+ migration is significantly lower than that indicated by the total impedance, which suggests that chemical modification may deliver useful increases in conductivity in this structural family.

These kinds of detailed insight need to be extended from isolated electrolyte materials to look at the interplay of chemistry and microstructure in delivering stable interfaces. This can be illustrated by two differing approaches to using composites to deliver solid-state batteries capable of extended cycling lifetimes.

A solid-state battery with excellent stability at up to 10 000 cycles, even at the high charging rate of 10 C has been realised by wetting the electrolyte interface with ionic liquids [208]. The solid electrolyte is an intimate composite of $Na_3Zr_2Si_2PO_{12}$ combined with adventitious $Na_3La(PO_4)_3$ introduced by an unsuccessful attempt to substitute La^{3+} into the Zr^{4+} site. The introduction of this impurity phase increases the density of the ceramic and so the presence of the passive impurity counterintuitively enhances the conductivity of the electrolyte composite beyond that of the pure $Na_3Zr_2Si_2PO_{12}$ phase. The capacity of

Figure 26. Formation of a composite between $Na_3Zr_2Si_2PO_{12}$ and NaF leads to increasing densification. The conductivity of the resultant material (a) increases to a peak value of 1.4 mS cm^{-1} when the density is maximised, as shown in (b).

90 mAh g^{-1} from the $Na_3V_2(PO_4)_3$ cathode combined with a metallic sodium anode is modest, but the stability and lifetime of the device show the efficacy of this approach for interface management. A similar capacity can be realised by casting ceramic particles in the NASICON phase in a polyvinylidene fluoride-hexafluoropropylene polymer to combine the conductivity of the ceramic with the mechanical properties of the polymer [209]. This solution-cast composite delivers a flexible electrolyte with a room-temperature conductivity of 2.25×10^{-3} S cm^{-1}, which matches that of the pure ceramic, whilst maintaining the ease of processing associated with the polymer.

Concluding remarks

Both oxide- and sulphide-based Na$^+$ electrolytes are now reaching the desired conductivity to enable solid-state batteries. The challenges in developing viable battery technologies lie in managing the interfaces between the solid electrolyte and the electrodes, and recent proof-of-concept studies have demonstrated the efficacy of an electrode/electrolyte composite approach. These examples serve as useful demonstrations of how chemical synthesis and materials processing must proceed in tandem to deliver cycling longevity from the management of electrolyte interfaces. Understanding the roles of the components and how they stabilise the interfaces will require a coordinated synthetic, experimental, and computational approach. There will also be a key role for *operando* measurements of crystal structure, lattice dynamics, and ion mobility in developing long-term electrochemical cycling in an all-solid-state sodium battery.

5. Testing protocols for Na-ion batteries

Juan D Forero-Saboya and Alexandre Ponrouch
Institut de Ciéncia de Materials de Barcelona (ICMAB-CSIC), Campus UAB, 08193 Bellaterra, Catalonia, Spain

Status

For all battery chemistries, a reliable electrochemical setup is essential. Half-cell configurations with typically two or three electrodes, using lithium metal as the counter electrode (CE) and reference electrode (RE), are standard setups for Li cells. However, several requirements need to be fulfilled to achieve reliable results (figure 27) [210, 211]. The CE must have high capacity, fast reaction kinetics, and should not contaminate the electrolyte solution with reaction byproducts. Meanwhile, the RE should ideally be nonpolarisable (a current flow should not affect its potential) and should have a reliable and stable potential. Although these conditions are satisfactorily met in Li half-cells, several studies point to various issues associated with the use of Na-metal CEs and REs [196, 212, 213].

Most of these issues are rooted in the low stability (and high solubility) of the SEI formed on the Na metal electrode (see the 'electrolyte/interface, SEI layer' section, by Reza Younesi). Considering the difficulty of developing new battery chemistries, in which both electrodes and electrolytes must be studied in parallel, the use of reliable electrochemical protocols is crucial in order not to discard potentially interesting material candidates or to make erroneous interpretations of the results. In this section, the most common issues arising from the use of Na metal CEs and REs are described, and recent strategies to overcome them are introduced.
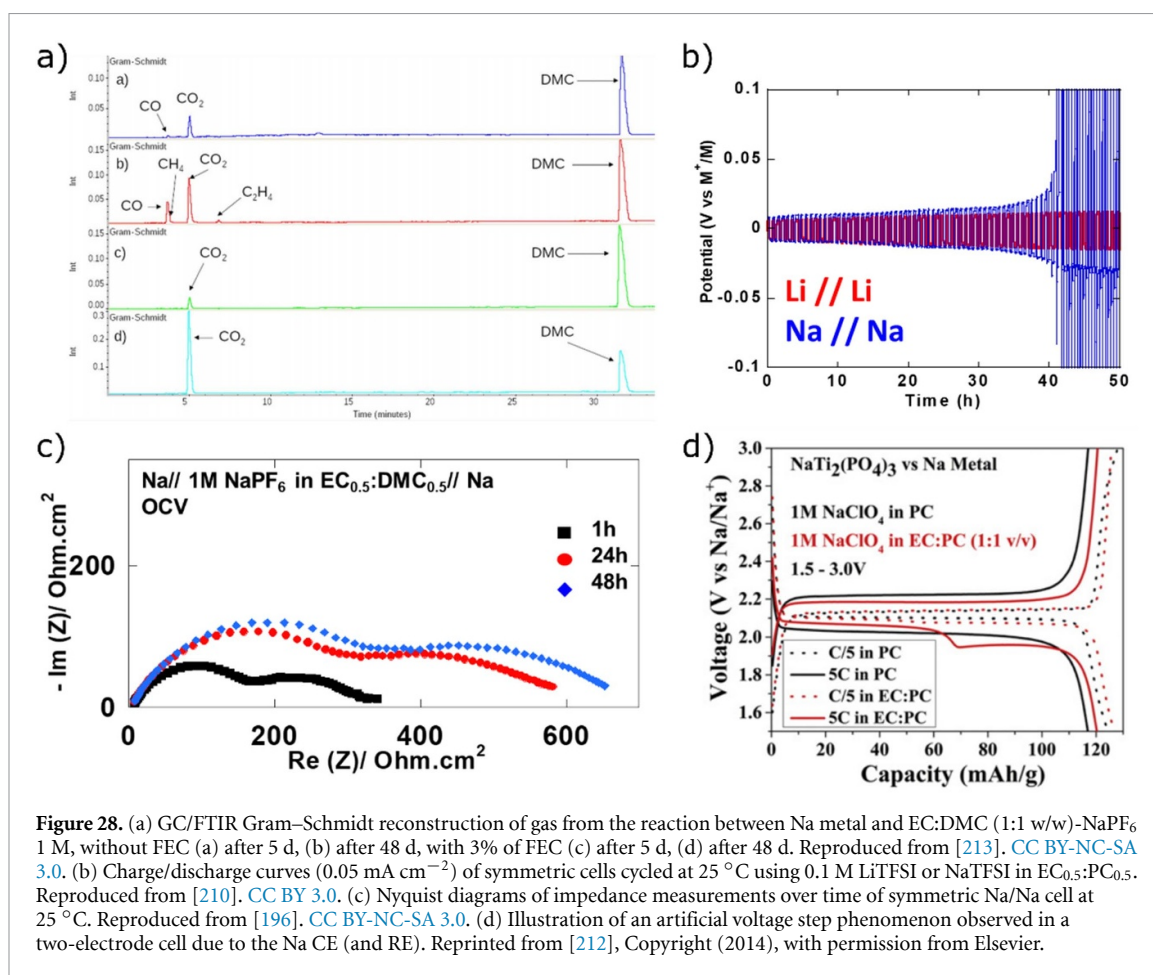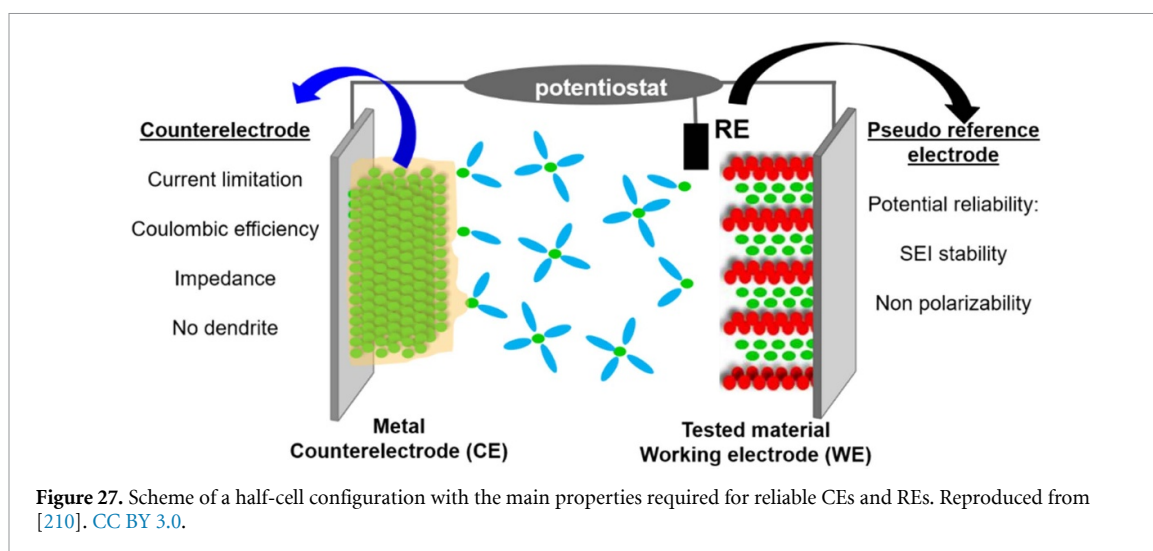
Current and future challenges

The instability of the Na metal–electrolyte interface has several consequences for any electrochemical test involving Na metal as both the CE and the RE. First, the constant SEI dissolution/reformation results in the contamination of the electrolyte with soluble/gaseous species. When alkyl carbonate-based solutions are in contact with Na metal, a growing amount of CO, CO_2, methane (CH_4) and ethylene (C_2H_4) is generated (figure 28(a)). The presence of soluble compounds, such as dimethyl 2,5-dioxahexane dicarboxylate (DMDOHC), has been observed in the solution, even after 5 d [213]. While the nature/amount of such contaminants is dependent on the electrolyte formulation, their impact on the working electrode interface and electrochemistry is clear. For instance, the impedances of hard carbon (HC)||HC (2-electrode) and HC||Na (3-electrode) cells left at OCV for 10 d indicate that the HC interface becomes more and more resistive when Na metal is present [196]. When comparing cyclic voltammograms of 1 M $NaClO_4$ in PC, Lee *et al* concluded that electrolyte decomposition products (formed on Na surface) diffuse to the working electrode (WE), where they are oxidised. Such parasitic reactions can obscure true measurements of the electrochemical performances of a given material [214]. Pfeifer *et al* observed that carbonate electrolytes (e.g., DMC, EC, PC) containing either $NaClO_4$ or $NaPF_6$ react readily in contact with Na, producing coloration or cloudiness of the electrolyte due to side reactions [302].

Sodium-ion intercalation into $Li_4Ti_5O_{12}$ was investigated using Na metal and activated carbon (AC) as CEs, with a significant cyclability improvement in the latter case. This was ascribed to a different passivation layer being formed, depending on the CE used, and possibly to more severe PVDF binder decomposition when Na is present. The highly inhomogeneous plating of Na, together with an increase in the Na metal impedance as a result of time and cycling, could also result in significant limitations on the cyclability of half cells (figures 28(b)) and (c)). Thus, when tests are performed on two-electrode half cells, the real performance of the active materials being tested as WEs can be significantly underestimated.

Finally, as the coulombic efficiency of Na plating/stripping is usually very low, the stripping of Na from the CE commonly involves two types of metallic Na: the freshly deposited one (Na_{plated}) and the Na bulk originally present as a disk or a foil. This can lead to an artificial voltage step that arises during the reduction of the active material used as the WE (figure 28(d)). Such a step can only be seen in two-electrode cells and was ascribed to the higher overpotential for Na_{bulk} when compared with Na_{plated} stripping [212, 213]. Once again, such an electrochemical response is only associated with the CE, and could be misleading.

Advances in science and technology to meet challenges

Several strategies have been developed to circumvent the problems associated with Na metal. One of the main approaches has been to control the nature and properties of passivation layers. Artificial passivation layers using freestanding composite layers consisting of Al_2O_3 particles and liquid electrolyte-swollen poly(vinylidene fluoride-co-hexafluoropropylene) polymers were developed, leading to an improved cycle life of Na||Na symmetric cells. However, evidence of dendrite formation and/or a cell impedance increase

Figure 27. Scheme of a half-cell configuration with the main properties required for reliable CEs and REs. Reproduced from [210]. CC BY 3.0.

Figure 28. (a) GC/FTIR Gram–Schmidt reconstruction of gas from the reaction between Na metal and EC:DMC (1:1 w/w)-NaPF$_6$ 1 M, without FEC (a) after 5 d, (b) after 48 d, with 3% of FEC (c) after 5 d, (d) after 48 d. Reproduced from [213]. CC BY-NC-SA 3.0. (b) Charge/discharge curves (0.05 mA cm^{-2}) of symmetric cells cycled at 25 °C using 0.1 M LiTFSI or NaTFSI in EC$_{0.5}$:PC$_{0.5}$. Reproduced from [210]. CC BY 3.0. (c) Nyquist diagrams of impedance measurements over time of symmetric Na/Na cell at 25 °C. Reproduced from [196]. CC BY-NC-SA 3.0. (d) Illustration of an artificial voltage step phenomenon observed in a two-electrode cell due to the Na CE (and RE). Reprinted from [212], Copyright (2014), with permission from Elsevier.

could still be seen at 0.5 mA cm^{-2} [215]. A similar layer using 2.8 nm-thick Al$_2$O$_3$ produced via low-temperature plasma-enhanced atomic-layer deposition was found to significantly increase the cyclability of Na symmetric cells up to 0.5 mA cm^{-2} [216].

Another avenue used to tune the SEI stability is to adjust the electrolyte formulation. Since this approach has already been discussed in section 4.4, here, we will focus on the impact of a few selected electrolytes on the reliability of Na-metal CEs and REs. Fluoroethylene carbonate (FEC) is a popular electrolyte additive in Na-ion batteries which limits the Na reactivity towards the electrolyte and helps in minimising the irreversibility of cathode materials. However, this does not come for free, and significant Na metal impedance increases can be measured together with a continuous release of small quantities of gases, even after 5 d [213]. Glyme-based electrolytes are among the most successful for Na metal. Schafzahl *et al*

demonstrated that improved cyclability and coulombic efficiency (reaching 97.7%) could be achieved in NaFSI/dimethoxyethane (DME) when compared with a carbonate-based electrolyte [217]. Superconcentrated glyme-based electrolytes were also investigated, reaching a coulombic efficiency for Na plating/stripping of 99.3% at 5 M NaFSI in DME [218].

Beyond the electrolyte formulation, several parameters can affect Na plating and stripping. Rupp and Vlad systematically investigated the roles of the electrolyte, separator, electrode preparation, cell architecture, cycling procedure, and the nature of the current collector [219]. The use of $NaCF_3SO_3$ in diglyme with a current density of 2 mA cm^{-2}, a Celgard 2325 separator and a high-density polyethylene gasket (to give better control of the current lines) led to a Na plating/stripping coulombic efficiency of 99.74%. Careful Na metal preparation could also result in limited surface contamination and an improved morphology [220].

While some of the strategies presented above could improve the Na plating/stripping coulombic efficiency and cyclability, the stability of the SEI (and its impedance) and the absence of soluble/gaseous contaminants remain to be ascertained. A radically different approach, relying on alternative CEs and REs, is also considered. A promising example consists of using the NASICON-type $Na_3V_2(PO_4)_3$ (NVP) as an intercalation-type CE [221]. Half cells with NVP as the CE exhibited stable cycling over a long period with low polarisation compared to Na as the CE. Measurements could also be performed at temperatures above the Na melting point, and due to the very flat voltage plateau of NVP, a two-electrode cell configuration could be assembled with a reliable potential measurement. Since NVP operates within the ESW of most electrolytes, it is also likely that such a CE does not produce undesirable contaminants. However, similarly to the use of capacitive electrodes (e.g., activated carbon), the sizing of the CE as a function of the expected capacity of the WE must be carefully considered [211].

The potential of the RE in a sodium cell is determined by the activity of the Na$^+$ ions in its vicinity, unlike the case for aqueous systems, where REs are commonly reversible to anions. As mentioned previously, SEI instability on Na metal has been shown to cause unreliable voltage measurements [210]. Lee and Tang evaluated alternative REs for Na-ion batteries: tin alloy, nickel hexacyanoferrate, activated carbon (AC) and silver ion [222]. Unfortunately, continuous potential drifts were recorded for tin alloy, nickel hexacyanoferrate and AC REs. Although silver ion (Ag$^+$/Ag) REs were found to be stable, they required the presence of a separate compartment and a porous glass frit to avoid the migration of silver cations; thus, they were not suitable for compact cell designs, such as Swagelok cells.

Concluding remarks

The use of Na metal for the CE and RE in a half-cell configuration results in several issues: electrolyte contamination, an increase in cell impedance, unstable potential, an artificial voltage step, and premature cell failure, among others. Most of these issues are rooted in the poor stability of the Na metal interface in most organic electrolytes. While several parameters can be tuned to mitigate such interfacial instability (e.g., electrolyte formulation, Na pre-treatment, cell geometry, etc.), there is currently no protocol which guarantees that reliable results can be obtained using Na metal. Since highly unsafe Na metal is mostly used in half-cells for material testing, one may wonder if research efforts need to be dedicated to making this challenging electrode work properly. Alternative CEs and REs such as NVP, AC, and silver-based electrodes are very attractive candidates for reliable electrochemical setups. While care must be taken when using such electrodes, their use can easily and routinely be integrated into most battery laboratories to obtain more reliable, and perhaps unexpectedly better results, than with Na half cells.

Acknowledgments

6. Advanced characterisation

6.1. Neutron characterisation of battery materials

Emily M Reynolds[1,2] *and Martin O Jones*[1,2]
[1] Science and Technology Facilities Council, North Star Avenue, Swindon SN2 1SZ, United Kingdom
[2] The Faraday Institution, Quad One, Harwell Science and Innovation Campus, OX11 0RA, United Kingdom

Status

Neutrons scatter from elemental nuclei and consequently interact weakly with condensed matter. This property offers considerable advantages in addressing the challenges associated with characterising the complex structure and dynamics of Na battery materials. Neutrons have a highly penetrating nature and can probe magnetic structure, resolve light elements and distinguish elements close to each other in atomic number. As a result, neutron diffraction (ND) can provide an insight into transition-metal (TM) distributions, magnetic structure, and Na diffusion pathways. Total scattering can distinguish between locally ordered TM distributions, observe local structural changes due to oxygen redox, characterise the structure of nanoparticles, and quantify disorder in hard carbon anodes. Inelastic techniques such as inelastic neutron scattering (INS) and quasi-elastic neutron scattering (QENS) can probe dynamics including Na diffusion, and techniques such as reflectometry and small-angle neutron scattering (SANS) allow us to observe the formation of the SEI layer and characterise the change in thickness/porosity of the SEI and electrode materials. Imaging techniques including radiography, tomography, and Bragg edge tomography can reveal the evolution of the components during cycling, and muon spectroscopy can probe the dynamics and energetics of Na diffusion. In addition to these specific techniques, neutrons remain a superior characterisation technique for *operando* studies of commercial and custom batteries due to their highly penetrating nature. Insight into the structural changes on cycling has revealed the mechanisms responsible for capacity fade [223], cycling-induced cation mixing [224], intermediate phases [224], dependence on cycle rate [225], and has led to the optimisation of commercial materials [226].

While the capabilities of neutron characterisation are vast, there is still scope for improvement through advances in facilities, instruments, and devices. For example, higher flux will increase temporal and spatial resolutions, and permit *operando* studies at higher cycling rates with an improved signal-to-noise (S/N) ratio. *Operando* neutron experiments are extremely challenging but are essential for a full understanding of battery operation and failure. Current abilities may be improved by developing a simultaneous characterisation facility that combines neutron scattering with electron paramagnetic resonance (EPR), NMR and X-ray spectroscopy techniques, optimising and improving existing sample environment cells, and developing new cells for scattering techniques currently without operando capabilities.

Current and future challenges

Disorder is a key feature in the most of the promising electrode materials, whether it be in structure, cation and anion distribution, stacking faults, or defects. Distinguishing between disordered states and correlating these to electrochemical properties is very challenging; however, cation disorder can improve Na transport, prevent unwanted phase changes, and reduce volume changes during cycling [227–229]. Furthermore, the structure of amorphous hard carbon (one of the most promising anode materials), and its Na storage mechanisms are difficult to characterise due to the lack of long-range order. While neutron characterisation, specifically total scattering, is well-equipped to address this, the routine characterisation of disordered materials remains a challenge. The analysis of such data often requires additional techniques to generate disordered models, either driven by physical/thermodynamic constraints, such as the Monte Carlo method, or driven by data, such as the reverse Monte Carlo. In addition, *operando* total scattering remains challenging, as any additional components from the battery setup interfere severely with data analysis.

Neutron characterisation excels in *operando* studies, despite the low neutron flux, which limits temporal and spatial resolutions. For diffraction, this limits the cycling rate, spatial resolution across an electrode, and the data quality achievable. For other techniques, such as quasi-elastic scattering (QENS), it has inhibited *in-situ* studies altogether. Cell design is also complex, as the requirements for good quality data and electrochemical cycling comparable to commercial battery operation are different and often incompatible.

In general, understanding and characterising the formation of the SEI on electrode materials, its chemical composition, evolution on cycling, and impact on diffusion are huge challenges for the battery community and are still in their infancy. Neutron reflectometry is an excellent technique for studying buried interfacial structures, and the highly penetrating nature of neutrons means that SEI formation can be observed *in-situ*, which is essential, as the interfacial structures are usually very sensitive to air. A major challenge for this technique is the development of an *operando* cell that presents a thin electrode with an extremely smooth surface.
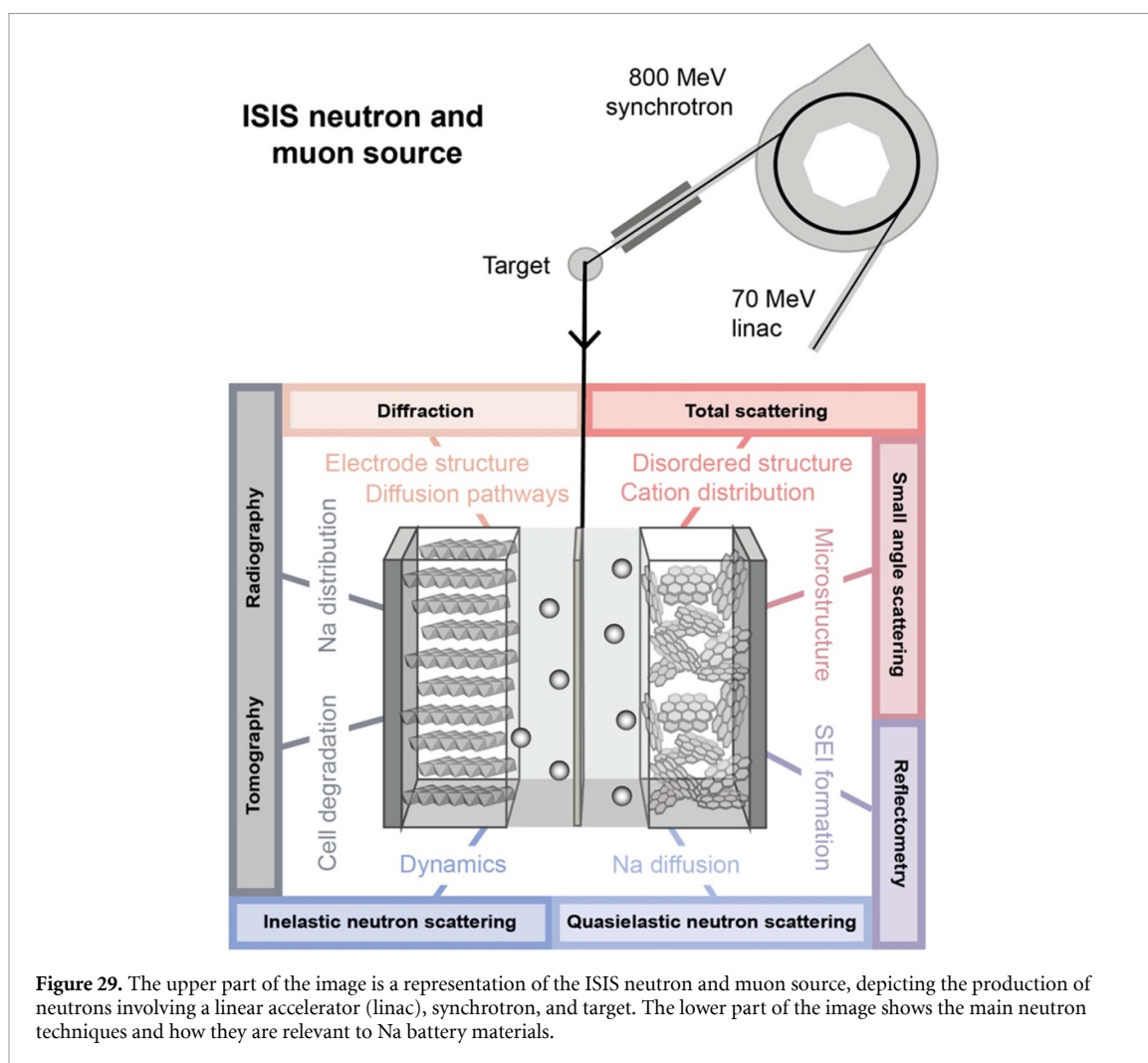
Figure 29. The upper part of the image is a representation of the ISIS neutron and muon source, depicting the production of neutrons involving a linear accelerator (linac), synchrotron, and target. The lower part of the image shows the main neutron techniques and how they are relevant to Na battery materials.

Advances in science and technology to meet challenges

Advances in instrumentation, such as guides and detectors used to obtain a higher flux in the sample will improve the temporal resolution and data quality of *operando* studies. This can also allow *operando* experiments for techniques where the current time resolution is too poor, such as QENS, as well as improving spatial resolution for imaging studies. Advances in cell development will also benefit *operando* studies, with the potential to reduce data collection times, allow the performance of simultaneous multicharacterisation studies, and facilitate total-scattering *operando* experiments. The development of *operando* total scattering is a significant challenge, as additional components from *operando* and/or multicharacterisation cells interfere heavily with pair distribution function (PDF) data collection and analysis; thus, new cells need to be developed with components that are either easily subtracted or have a small contribution to the total scattering.

Alternatively, the temporal resolution may be improved through the development of stroboscopic measurement techniques, whereby multiple identical experiments are carried out and the data are carefully time marked to allow the data from the individual experiments to be combined, enhancing the S/N ratio and resolution through overlapping data sets.

Advances in sample environments and equipment are essential, in particular, for *in-situ* and *operando* experimentation, which enable simultaneous data collection from complementary techniques—so-called 'multimodal characterisation'. Examples include simultaneously collecting NMR or EPR data whilst performing neutron diffraction, or the combination of two different neutron techniques, such as diffraction and imaging, a facility that is currently under development. The development of new multimodal characterisation sample environments that can be utilised with different instrumentations and across techniques with the same sample is vital. A full understanding of the physical phenomena that underpin functional properties can only be obtained through this type of experimentation.

While advances in flux and sample environments will benefit disorder studies, data-analysis tool development will allow heavily disordered systems to be understood. It would be helpful to improve analysis

tools such as 3D-PDF [230, 231] that can identify Na sites when disordered, component analysis that can separate multiple phases in the PDF, and machine-learning algorithms that can be used to identify potentially interesting structures, including disordered ones.

Concluding remarks

Neutron characterisation techniques deliver significant capabilities to the energy materials community, giving the possibility of full, multimodal characterisation of all functional properties and related structural and spectroscopic phenomena. The development of new sample environments to permit these multimodal studies across different instrumentations and techniques is essential to support progress in this area. Equally, investment in neutron facilities to improve instrumentation, detectors, and neutron flux will result in advances in the temporal and spatial resolution of neutron-scattering techniques. This combination of developments will facilitate a comprehensive understanding of battery systems and thus promote the creation of new and improved battery systems.

Acknowledgment

6.2. Solid-state NMR for the characterisation of Na-ion batteries

Valerie R Seymour[1,2] and John M Griffin[1,2]
[1] Department of Chemistry, Lancaster University, Lancaster LA1 4YB, United Kingdom
[2] The Faraday Institution, Quad One, Harwell Science and Innovation Campus, OX11 0RA, United Kingdom

Status

In order to develop and optimise new Na-ion battery materials, it is crucial to understand the underlying structural chemistry in detail. In general, diffraction techniques are the go-to methods for studying crystalline battery materials, and these continue to be the 'gold standard' in delivering atomic-level pictures of the long-range structure. However, many structures and mechanisms involve short-range phenomena such as disorder, dynamics, and defects that can be challenging to characterise by diffraction. In this regard, solid-state NMR stands out as a powerful complementary approach due to its sensitivity to the local chemical environment. Indeed, solid-state NMR has no requirement for long-range order, making it applicable to the study of crystalline, disordered, and amorphous materials. It is also sensitive to dynamics over a wide range of timescales, making it useful for studying ion migration and diffusion.

Solid-state NMR experiments on batteries can be carried out *ex situ* on materials extracted from cells, or *in situ* using bespoke cells that are designed to fit inside the NMR detection coil (figure 30) [232]. *Ex situ* experiments have the benefit that they are compatible with magic-angle spinning (MAS), meaning that high-resolution results can be obtained. *In situ* experiments have the advantage that they give a better chance of observing any short-lived or metastable states, since the cell is not disassembled for analysis.

Solid-state NMR studies of Na-ion battery materials are not yet as prevalent as for Li-ion battery materials, but both *ex situ* and *in situ* approaches have been applied in a number of studies. For $NaMnO_2$, *ex situ* measurements were used to follow changes in the domain structure during cycling. The spectra revealed signals associated with the α- and β-phases, as well as the stacking-fault interfaces between these domains (figure 31(a)) [233]. During desodiation, the peak corresponding to the β-phase reduced faster than the interfacial resonance, indicating preferential extraction from this phase and/or loss of long-range order. For the candidate cathode material Na_2FePO_4F, ^{23}Na 2D exchange NMR experiments showed that the Na ions move between crystallographic sites in the structure at a frequency of approximately 200 Hz [234]. *Ex situ* measurements showed the formation of the fully oxidised $NaFePO_4F$ phase during cycling, suggesting a two-phase desodiation mechanism. NMR performed on *in situ* ^{23}Na has been applied to hard carbon-anode materials, where it clearly revealed structural transitions during sodiation and desodiation [77]. At low sodiation levels, the isolated Na ions showed a characteristically diamagnetic chemical shift; however, at high sodiation levels, a marked change to paramagnetic chemical shifts signified the growth of quasi-metallic clusters (figure 31(b)). Recently, *in situ* ^{23}Na NMR and MRI have also been applied to observe the growth of dendritic and mossy microstructures on Na metal anodes [235]. The results revealed a two-step mechanism in which nucleating microstructures led to an increasing overpotential which triggered a rapid breakdown of the electrolyte, causing cell failure.

Current and future challenges

One of the key challenges in the solid-state NMR of battery materials is the presence of strong paramagnetic interactions arising from the unpaired electron spin density of transition-metal ions that are present in many systems. These interactions can result in large resonance shifts and extensive line broadening which complicate the acquisition and interpretation of NMR spectra. In most cases, the resolution is maximised by performing measurements at fast MAS rates ($\geqslant$60 kHz) and using moderate or low magnetic fields. However, even under these conditions, the resolution can still be compromised, making it difficult to identify all the species that are present. In addition, the assignment of spectral resonances is often not straightforward. For extended diamagnetic systems, plane-wave DFT codes can usually predict NMR parameters with sufficient accuracy to allow assignment to a model structure. However, due to the greater complexity of paramagnetic structures, progress in the development of accurate DFT methods for the calculation of NMR parameters has been slower, and spectral assignment still largely relies on empirical trends.

Another challenge is the intrinsically low sensitivity of some NMR-active nuclei, which hinders or precludes their observation. For some nuclei (e.g., ^{17}O or ^2H) the natural abundance is so low that their observation is rarely possible under normal conditions. Isotopic enrichment of these nuclei is possible, but is very costly and can require modification of the synthesis procedure, depending on the isotopically enriched precursor available. Sensitivity is also a significant challenge in the detection of surface and defect species, which play an important electrochemical role in many systems. Since NMR is quantitative, the detection of such low-concentration species within a bulk sample can be very challenging, even when they contain
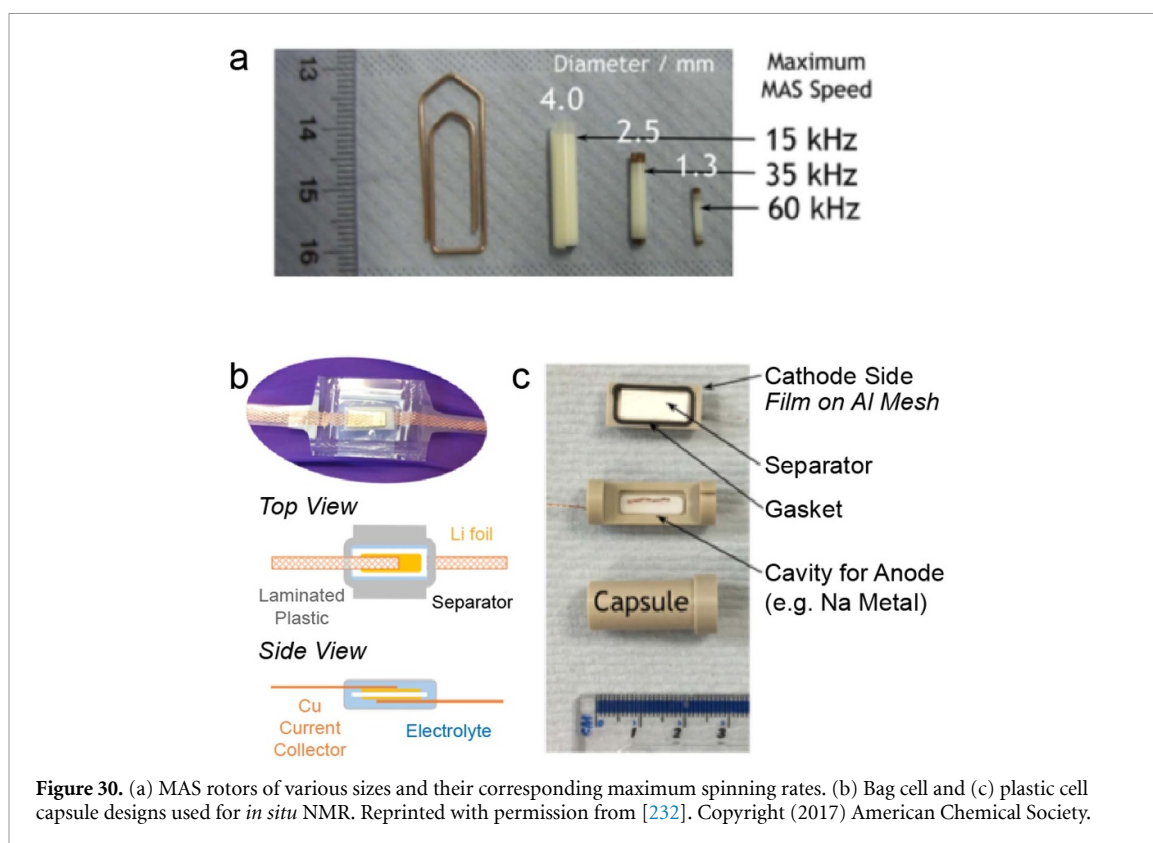
Figure 30. (a) MAS rotors of various sizes and their corresponding maximum spinning rates. (b) Bag cell and (c) plastic cell capsule designs used for *in situ* NMR. Reprinted with permission from [232]. Copyright (2017) American Chemical Society.
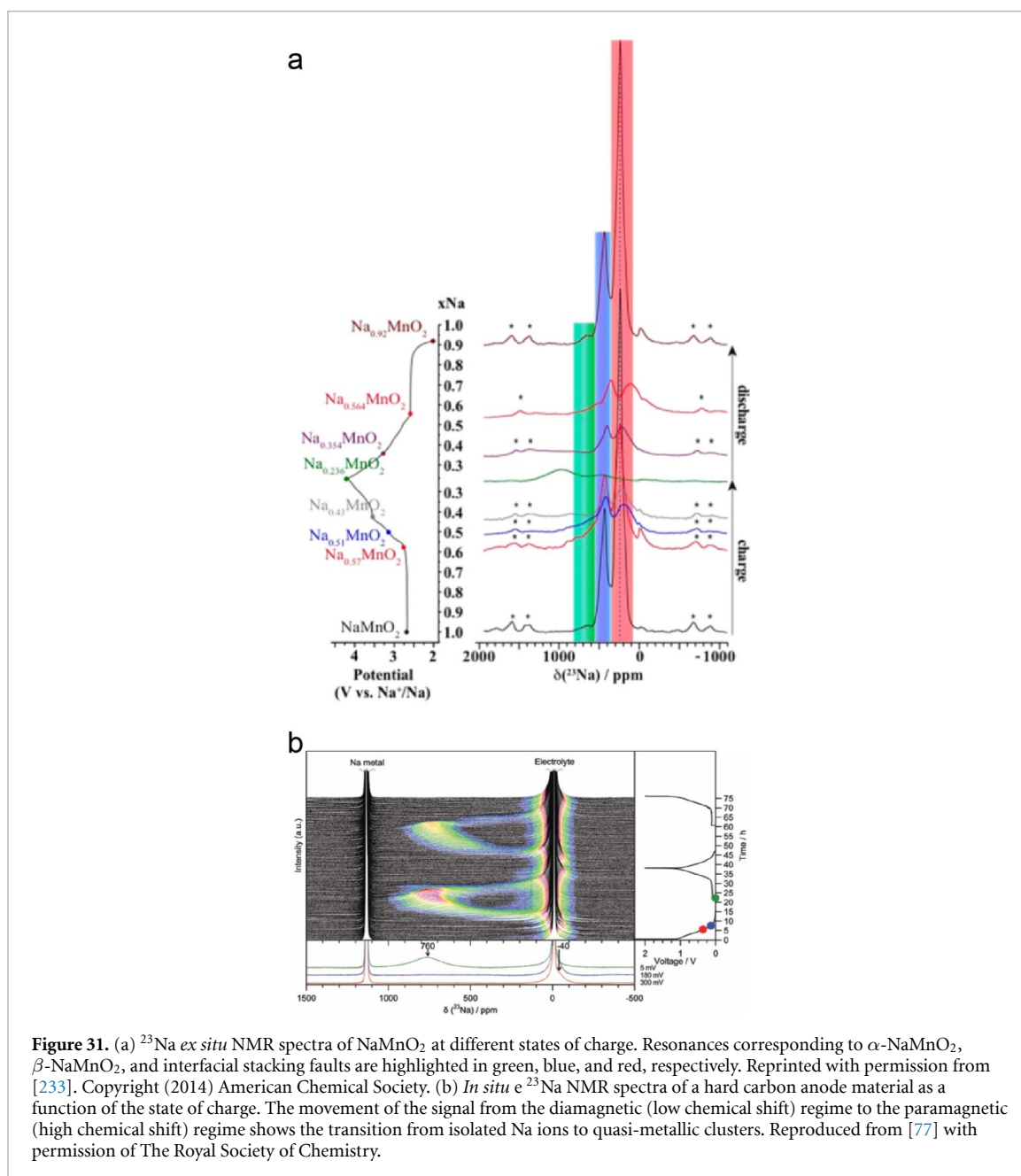
high-sensitivity nuclei. This challenge is exacerbated by *in situ* measurements, in which the sensitivity is typically further reduced due to the requirement for a large-diameter detection coil and a low filling factor due to the cell components, which reduces the sensitivity further.

Advances in science and technology to meet challenges

An important area of NMR hardware development is MAS probe design. As discussed above, fast MAS can help to remove the effects of paramagnetic interactions, which broaden and complicate solid-state NMR spectra in battery materials. Fast MAS frequencies remove these interactions more efficiently, thereby improving both the resolution and sensitivity of NMR spectra, so that more information can be obtained. Very recently, a probe capable of MAS frequencies up to 170 kHz has been demonstrated [236]. Although this ultra-fast MAS technology has not yet been widely applied, it represents a significant step forward, which can be expected to support new insights into battery materials in the future.

Advances in DFT methods for the calculation of paramagnetic NMR shifts will play a key role in addressing the issue of spectral interpretation and assignment. Although this remains a significant challenge, progress has been made in recent years, and a number of methods have been successfully demonstrated for model systems [237, 238]. Further development of these methods will enable them to be applied more widely beyond proof-of-concept studies, although due to the complex and highly system-dependent nature of the calculations, it is not clear whether paramagnetic shift calculations will become routine in the same way as for non-paramagnetic materials.

Concerning the challenge of detecting insensitive nuclei and surface or defect species, significant progress has been made in recent years through the development of dynamic nuclear polarisation (DNP). DNP transfers strong electron spin polarisation from either native or exogenous radical species to nuclei within the material of interest. Since the transfer is distance-dependent, exogenous radical species have a tendency to selectively enhance surface groups [239]. Radicals native to the material structure have also been used to enhance insensitive nuclei in the bulk structure [240, 241]. This approach holds considerable promise for the study of unstable or reactive battery materials which may not be amenable to the addition of exogenous polarising agents. Despite the promise that DNP holds, further developments are required to properly understand polarisation transfer mechanisms, and also to widen the temperature range over which it is effective, so that materials can be studied under ambient or variable-temperature conditions.

Figure 31. (a) ^{23}Na *ex situ* NMR spectra of NaMnO$_2$ at different states of charge. Resonances corresponding to α-NaMnO$_2$, β-NaMnO$_2$, and interfacial stacking faults are highlighted in green, blue, and red, respectively. Reprinted with permission from [233]. Copyright (2014) American Chemical Society. (b) *In situ* e ^{23}Na NMR spectra of a hard carbon anode material as a function of the state of charge. The movement of the signal from the diamagnetic (low chemical shift) regime to the paramagnetic (high chemical shift) regime shows the transition from isolated Na ions to quasi-metallic clusters. Reproduced from [77] with permission of The Royal Society of Chemistry.

Concluding remarks

Although widely applied as an analytical technique, solid-state NMR continues to be a highly active area of research in itself, which engenders continual developments in experimental hardware and methodology. These ongoing advances are helping to deepen and transform our understanding of battery material structures and mechanisms, so that their material properties can be optimised. For the study of Na-ion battery materials in particular, NMR has already provided considerable insight and will continue to do so as faster MAS rates become more widely available and advances in DNP methodology provide ever higher sensitivity and selectivity.

Acknowledgments

6.3. Nanoscale characterisation of the local physical properties of Na-ion batteries, electrodes, and interfaces

Oleg V Kolosov[1,2] *and Yue Chen*[1,2]

[1] Department of Physics, Lancaster University, Bailrigg, Lancaster LA1 4YB, United Kingdom
[2] The Faraday Institution, Quad One, Harwell Science and Innovation Campus, OX11 0RA, United Kingdom

Status

The majority of characterisation techniques enabling the current fast development of rechargeable batteries fall into three major categories—the traditional electrochemical performance measurements, such as galvanostatic charge/discharge and cyclic voltammetry; crystal and nanostructural characterisation, such as x-ray diffraction and electron microscopy (EM); and NMR, XPS, and soft x-ray spectroscopy, which also provide chemical component analysis. The long history of battery technology development has amassed an in-depth understanding of electrochemical processes based on the characterisation of these electrochemical, structural, and chemical properties, derived from the above electroanalytical methods and their techniques. While these properties are essential, as shown in figure 32, the physical properties, including the mechanical, thermal, and electrical properties, of the materials deployed in Na-ion batteries are no less important.

Growing attention has recently been paid to revealing the nanomechanical properties of sodium nanodendrites in high-capacity Na-metal anodes [242], and the generation of interfacial stress in layered TMD [243] anodes due to the intercalation of the larger Na ions compared to Li ions. It is also well established that the Young's moduli of the SEIs on the negative electrodes define the battery's resistance to dendrite growth whereas the stability of polycrystalline cathodes crucially depends on the mechanical integrity of their components during the charge–discharge cycle expansion and their resistance to crack propagation [244]. The electrical conductivity of the electrodes and the ionic conductivity of the interfacial layers are the key limiting parameters for battery rate performance, and the thermal conductivity is another factor that defines battery operation in demanding applications. Therefore, measuring mechanical moduli, local stress, electrical conductance, and thermal transport in real-life batteries and model systems, and correlating these data with electrochemical and structural analyses will provide an essential platform for overcoming existing challenges and for the development of novel paradigms in Na-ion batteries.

Current and future challenges

One of the major challenges in the nanoscale measurement of the physical properties of electrodes and interfaces in NIBs is linked to the wide range of length scales involved. The electrode thicknesses are typically a few tens of micrometres (μm), the individual cathode electrode particles are a few μm across, and hard carbon particles in the battery anodes are on the nm length scale. The SEI layers are several tens of nm thick, while the cathode electrolyte interphase (CEI) can be as little as a few nm thick [245]. Na-ion incorporation occurs at interatomic distances that are on the sub-nm length scale. The successful investigation of this phenomenon requires a means of characterisation that can provide local measurements of physical properties with the commensurate nanoscale lateral resolution. Another major challenge is the extreme heterogeneity of the battery components. For example, the mechanical moduli range from sub-MPa values for the outer layers of an SEI-facing electrolyte to hundreds of GPa for cathode polycrystalline particles, and the ionic conductivity of the sodium ranges from $\sim 10^{-2}\ \mu$S cm^{-1} when crossing the SEI layers at the electrode–electrolyte interface to $\sim 10\ \mu$S cm^{-1} within the interlayers of the TMD anode. Lastly, but most importantly, the dynamic evolution of nanoscale physical properties, which are closely related to the sodium ion transport and electrolyte electrochemical/thermal decomposition, is exceptionally difficult to 'look' at, since sodium battery active materials and interfaces are buried deep within the volatile liquid electrolyte under battery operating conditions.

To satisfy these complex characterisation capability requirements at multiple length scales and address the electrode heterogeneity and the fluidic electrochemical environment, scanning probe microscopy (SPM) has been applied for the micro/nanoscale characterisation of the dynamic and local physical properties of battery electrodes and interfaces. In these studies, model systems are often used, e.g., highly oriented pyrolytic graphite (HOPG) [246, 247] or the physical vapor deposition/chemical vapor deposition of binder-free electrodes [245] as a proxy for the battery electrode, enabling the direct observation of SEI formation and ion intercalation through nanomorphology measurements of the electrode surface. However, it is not sufficient to only investigate the surface physical properties of these structures; tools are required that can access the inner structures of electrodes and interfacial layers. The direct nanoscale characterisation of multiple complementary physical properties of real-life batteries, for *ex situ* and *in-situ*/*operando* cases, remains the holy grail of Na-ion characterisation requiring an innovative solution for three-dimensional (3D) sample preparation.
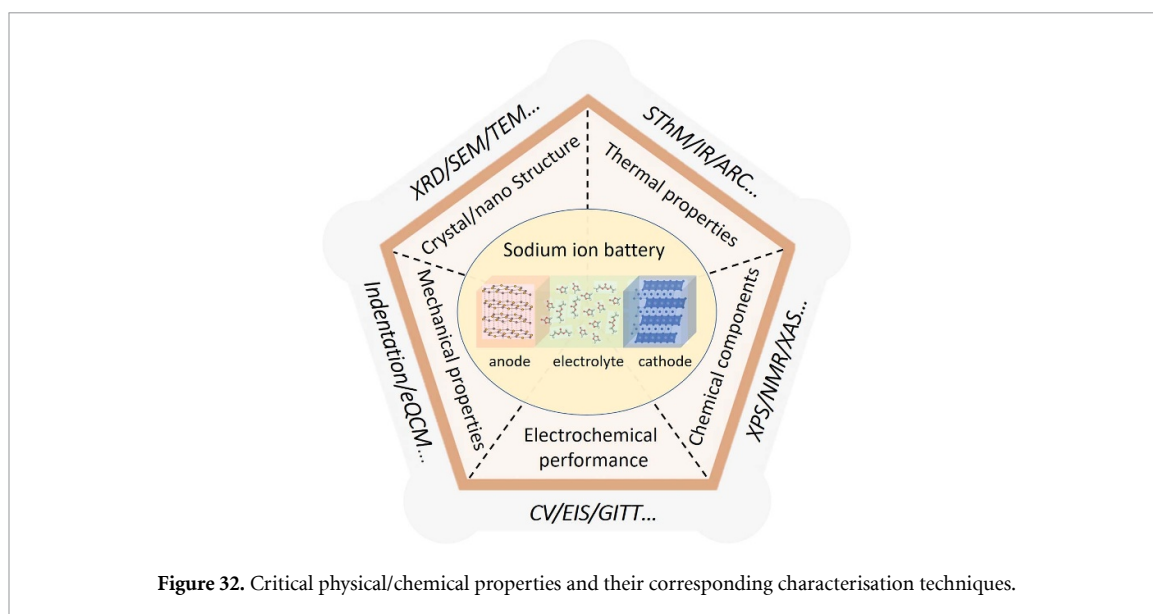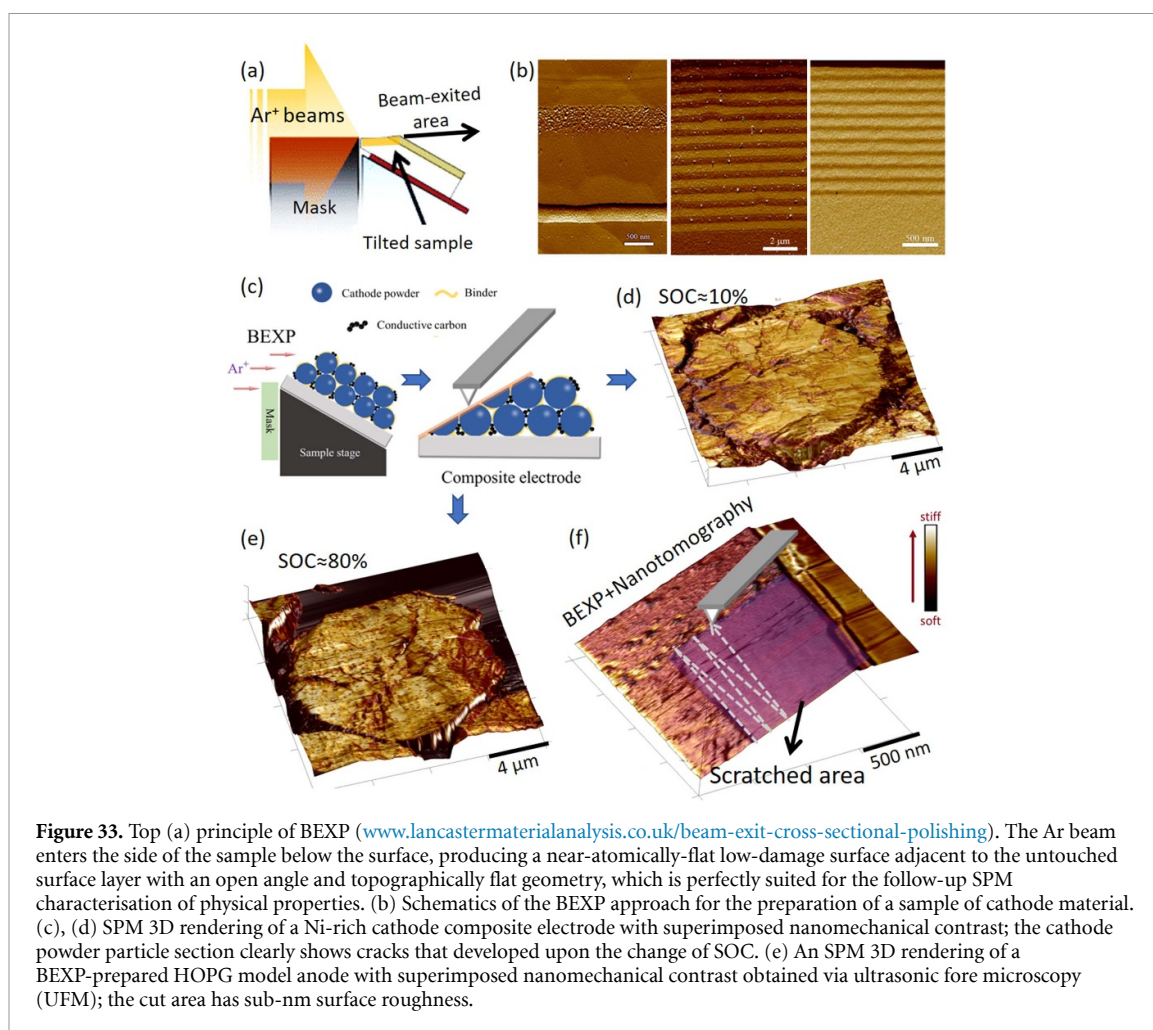
Figure 32. Critical physical/chemical properties and their corresponding characterisation techniques.

Advances in science and technology to meet challenges

Among the vast number of techniques used for sodium battery interface analysis [248], SPM occupies a unique place, as it can provide both the required nanoscale spatial resolution, as well as being sensitive to the local physical properties of the studied material. Using SPM in the electrochemical environment on the model HOPG substrate allowed the study of the initial stages of SEI growth [246], revealing the dynamics of ion intercalation. The downside of SPM is that it requires nanoscale flat samples and mainly allows the investigation of surfaces rather than 3D structures. Focused ion beam (FIB) sectioning, widely used in EM measurements, is inadequate for SPM, as the sections produced are too small to be measured efficiently and, more significantly, the Ga ions can drastically change the physical properties of the studied material during sectioning. As shown in figure 33(a), a much more suitable approach is to use advanced nanosectioning using multiple Ar-ion beams, known as beam-exit cross-section polishing (BEXP), which produces a close to atomically flat surface with minimal damage, due to the non-reactive nature of Ar atoms. In the BEXP method, the open-angle tilted section adjacent to the intact surface of the sample produces a perfect area for the material-sensitive SPM, additionally expanding the interfacial area by a factor of 5–10, allowing the study of interfaces a few nm thick (such as the superlattice in figure 33(b)) with a total section area on the sub-mm length scale. By using a dedicated material-sensitive SPM contrast, such as nanomechanical via sample excitation, ultrasonic force microscopy (UFM), or tip-excitation waveguide UFM [249], the conductance of the cross-sectioned samples can reveal the local physical properties of the internal structure at nanoscale resolution. Figures 33(c)–(e) show a diagram of a commercial Ni-rich cathode polished by BEXP and the prepared sample's cross-sectional UFM images. In figures 33(c) and (d), the cathode particles at different states of charge (SOC) in the binder and the conductive carbon black matrix can be clearly distinguished. Additionally, the crack network within the grain section is visible in the nanomechanical UFM images, which could serve as a perfect model for *operando* SPM studies of dynamic crack propagation in cathode polycrystalline particles, revealing the fundamentals of capacity degradation in sodium–transition-metal oxide cathodes.

Another approach for examining 3D structures is to use direct *in situ* sectioning of the sample through nanotomography [250], in which the tip mills out the surface along the section plane, followed by nanomechanical, nano-electric, or surface-potential measurements. Such an approach is more suitable for the sectioning of softer layers, such as the SEI, in which follow-up nanomechanical SPM probes all the layers, starting from the double layer in the electrolyte, through to the soft and then more compact SEI layers at the interface with the anode. As shown in figure 33(f), when BEXP and nanotomography are combined, the organic adsorption layer that forms on the atomically flat cut slope of the HOPG anode can be scraped by the SPM tip. This allows for the uncovering of the subsurface physical properties of electrodes and interfaces, which could be the 'buried treasure' in the study of Na-ion batteries.

Overall, SPM will allow the investigation of the highly important Na-ion intercalation phenomena in carbon-based [247] and other electrodes by observing both the nanoscale morphological (*operando* dimensional change) and physical parameters (*operando* mechanical compliance that was shown to affect the mechanical properties during atomic intercalation) [251]. Other physical parameters, such as the surface

Figure 33. Top (a) principle of BEXP (www.lancastermaterialanalysis.co.uk/beam-exit-cross-sectional-polishing). The Ar beam enters the side of the sample below the surface, producing a near-atomically-flat low-damage surface adjacent to the untouched surface layer with an open angle and topographically flat geometry, which is perfectly suited for the follow-up SPM characterisation of physical properties. (b) Schematics of the BEXP approach for the preparation of a sample of cathode material. (c), (d) SPM 3D rendering of a Ni-rich cathode composite electrode with superimposed nanomechanical contrast; the cathode powder particle section clearly shows cracks that developed upon the change of SOC. (e) An SPM 3D rendering of a BEXP-prepared HOPG model anode with superimposed nanomechanical contrast obtained via ultrasonic fore microscopy (UFM); the cut area has sub-nm surface roughness.

potential and conductance changes, when measured *ex-situ*, can provide additional information in such studies.

Concluding remarks

The real-space physical-property nanomapping of battery electrodes and interfaces via multifunctional SPM, combined with the efficient and artefact-free sample preparation approach via BEXP and nanotomography will provide a valuable characterisation toolbox for the development of the next generation of Na-ion batteries. Furthermore, it will allow the direct investigation of SEI stability and composition, the development of more robust cathode/anode–electrolyte interfaces, and the exploration of Na-ion intercalation, enabling the selection of a winning electrode–electrolyte combination.

6.4. Dissolution benchmarking of sodium-ion electrodes

Shahin Nikman[1,2] *and Stijn F L Mertens*[1,2]

[1] Department of Chemistry, Lancaster University, Lancaster LA1 4YB, United Kingdom
[2] The Faraday Institution, Quad One, Harwell Science and Innovation Campus, Didcot OX11 0RA, United Kingdom

Status

Loss of battery electrode inventory to dissolution processes is one of the major sources of capacity fading. In the lithium-ion field, much research has been conducted into the charge–discharge profiles and electrolyte formulations that contribute to dissolution, in particular, for electrodes based on manganese, nickel, and cobalt, which can be translated to sodium-ion chemistries (with some caveats) when similar electrode materials and electrolytes are used [252]. Na^+ ions have a 34% larger radius than Li^+ (1.02 vs. 0.76 Å) which causes a greater strain on the electrode materials during insertion and extraction. Sodium-ion electrodes also span a larger compositional range than current LIB materials, encompassing transition-metal oxides, alloying reactions, and conversion-reaction materials, and therefore enhance both the possible sources and consequences of electrode dissolution. While direct loss of active electrode material due to dissolution into the liquid phase is typically in the single-digit percentage of overall capacity loss, the presence of dissolved transition metals in the electrolyte is known to rapidly accelerate SEI formation, leading to near-complete passivation of the negative electrode. This so-called dissolution–migration–deposition (DMD) process is estimated to account for up to 30% of the overall capacity loss in manganese-oxide-based intercalation batteries [253].

Several strategies already exist to counteract electrode dissolution, such as heteroatom doping [254], coatings, and the use of concentrated electrolyte formulations, figure 34. These indeed improve the long-term stability, but typically at the expense of the power and/or energy densities of the electrode. Fast throughput techniques that can determine electrode dissolution rates as a function of electrode potential, time, and electrolyte formulation are therefore essential and urgent. Understanding the effect of electrolyte, solvent, and electrode composition on dissolution and battery longevity will lead to better-informed materials discovery for durable and efficient NIBs.

Current and future challenges

Due to their propensity to dissolve manganese, $LiMn_2O_4$ and Na_xMnO_2 electrodes are widely used for model studies. A primary challenge is to accurately identify the cause of electrode dissolution. For example, Hunter's mechanism of Mn^{3+} disproportionation into soluble Mn^{2+} and insoluble Mn^{4+} was confirmed in an aqueous solution but may differ in non-aqueous, fluoride-containing carbonate-based electrolytes. Recent studies have suggested that in non-aqueous electrolytes, Mn(III) is the dominant dissolved oxidation state. Other elements may also dissolve into the electrolyte, for example, vanadium from NaV_3O_8 cathodes [255].

As the rate of dissolution is proportional to the electrochemically exposed surface area, bulk characterisation techniques, such as x-ray diffraction may not be adequate. *In situ* surface-sensitive methods, such as electron energy-loss spectroscopy, extended x-ray absorption fine structure, and high-angle annular dark-field imaging show that de-intercalated λ-MnO_2 is chemically unstable [256]. However, only the surface layers break down to $Li_2Mn_2O_4$ and Mn_3O_4, where the average Mn oxidation state is much closer to three. The stability of the electrode therefore cannot be predicted, based on the bulk composition or the cell potential, which would indicate only an insoluble product. Such structural changes also induce stress in the host material due to changes in the lattice constant, leading to cracks and again increasing the exposed surface area. Although such methods have not yet been employed to elucidate sodium-ion electrode dissolution, the intercalation of Na^+ induces more strain than the intercalation of Li^+ due to its larger radius, potentially leading to more cracks, a greater exposed surface area, and hence, enhanced dissolution. Heteroatom dopants, such as iron and nickel in, for example, $Na_{0.67}Fe_{0.5}Ni_{0.15}Mn_{0.65}O_2$ may increase stability against manganese dissolution [257], but may themselves dissolve following chemical or electrochemical pathways and increase the potential range in which dissolution takes place. The dissolution problem is further compounded in sodium-ion anodes, in which elements such as tin, antimony, phosphorus, titanium, copper, iron, or sulphur can produce soluble byproducts during operation, whereas graphite does not.

Solvents, electrolytes, and contamination from moisture or CO_2 can further accelerate the degradation of sodium cathode host materials at a much higher rate than their lithium counterparts [258]. The dissolution of ions into the electrolyte solution depends on the particular electrolyte formulation, ion solubility, and potential programming of the battery cell, which encompasses a huge array of variables. The lack of direct, real-time dissolution measurements greatly compromises the time and potential resolution of dissolution information. To date, most dissolution diagnosis has been conducted post-mortem. For example, inductively coupled plasma (ICP)-based elemental analysis of the electrolyte has been used to identify ppm-range
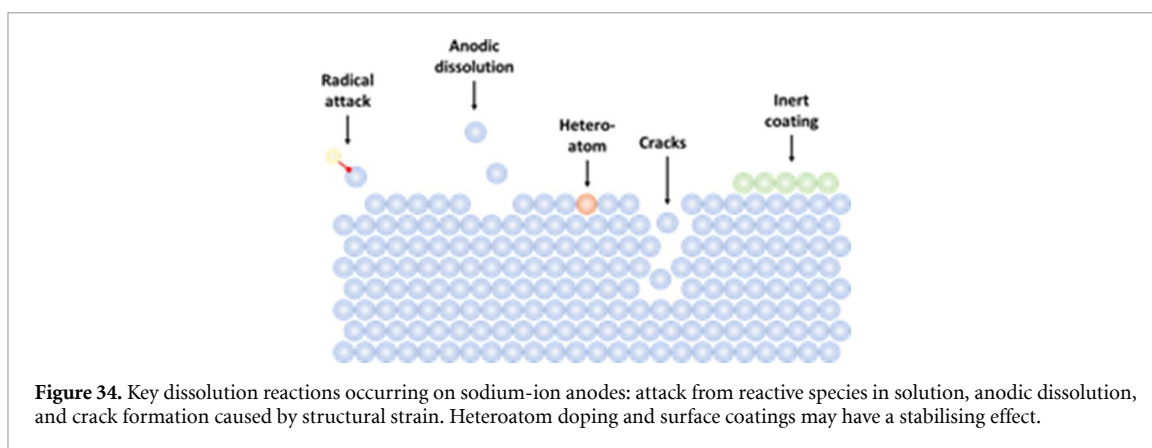
Figure 34. Key dissolution reactions occurring on sodium-ion anodes: attack from reactive species in solution, anodic dissolution, and crack formation caused by structural strain. Heteroatom doping and surface coatings may have a stabilising effect.
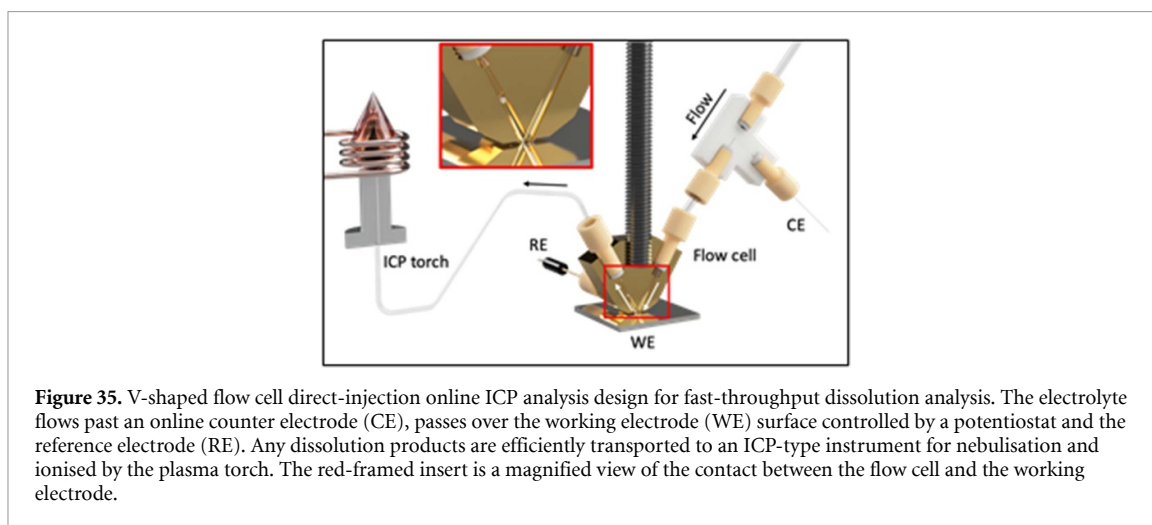

Figure 35. V-shaped flow cell direct-injection online ICP analysis design for fast-throughput dissolution analysis. The electrolyte flows past an online counter electrode (CE), passes over the working electrode (WE) surface controlled by a potentiostat and the reference electrode (RE). Any dissolution products are efficiently transported to an ICP-type instrument for nebulisation and ionised by the plasma torch. The red-framed insert is a magnified view of the contact between the flow cell and the working electrode.

concentrations of dissolved iron from sodium iron hexacyanoferrate electrodes as a function of the surface coating strategy [259]. Energy-dispersive x-ray spectroscopy (EDS) is also commonly used, for example, to analyse the separator in order to identify trapped ions, or to analyse the negative electrode to identify DMD products from $Na_{0.67}MnO_2$ electrodes [260]. The preparation and *ex situ* handling of such samples increases experimental error and may compromise the reliability of the conclusions. Furthermore, full and half cells prepared in CR2032 coin cells do not isolate a single cause of dissolution, as the effects of electrode arrangement, cell pressure, the counter-electrode material and current collectors must also be considered.

Open questions are whether electrode dissolution is electrochemically or chemically induced, i.e., which are the most significant dissolution pathways, and their accurate quantification. Methods of detection must be highly sensitive, as dissolution only affects a small part of the overall electrode mass, and setups must rigorously exclude agents known to accelerate dissolution, such as water, as otherwise, artefacts will arise. An adequate dissolution monitoring system must therefore be carefully designed.

Advances in science and technology to meet challenges
ICP-based instruments are routinely available, and allow highly sensitive elemental analysis, with detection limits of sub-ppb using optical emission spectroscopy (ICP-OES) or even sub-ppt using mass spectrometry (ICP-MS). Primarily used for aqueous samples, these are, to a certain degree, forgiving towards non-aqueous battery solvents and electrolyte salts (up to 0.1 M (ICP-MS) or 1 M (ICP-OES) without dilution). The observation of dissolution in non-aqueous electrolytes is challenging, due to the need for oxygen and water to be excluded from the electrolyte. Prohibitive factors include instrument corrosion from highly reactive electrolytes and the high cost of many high-quality non-aqueous electrolyte solutions.

Recent advances in electrochemical flow cell design have enabled direct observations of the dissolution of candidate electrode surfaces in non-aqueous environments under potential or galvanostatic control. Typically, the electrochemical flow cell outlet is directly connected to the ICP nebuliser by tubing, in the so-called direct-injection analysis. Successful examples include the flow-through scanning flow cell (FT-SFC) introduced by Mayrhofer *et al* [261], which incorporates a V-shaped channel design for efficient transport of dissolution products, figure 35. This type of cell has also been manufactured by 3D printing and successfully

used for fast and high-throughput dissolution detection [262]. However, intricate new cell designs are not always necessary. Markovic's group [263] fitted an ICP-MS inlet to a rotating disc electrode tip in a stationary probe rotating disc electrode (SPRDE-ICP-MS), adding the advantage of uniform and well-characterised convection. Hence, hyphenation of existing apparatus to increase time- and potential-dependent dissolution information output in accelerated degradation tests becomes possible.

While ICP-based analytical instruments identify the atomic mass/charge ratio (ICP-MS) or element-specific emission spectra (ICP-OES), valuable information about the oxidation state of the dissolved species, i.e., speciation, is lost. Other *in situ* techniques may additionally allow speciation, e.g., rotating ring–disc electrode [264], electron paramagnetic resonance, or UV–vis [265] measurement of the electrolyte in *operando* cells. However, interference from solvents, electrolytes, or other solution species must be accounted for.

Concluding remarks

Post-mortem analyses and *ex-situ* observations of battery electrodes limit our understanding of the degradation processes that are the main causes of capacity fading and the premature failure of batteries. Today, a detailed understanding of the atomistic causes of the dissolution of electrode materials remains elusive, even for the most basic model electrodes. The development of online analysis techniques that quantify time-resolved dissolution as a function of potential and other experimental parameters can revolutionise our understanding of battery electrode degradation, as an essential step towards its mitigation and the rational design of resilient new battery electrode materials. Advances in spectroelectrochemical cell design and analytical instrumentation can unlock detailed dissolution probing, revealing not only elemental quantities but also chemical speciation.

Acknowledgments

7. Scale-up and manufacturing

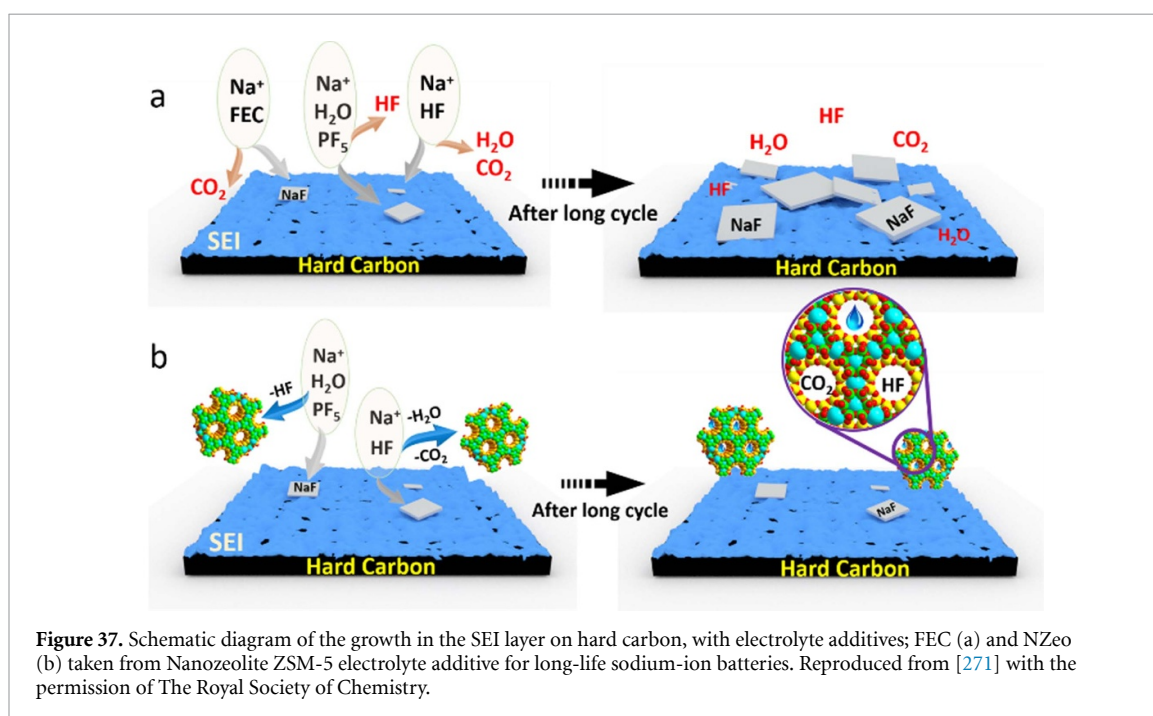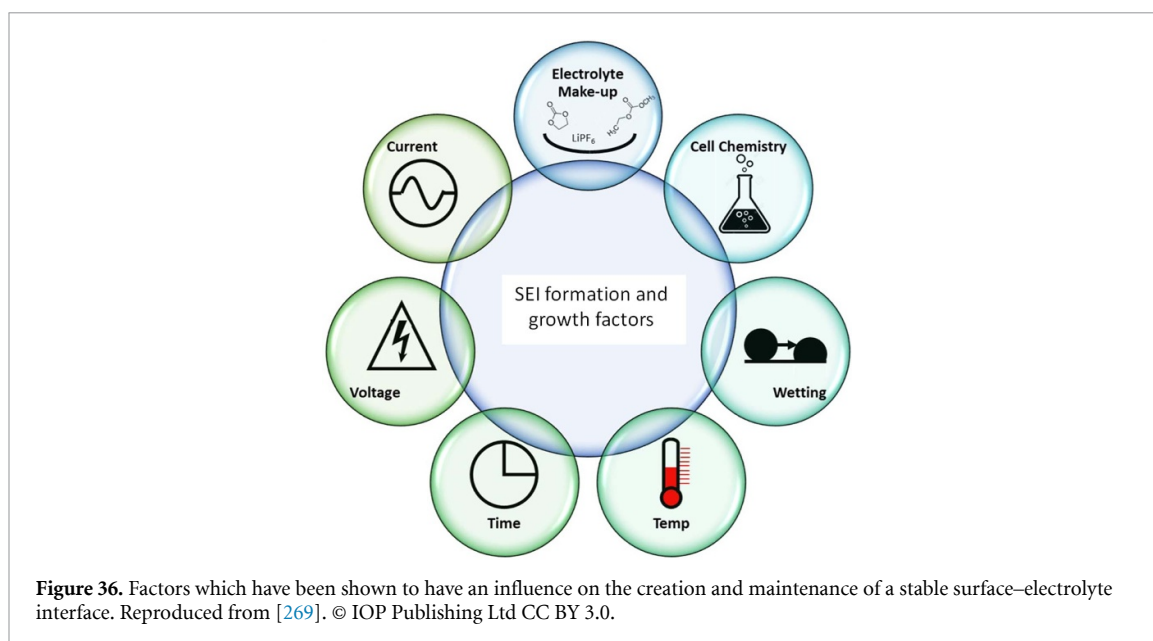## 7.1. Cell performance and requirements
Emma Kendrick
School of Metallurgy and Materials, University of Birmingham, Edgbaston, Birmingham BT15 2TT,
United Kingdom

Status
Research into Na-ion batteries (NIBs) began in the 1970s and 1980s and was usurped by LIBs in the 1990s. NIBs have recently re-emerged as a potential sustainable and lower-cost alternative to LIBs [266]. They offer an energy storage solution which is not as reliant upon geographically localised raw or critical materials. Several commercial entities have built up around this technology, with demonstrator cells and prototype battery packs, offering the potential for lithium-ion and lead-acid battery substitutions in current markets [71]. Sodium can be extracted from seawater, anode materials can be obtained from renewable sources, and cathodes generally contain iron and manganese, rather than high levels of cobalt and nickel. The manufacturing processes are expected to be the same as those for LIBs, and therefore, no investment is required in new manufacturing lines. The cost difference between LIBs and NIBs can therefore be considered to be due to materials and performance only [184]. NIBs are unlikely to ever reach the energy densities (gravimetric and volumetric) of LIBs, due to their lower operating voltages and lower active component densities [267]. The 'drop-in' manufacturing approach also creates limitations on NIB development, in terms of the design of components and cells. The thickness and design of the electrodes are limited by these tape-casting methods. Opportunities for differentiation consequently lie in high power, safe, and long-life NIB technologies. A sustainable circular-economy perspective on materials, manufacturing, and end-of-life could also offer significant advantages over current battery technologies. Alternative manufacturing methods may offer solutions for improved electrode kinetics, the engineering of more efficient electronic and ionic transport pathways, and simplified recycling. Sustainability needs to be considered within a greater holistic outlook, however; the use of low-cost and highly abundant materials may mean, for example, that the reclamation and reuse of these materials never becomes economically viable. Consideration of the hierarchy of recycling, re-use, or second life within the circular economy is required. Therefore, lifetime, in particular, is a key performance parameter for sodium ion batteries, as the value of the materials reclaimed from recycling will not be sustainable if low-cost and abundant materials are used [268].

Current and future challenges
There are several research challenges which need to be addressed in the field of NIB technologies, one of which is long life, which is required to improve sustainability. Advancements in LIB energy density, both volumetric and gravimetric, are required for applications reliant upon this technology, and there is an immense amount of work ongoing to develop new anode and cathode materials. However, the lifespan of the cells is governed by various chemical and cell engineering optimisations relating not only to the materials but also to the design of electrodes and cells and their operation (figure 36) [269]. For NIBs, mass balance optimisation between positive and negative electrodes is critical for high-energy and long-life batteries. Each cathode and anode material has a first-cycle coulombic inefficiency related to electrolyte decomposition and irreversible sodium movement from the positive to the negative electrode. As a result, an interface (surface–electrolyte interface (SEI)) forms on the anode, causing less sodium to be available (reducing capacity) for shuttling between the positive and the negative electrodes. The mass balance and the voltages chosen therefore have a large effect upon the effectiveness of this interface formation at stabilising the electrolyte against decomposition, and consequently, the energy density of the cell [270]. The stability of the interfaces on the positive and negative electrodes is reliant on many factors, and it is known that the stability of NIB interfaces is inferior to those of LIBs due to the highly soluble nature of sodium salts. Much work is required to understand the formation and changes that occur at these surfaces and interfaces during the lifetime of the cell, and some progress has been made in this area (figure 37) [271]. These interfaces are not only important for longevity but also for safety. Dendrites and plating can occur very readily in sodium-ion cells, and this is not only controlled by the electrolyte composition and the ability to form low-resistance, stable interfaces, but also through electrode design. For example, low and inhomogeneous electronic conductivities within the electrode can lead to changes in current density across the electrode, resulting in sodium plating and dendrite growth in areas with high resistance. Improving the electronic conductivity of the electrode with conductive additives, such as carbon black, can aid electron transport but additionally leads to increased electrolyte side reactions and hence ongoing growth in the SEI. This, in turn, blocks pore networks for ionic transport and increases local resistance [272]. Understanding the combined effects of

Figure 36. Factors which have been shown to have an influence on the creation and maintenance of a stable surface–electrolyte interface. Reproduced from [269]. © IOP Publishing Ltd CC BY 3.0.

Figure 37. Schematic diagram of the growth in the SEI layer on hard carbon, with electrolyte additives; FEC (a) and NZeo (b) taken from Nanozeolite ZSM-5 electrolyte additive for long-life sodium-ion batteries. Reproduced from [271] with the permission of The Royal Society of Chemistry.

these changes upon the lifetime, capacity, and ultimately the degradation mechanisms will be essential to extend the lifetime of cells and make further NIB optimisations.

Advances in science and technology to meet challenges

In order to achieve longer lifetime NIBs, a greater understanding of the interaction of all the cell components and competing ageing and degradation processes is required. This will be different for each cell chemistry, voltage window, and electrode design. An understanding of the interfaces is of the greatest importance for both cathodes and anodes. These interfaces control the transport properties of sodium into the electrodes and influence the type and extent of microstructural changes during the ageing of the electrode. The compositional makeup of these interfaces requires optimisation through electrode and electrolyte design. Changes in these interfaces and their effects on the physical and chemical properties will also affect performance and safety. This offers opportunities for advanced, data-driven, and multiphysics models to be partnered with experimental data to provide greater in-depth information about the changes in the fundamental kinetic and thermodynamic properties of the cell for various compositions and designs.

Advances in parameterisation methods for LIBs could be translated to NIBs, offering novel, unique insights into cell construction and component optimisation [273].

Moving away from traditional LIB manufacturing processes is essential to achieve step changes in sustainable cell designs. Novel processes are required to provide improvements in electrode 3D electronic and ionic transport pathways. With improvements in electrode design, less current collector and packaging materials are required, which improves energy density and reduces waste at the end of battery life. Novel methods of embedding electronic conductors in active materials without using high-cost and highly resistive polymeric binders to adhere them to metallic current collectors could provide the step change required. In addition, designs that enable simple manufacturing and subsequent disassembly for material reclamation will enable greater value from material recovery and reuse, creating a sustainable circular economy for NIBs. The ultimate design intent would be to use no binder, however moving to renewable sources for water-soluble binders, such as those based on algae and cellulose, may also improve recyclability prospects. Designing for recycling and disassembly is a key area which can capitalise on the benefits of this set of materials and unlock the potential of NIBs.

Concluding remarks

An economically viable NIB should be considered with respect to the sustainability potential of a circular economic model rather than purely the first-life cost of materials and manufacturing. Consideration of lifetime performance is required for both first life and second life, with recovery and recycling of cell components at the end of life. The current focus is upon matching LIB performance criteria. However, with rapidly changing markets for energy storage solutions, NIBs offer different opportunities for new cell design and manufacturing processes, allowing a holistic approach to sustainability. A focus upon developing longer-life batteries is required to achieve this. The optimisation of electrolyte and electrode designs to reduce interface resistance and dendrite growth will improve both longevity and safety, while new manufacturing processes and cell designs are required for sustainable end-of-life solutions. Materials and components can then be easily and repeatedly manufactured, reconditioned, disassembled, and remanufactured. In this way, the challenges of both the performance and economics of sodium-ion batteries can be overcome by combining novel materials, processes, and products with advanced material recovery, repurposing, and recycling.

Acknowledgment

7.2. Applications and scale-up: manufacturing

Stewart A M Dickson[1,2] *and John T S Irvine*[1,2]

[1] School of Chemistry, University of St. Andrews, St. Andrews KY16 9ST, United Kingdom
[2] The Faraday Institution, Quad One, Harwell Campus, OX11 0RA, United Kingdom

Status

The manufacture of batteries is often overlooked at a research level, due to the importance of finding new, higher-energy electrode materials, and solving the challenges faced in cell chemistries at smaller scales. However, when producing large-format cells, its importance in achieving the optimal cell performance is paramount. As demand increases further, together with the growing applications of LIBs, the availability of manufacturing facilities has also increased. Europe has multiple 'Gigafactories' in the pipeline, with examples such as Northvolt, who are expected to reach 32 GWh by 2023. Similar or larger-scale factories in China and beyond are also in the pipeline, backed by larger companies such as Tesla. As noted by the Faraday Institution, eight 'Gigafactories' will be needed by 2040 to satisfy UK battery demands, which requires one to be established at least every two years from 2020 [274]. Projects such as those recently proposed by AMTE Power and Britishvolt are the start of promising large-scale manufacturing of LIBs within the UK, with the hope that this can complete the chain to take materials from powder to power, thus attracting end users of battery technology by shortening supply chains [275].

NIBs are beginning to reach a technology readiness which requires large-scale production, as demonstrated by Faradion, with recent orders from Australia and India [276]. NIBs will see use in large, decentralised power applications, and small-scale deployments will be required to assist in load balancing from intermittent-power farms, such as wind and solar [277]. Factories can switch between lithium and sodium chemistries, due to their 'drop-in' nature, as long as the technologies remain similar enough in their production (figure 38).

This helps to reduce barriers to entry and initial costs, as the creation of new facilities is not required; however, the gap between commercial and laboratory technologies still needs to be bridged to facilitate material advances and their application in larger cells. Additionally, research institutions often lack access to facilities which can help to realise materials at larger scales. By improving this connection, especially through links between industry and academia, it is hoped that an acceleration of research towards manufacturing readiness can be achieved.

Current and future challenges

Although some good parallels can be drawn from LIB manufacture, there are still limitations to how this can be applied to NIBs, due to differences in the materials used. When changing any physical property of a material, such as particle size, crystal structure, morphology etc., this also alters the processing parameters, thus impacting electrochemical performance. Similarly, changing the processing procedures of an electrode material, for example, slurry preparation or electrode modifications, can also influence both its structure and its maximum performance (figure 39) [278]. Therefore, every material must be treated differently to achieve this fine balance between every parameter.

Most of the challenges within manufacture lie at a materials level. Complex multi-step procedures can be used to produce grams of material for research purposes. However, these techniques may not be feasible when producing the kilogram amounts required for larger cells. Material morphologies, such as the creation of high-surface-area particles, will assist with electrochemical performance. Additionally, some layered sodium oxides of interest are extremely sensitive to air and moisture, which can make handling of large quantities more complex, and imposes additional requirements such as additives in slurries to improve their longevity. It is possible to modify these materials to improve their stability in air or to reduce the sodium content, but this can be detrimental to electrochemical performance [279].

Electrode slurries at the coin-cell level also have standardised formulations; little attention is paid to metrology and dry powder mixing, and they include large amounts of binder and carbon to overcome material limitations, such as poor conductivity. Reducing these amounts to increase the energy density of cells is vital at large scales, as commercial cells sometimes reach up to 98 wt.% active material. However, such changes require specific testing and optimisation of every electrode slurry. After coating, the influence of drying and the application of calendering as a technique to improve electrode density and adherence are also not routinely considered within the research environment. These steps also require individual tailoring to maximise electrochemical performance without negatively impacting electrode structure.

Although materials and processing are key to cell performance, other considerations, such as electrode balancing and geometry, tab placement, and safety aspects related to long-term storage and long-term cycling which are not routinely studied at smaller scales also become relevant. Due to the infancy of NIB technology, little research exists for many of these other areas, though it is fortunate that many of these can
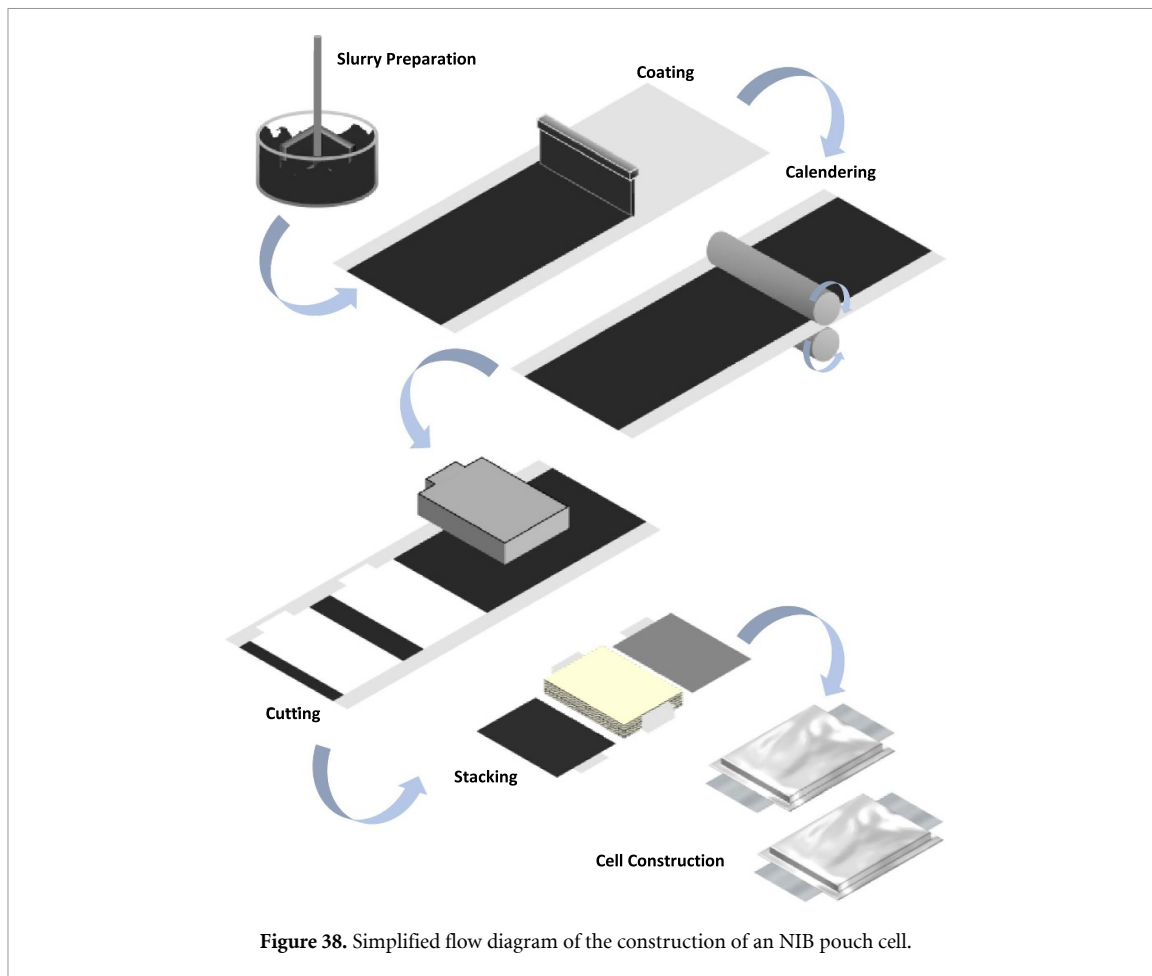
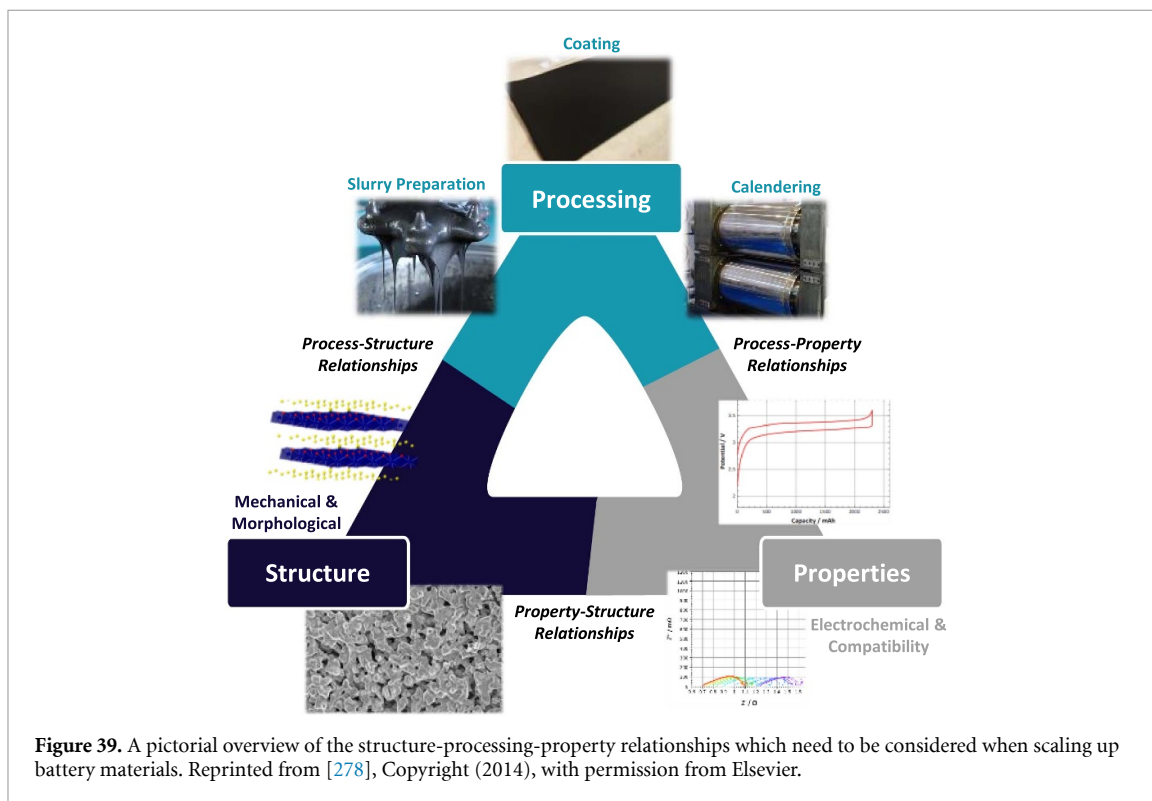**Figure 38.** Simplified flow diagram of the construction of an NIB pouch cell.

Figure 39. A pictorial overview of the structure-processing-property relationships which need to be considered when scaling up battery materials. Reprinted from [278], Copyright (2014), with permission from Elsevier.

be directly transferred from LIB research, and challenges can be jointly tackled. Some advantages and benefits which can be discovered are, however, solely for NIBs, such as the ability to internally short a pouch cell with no performance impact, as demonstrated by Faradion [277].

Advances in science and technology to meet challenges

In general, a better understanding is required of how to produce and process materials, as there is very little information that specifically relates to NIBs at larger scales. Ideally, techniques already used to scale up electrode materials to significant quantities could be implemented. Co-precipitation is the most widely utilised approach for materials scale up, and several researchers have produced well-defined structures of layered sodium oxides for NIBs, which required additional firing steps after the initial precipitation, which can be energy intensive [280]. Prussian blue analogues (PBAs) can also be produced by co-precipitation, and do not require further processing, reducing cost and time. Co-precipitation is not necessarily suitable for all electrode materials, depending upon their stability and composition. Therefore, new routes such as microwave synthesis could be optimised to provide alternatives.

Electrode processing is also a significant focus, as it contributes a large amount to the cost of cell production. Tape casting is the technique most widely utilised to produce electrode sheets; however, the use of N-methyl pyrrolidone (NMP) increases expense, due to the need for solvent-recovery systems. The development of newer electrode slurry combinations, particularly aqueous chemistries, would reduce this cost. Additionally, several researchers have begun to develop 'solvent-free' casting techniques in a bid to remove this issue entirely and have greater control of electrode morphologies, though these advances are likely to take some time to become commercially viable [281, 282].

Perhaps one of the biggest advances which will help manufacturing immensely is the use of simulation and modelling. Computational modelling of cells and packs has become much more viable in recent years and by varying parameters, can allow for rapid analysis of changes to electrode composition and cell design, obtaining incremental performance gains when applied experimentally. One example of modelling to identify improvements in pouch cells is that of tab placement, where the benefits of an opposite-ended tab design were shown to improve electrode usage and temperature management [283]. Greater practical application is required to demonstrate the benefits of these findings, and whether there are correlations with simulations.

Finally, in terms of NIBs, there needs to be a much greater understanding of the long-term performance of cells, especially as size increases, which will become better understood with time. Additionally, the use of half cells with metallic sodium does not realise true cell chemistries, which instead use hard carbon anodes, though the use of half cells is also a common practice for new LIB materials. Any performance issues or irregularities in a half-cell setup are not a true representation of what may occur in a scaled-up cell configuration; thus, a greater emphasis on testing materials in three-electrode or small full-cell setups is essential to ensure that materials can be scaled up without issue.

Concluding remarks

Unquestionably, as the field of NIBs expands over the next decade, greater cooperation between materials development and manufacturing will be required to ensure that advances can be easily transferred from small scale to large scale. Though pouch cells have been considered in this text, there are multiple formats for batteries which should all benefit from this focus. If LIB manufacturing lines can be converted to produce NIBs, this would help to drastically reduce costs further and allow for better knowledge transfer, making NIBs an attractive low-cost option. However, there are still many NIB-specific challenges which need to be tackled, mainly by improving knowledge about the processing of electrode materials, and their inherent long-term safety, which both require greater study.

Acknowledgment

8. Industrial targets and techno-economic analysis

8.1. Industrial targets
Ashish Rudola, Ruth Sayers and Jerry Barker
Faradion Limited, The Innovation Centre, 217 Portobello, Sheffield S1 4DP, United Kingdom
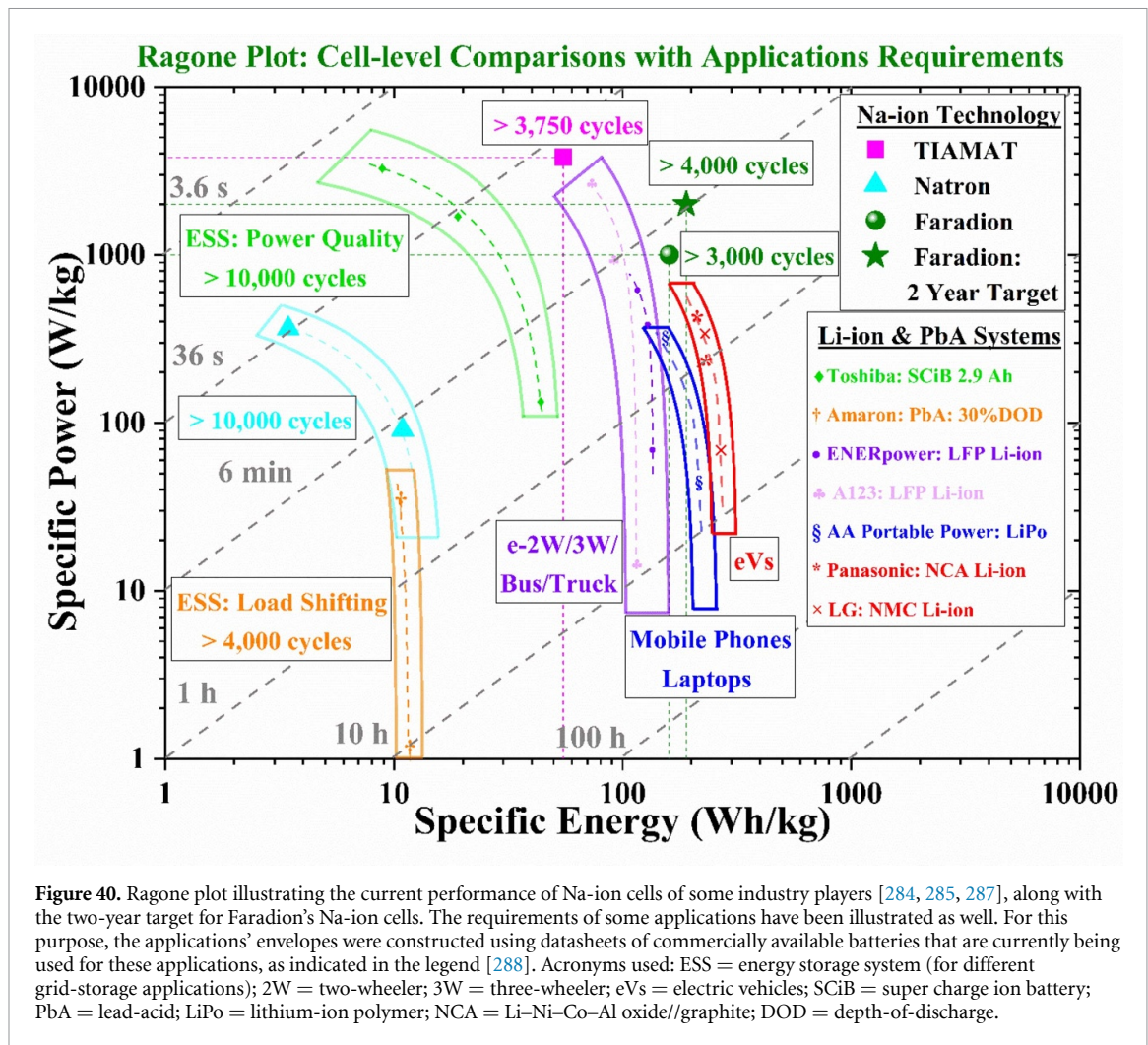
Status

Faradion Limited, established in 2011, was the first non-aqueous Na-ion battery company in the world. Since then, several Na-ion companies have been founded, covering a wide range of sodium-based chemistries. Faradion's technology utilises mixed-phase O3/P2-type Na–Mn–Ni–Ti–Mg layered oxide cathodes, hard carbon anodes, and non-aqueous electrolytes [284]. Other companies reliant on carbon-based anodes and non-aqueous electrolytes include the French company, Tiamat, whose cathodes are based on the polyanionic $Na_3V_2(PO_4)_2F_3$ [285], the Chinese company HiNa Battery, which utilises O3-type Na–Cu–Fe–Mn layered oxide cathodes [286], and the Swedish company Altris AB, based on Prussian blue analogue (PBA) cathodes. In contrast, US-based Natron Energy has built its Na-ion technology around aqueous solvents and PBA-based cathodes and anodes [287].

From the above, it can be seen that there is already a diverse array of Na-ion chemistries available in the industry. This is important, as different markets/applications have different requirements and might require unique solutions – the battery of choice needs just the right combination of cost ($ kWh^{-1}), energy density, stability/reliability, power rating, charge acceptance, and temperature performance. As such, figure 40 presents a Ragone plot covering several main market applications with their specific energy/power envelopes (gauged by the datasheets of existing battery technologies that are currently deployed in the market for these specific applications) [288, 289]. It should be stressed that these are just a few examples of applications—there are others with different performance requirements. We have also indicated the maximum performance of Na-ion cells from some industry players, as given by their datasheets or published reports [284, 285, 287]: for Tiamat and Natron, the values mentioned are correct as of mid-2018 and mid-2019, respectively, while for Faradion, values are accurate as of mid-2020. A Na-ion cell might be appropriate for utilisation for a particular application, as long as the application's envelope lies within its energy/power capabilities (gauged by the area below its respective dotted lines in figure 40) and it can meet other requirements such as cycle life. It is evident that current Na-ion technology could be attractive for most applications, apart from some types of consumer electronics and long-range electric vehicles.

Current and future challenges

Referring to figure 40, it can be seen that different Na-ion chemistries are better suited for different applications. For example, Natron's aqueous Na-ion chemistry has the lowest specific energy/power—this is expected, as aqueous electrolyte-based batteries cannot match the energy densities of their non-aqueous counterparts owing to the limited voltage window of water as an electrolyte solvent. Thus, Natron's Na-ion systems would be ill-suited for higher-energy applications, such as electric vehicles. However, Natron batteries' expected low cost, exceptional cycling stability, safety and efficiency would make them attractive for different ESS applications [287]. Tiamat's use of fluorinated vanadium-based polyanionic cathodes delivers Na-ion chemistry with excellent power capabilities albeit at the expense of energy density and raw material handling and availability [285]. Polyanionic cathodes represent an attractive avenue for high power and durable Na-ion systems. The challenge is to base them on more Earth-abundant elements, such as Fe and Mn. Unfortunately, pure Fe/Mn-based polyanionic cathodes generally either demonstrate relatively low operating potentials which limit their specific energies, or rely on bulky anionic groups [290], which limit their tap densities and, in turn, volumetric energy densities [284]. On the anode side, hard carbon can be prepared from a variety of precursors, including low-cost options, and has an attractive combination of desirably low operating potentials and high capacity (current hard carbon capacities almost match those of graphite Li-ion anodes). Hence, it is unlikely to be displaced as the anode of choice for high-energy applications in the foreseeable future. Furthermore, an intense research focus on hard carbon has resulted in significant improvements, not only in its cycling stability and rate performance but also in its charge acceptance capabilities—these, along with excellent compatibility with high-flash-point electrolytes, confer a high degree of safety to Na-ion systems [284].

Faradion's Na-ion cells currently deliver a good mix of energy and power densities with attractive costs, due, in large part, to cathodes devoid of costly and scarce elements, such as Co and V [284]. Table 2 illustrates how Faradion Na-ion cells compare with two types of state-of-the-art Li-ion cells: Li–Ni–Mn–Co oxide (NMC)//graphite and LiFePO$_4$ (LFP) cathode//graphite chemistries.

Figure 40. Ragone plot illustrating the current performance of Na-ion cells of some industry players [284, 285, 287], along with the two-year target for Faradion's Na-ion cells. The requirements of some applications have been illustrated as well. For this purpose, the applications' envelopes were constructed using datasheets of commercially available batteries that are currently being used for these applications, as indicated in the legend [288]. Acronyms used: ESS = energy storage system (for different grid-storage applications); 2W = two-wheeler; 3W = three-wheeler; eVs = electric vehicles; SCiB = super charge ion battery; PbA = lead-acid; LiPo = lithium-ion polymer; NCA = Li–Ni–Co–Al oxide//graphite; DOD = depth-of-discharge.

Advances in science and technology to meet challenges

Faradion's Na-ion cells currently deliver energy and power metrics in between those of NMC//graphite and LFP//graphite cells (table 2). They can respond at 10 C (continuous discharge), which compares favourably with LFP//graphite pouch cells (1–3 C) [293]. Faradion's Na-ion chemistry could be considered as a replacement for most applications where LFP//graphite is currently deployed. Table 2 also outlines targets for an 'energy cell' and a 'power cell,' that would solidify Na-ion technology as the go-to battery choice for different applications. The 'energy cell' is based on Faradion's Na-ion chemistry and seeks to satisfy some of the more energy-demanding applications, such as mobile phones, laptops, and some EVs. For this purpose, Faradion has devised a clear roadmap to achieve these targets by enhancing reversible capacities, increasing electrode densities, and boosting coulombic efficiencies with novel electrolytes and additives. In fact, we recently showed that the rates of increase of Faradion's Na-ion specific energies (and cycle lives) are significantly faster than those of Li-ion [284].

Even though current Na-ion technology can deliver high power, for applications such as power tools or drones, both power and energy densities need to be simultaneously acceptable. For such a 'power cell,' it might be challenging to meet the power and energy requirements using polyanionic cathodes at acceptable costs. We thus anticipate layered oxide cathodes will be used for such cells, relying on a majority, or a pure, P2 phase; it is well known that many P2-based Na-ion oxide cathodes can deliver excellent rate performance. Faradion's low cell BOM (bill-of-materials) is based on the absence of expensive cobalt, the use of aluminium (as opposed to expensive copper) current collectors, and the natural abundance of sodium, resulting in active materials and electrolyte salts that are cost-effective to produce. Future cell BOMs ($ kWh^{-1}) can primarily be reduced in three ways: (a) increasing energy density; (b) large-scale industrialisation of the material supply chain with (c) increasing production volumes, all reducing cost ($) with scale. The technical approach to achieving these target energy densities (stated in table 2) is listed above. The development of material supply chains and an increase in production volumes are already happening with the ever-increasing realisation of the performance benefits of Na-ion batteries (figure 40) and the ever-rising demand.

Table 2. Performance metrics of current NMC//graphite and LFP//graphite Li-ion technologies and those of Faradion's Na-ion cells. Industry targets for a Na-ion energy cell and a Na-ion power cell are also shown.

Parameter	Current technology			Na-ion energy cell: production[c] pouch cells		Na-ion power cell: production[d] ≤12 Ah pouch cells	
	NMC//graphite: cylindrical	LFP//graphite: 25 Ah—280 Ah pouch/ prismatic	Faradion Na-ion	2 year target	5 year target	2 year target	5 year target
Cell BOM* at equivalent cell sizes and volumes ($ kWh^{-1})			25%–30% lower than LFP//graphite pouch cells [282]	Future cell BOM targets are in line with maintaining 25%–30% lower than LFP//graphite, and taking into account the forecasted annual reductions in Li-ion costs [289]			
Specific energy (Wh kg^{-1})	240–270	140–175	160 (32 Ah pouch)	>190	>210	>140	>160
Energy density (Wh l^{-1})	670–750	240–360	290 (32 Ah pouch)	>350	>380	>230	>260
Specific power (W kg^{-1})	340–420	175–425	1000 (2 Ah pouch)	>1500	>2000	>2500	>4000
Power density (W l^{-1})	960–1200	360–770	1300 (2 Ah pouch)	>2700	>3600	>4000	>6400
Cycle life^a @ 80% DOD at ±1 C	600 [292]	3500–6000	3000 [284]	4000	8000	2000	4000
Pulse discharge	5–7 C for 10 s	4 C for 10 s	20 C for 10 s	20 C for 10 s	30 C for 10 s	30 C for 10 s	50 C for 10 s
T range, T_{min} to T_{max} (°C)	−20 to 60	−20 to 60	−30 to 60	−30 to 80	−30 to 80	−30 to 80	−30 to 80
RTEE^b at ±C/2 (%)	91	94	>93	>94	>95	>95	>95
Impedance (mΩ) at 1 kHz	<25 (21 700 cell)	<1.2 (25 Ah cell) <1 (120 Ah cell) <0.25 (280 Ah cell)	<2.5 (12 Ah cell)	<1.5 (12 Ah cell)	<1.2 (12 Ah cell)	<1.2 (12 Ah cell)	<1 (12 Ah cell)

* BOM: bill of materials. ^{a}Number of cycles to 20% capacity fade. ^{b}Round-trip energy efficiency, calculated from datasheets. ^{c}Production energy cell pouch: capacity ⩾10 Ah. ^{d}Production power cell pouch: capacity ⩽12 Ah, as power cells typically have thinner electrodes which result in lower capacities and smaller cell sizes. Note that LFP//graphite chemistry (like any battery chemistry) can deliver much higher power ratings in cylindrical cells (refer to figure 40), but in large-scale pouch cells between 25–280 Ah, the manufacturers recommend a maximum continuous discharge from 1 to 3 C [293].

Concluding remarks

Na-ion technology is rapidly catching up with the established Li-ion battery. It is revealed here that the energy/power densities of Faradion's Na-ion chemistry, which is devoid of scarce elements, such as Co and V, already surpass those of LFP//graphite systems. For most applications, the different types of Na-ion battery already possess the required performance attributes at the cell level, from negligible self-discharge to excellent temperature performance and the ability to be shipped/stored at 0 V [284], to name a few. Such performance must now be shown in actual demonstrations of large-scale systems, cycled according to the duty cycles required for an application in real-world settings. These demonstrations by various Na-ion companies are already underway, and with each successful demonstration, the market's confidence in this technology will progressively grow. If the near-term industrial targets for Na-ion energy and power cells can be met, mass penetration of Na-ion batteries in the market will be almost inevitable.

Acknowledgments

8.2. Techno-economic assessment

Emmanuel I Eweka[1] *and Grant S Stone*[2]
[1] Amte Power Ltd, 153A Eastern Avenue, Milton Park, Oxford OX14 4SB, United Kingdom
[2] Amte Power Ltd, Denchi House, Thurso Business Park, Thurso, Caithness KW14 7XW, United Kingdom

Status

Batteries using conventional Lithium-ion chemistries (LIBs) have long since been the power source solution of choice in a range of applications due to their high volumetric and gravimetric energy densities. Energy-dense, state-of-the-art LIBs in the pouch and cylindrical formats are currently achieving energy densities of up to 250 Wh kg^{-1} [294]. Beyond the current LIB designs, bulk all-solid-state batteries (ASSBs) are also being developed [295] to provide a significant increase in energy density (>400 Wh kg^{-1}) and safety and to address the range anxiety with electric vehicles. However, it is not believed that the first generation will be a cost-effective solution for stationary (grid, renewables, telecoms, and domestic) applications, and timescales to market for a competitively performing product are expected to be way beyond 2025. Other 'beyond-lithium' chemistries, such as Li-air and rechargeable magnesium batteries, are still at very early stages of R&D [294]. Current analyses are focused on non-aqueous battery systems. For stationary and telecoms applications, size and weight are less limiting than, say, cost, safety, ease of maintenance, reliability, and cycle life. Therefore, this techno-economic assessment focuses on applications where it is believed that NIBs will be competitive, at least in the near term (5–10 years) based on their current state of development. Some of these application areas include stationary and telecoms.

Their inherently low material cost and high technology safety make NIBs a very attractive proposition for stationary applications [252]. In addition to being made in similar formats to LIBs, NIBs can be made on existing LIB manufacturing lines—significantly reducing development costs and timescales. Current high-performance LIBs are considered less accessible (and safe) for these applications, although they have been proposed for second-life use [296]. Based on economics, Pb-acid and LiFePO$_4$ (LFP) are the current cathode chemistries of choice for stationary applications, compared to either LiNi$_{1-x-y}$Mn$_x$Co$_y$O$_2$ (NMC) or LiNi$_{1-x-y}$Co$_x$Al$_y$O$_2$ (NCA).

NIBs using a layered oxide, NaMO$_2$ (where M stands for Ni, Mn, Mg, or Ti) P2/O3-type structure and hard carbons (HCs) have been significantly advanced by Faradion and look very promising for stationary applications [297]. Low-cost NIBs based on Prussian blue analogue (PBA) anodes and cathodes and sodium vanadium fluorophosphates (NVPF) are also being developed by Natron energy and Tiamat respectively [298], but are considered less competitive for these applications, predominantly on a gravimetric and volumetric energy basis.

Using various cost models including BatPac, € kWh^{-1} has been estimated for NIB (NaMO$_2$/HC), LFP and NMC (40%Ni:40%Mn:20%Cobalt), 18 650 cells, respectively [267, 296]. The BatPac model included cell-design elements, depreciation, and warranty in addition to material and processing costs. The outputs from these models indicate comparable costs for LFP cells and NIBs (and lower costs for NMC cells). The models also indicate that the € kWh^{-1} for NIBs can be significantly decreased with volume-scale manufacturing and if the Wh kg^{-1} and Wh l^{-1} can be increased.

Current and Future challenges

Global energy demand is predicted to grow by up to 40% in the next ten years, including an increase of 2500 TWh in the transport sector, and the global power capacity of solar and wind are planned to be 2 TW and 1.5 TW, respectively, in the same timescale [299]. Combined with a global push to reduce fossil-fuel reliance, this will create a massive market for energy storage. Competitive battery technologies covering a wide performance, safety, and cost matrix will be required to support this growth [300].

In the short term, the first generation of NIBs has to prove that it is a contender in the energy-storage market, in terms of competitive performance, safety, cost, and maintenance, compared to incumbent technologies, such as Pb-acid, LIBs (LFP and NMC), and redox-flow batteries. The cost of development, production, and time to market will also have to be factored in. One of the major challenges in this space will be to match or, if possible, outperform state-of-the-art LIB cathodes such as NMC on a cost/performance, (€ kWh^{-1}) basis and fit in with existing infrastructure. The majority of new stationary energy-storage installations use LIBs (currently, mostly LFP), which have benefitted from cost reductions and innovations in the EV market [300], and a bulk cost reduction could allow for a quick entrance into this application. Another major short-term challenge facing all new energy-storage markets is regulation and policy. Concerns around safety and the decisions to invest in different types of infrastructure will have a huge impact on the demand for energy storage and the associated costs of installation and use [300]. Future challenges will lie in securing and maintaining a competitive edge over other developing technologies. LIB roadmaps are looking at novel materials and architectures to increase energy density and reduce cost per

kWh. Ease of recycling is another challenge that will need to be addressed, since the financial and environmental costs of disposal increase with the scale of adoption.

Advances in science and technology to meet challenges

In recent years, there has been a significant increase in worldwide NIB R&D activities [252, 267], driven by potential cost and safety benefits compared to LIBs, as well as compatibility with LIB manufacturing processes and applications. Next-generation cells will seek to improve energy density beyond 170 Wh kg^{-1} [301] and improve other cell characteristics without compromising safety. This will further reduce the € kWh^{-1} cost and make them more competitive for automotive and other applications [252, 267].

Advanced NIBs based on current-generation chemistries will improve in gravimetric and volumetric energy density, simply based on material, electrode, cell design, and engineering improvements. One area of improvement will be to increase the physical and active content and loadings and the density of the electrodes (and tap densities of active materials) to maximise the volumetric capacity. Electrolyte loadings can also be optimised to reduce cell weight.

First-cycle efficiencies (FCEs) for hard carbons are also quite low compared to that of graphite (<78% compared with >92%); investigating the use of a range of hard carbon/electrolyte combinations with higher FCEs will further increase the energy density. Hard carbons with lower average discharge voltages will increase the average cell operating voltage and the overall gravimetric and volumetric energy densities of the cells. Implementing these design and engineering optimisations could increase the energy density of first-generation NIBs to 160 Wh kg^{-1} [301].

Next-generation cathode chemistries are also being investigated [252]. These will seek to reduce the amount of Ni in the cathode by replacing it with Fe and/or Mn to significantly reduce the cost. Lower processing costs are also an area to explore to improve € kWh^{-1} for first-generation NIBs.

Alloying elements such as Sb, Si, Ge, As, Sb, Se, Pb, and Bi are also being investigated as alternatives to hard carbon anodes [252]; it is believed that the second generation of anodes will use these as blends with hard carbon. Titanium phosphates (e.g. $NaTi_2(PO_4)_3$) and titanium oxide ($Na_2Ti_3O_7$) insertion compounds are also being investigated as alternatives to hard carbons [252].

Compared to LIBs, the NIB anode and cathode spaces are relatively unmined, so there is still significant potential to further increase the energy density of second-generation NIBs beyond 170 Wh kg^{-1}; 190 Wh kg^{-1} has been predicted by Barker [301]

Concluding remarks

This short techno-economic assessment has shown that the current generation of NIBs, if advanced to mass production, can be competitive against LFP (and replace Pb-Acid) and NMC cells for stationary and telecoms applications. NIBs show massive advantages in safety, compared to either LFP or NMC cells, and have the potential for reduced cost (predominantly because Na is significantly more abundant than Li) and improved cycle life. The current generation of NIBs has the potential to exceed 150 Wh kg^{-1} through electrode and cell design optimisation. As a new technology, NIBs also have the added advantage of being a 'drop-in' replacement for LIBs, as the manufacturing processes are compatible.

Other potential benefits include the potential to store NIBs at 0 V without impacting safety and performance; this will allow for cheaper storage and transportation.

Due to the significant worldwide research in NIB materials, advances will probably lead to second-generation energy densities of >180 Wh kg^{-1}.

However, timescales for commercialisation may be long, and the timing of introduction to the market will be crucial to displace existing technologies. Satisfying existing regulatory and policy requirements is also a factor to be considered in the timescales for the commercialisation of NIBs. If Ni can be removed from the cathode formulation, then upcycling and disposal could be potentially easy and inexpensive.

Data availability statement

All data that support the findings of this study are included within the article (and any supplementary files).

ORCID iDs

Nuria Tapia-Ruiz ⦿ https://orcid.org/0000-0002-5005-7043
A Robert Armstrong ⦿ https://orcid.org/0000-0003-1937-0936
Hande Alptekin ⦿ https://orcid.org/0000-0001-6065-0513
Heather Au ⦿ https://orcid.org/0000-0002-1652-2204
Jerry Barker ⦿ https://orcid.org/0000-0002-8791-1119
William R Brant ⦿ https://orcid.org/0000-0002-8658-8938
Yong-Seok Choi ⦿ https://orcid.org/0000-0002-3737-2989
Sara I R Costa ⦿ https://orcid.org/0000-0001-8105-207X
Maria Crespo Ribadeneyra ⦿ https://orcid.org/0000-0001-6455-4430
Serena A Cussen ⦿ https://orcid.org/0000-0002-9303-4220
Aamod V Desai ⦿ https://orcid.org/0000-0001-7219-3428
Juan D Forero-Saboya ⦿ https://orcid.org/0000-0002-3403-6066
John M Griffin ⦿ https://orcid.org/0000-0002-8943-3835
John T S Irvine ⦿ https://orcid.org/0000-0002-8394-3359
Patrik Johansson ⦿ https://orcid.org/0000-0002-9907-117X
Martin Karlsmo ⦿ https://orcid.org/0000-0002-0437-6860
Emma Kendrick ⦿ https://orcid.org/0000-0002-4219-964X
Eunjeong Kim ⦿ https://orcid.org/0000-0002-2941-068
Oleg V Kolosov ⦿ https://orcid.org/0000-0003-3278-9643
Stijn F L Mertens ⦿ https://orcid.org/0000-0002-5715-0486
Laure Monconduit ⦿ https://orcid.org/0000-0003-3698-856X
Andrew J Naylor ⦿ https://orcid.org/0000-0001-5641-7778
Philippe Poizot ⦿ https://orcid.org/0000-0003-1865-4902
Stéven Renault ⦿ https://orcid.org/0000-0002-6500-0015
Ashish Rudola ⦿ https://orcid.org/0000-0001-9368-0698
Ruth Sayers ⦿ https://orcid.org/0000-0003-1289-0998
Valerie R Seymour ⦿ https://orcid.org/0000-0003-3333-5512
Begoña Silván ⦿ https://orcid.org/0000-0002-1273-3098
Moulay Tahar Sougrati ⦿ https://orcid.org/0000-0003-3740-2807
Lorenzo Stievano ⦿ https://orcid.org/0000-0001-8548-0231
Chris I Thomas ⦿ https://orcid.org/0000-0001-8090-4541
Maria-Magdalena Titirici ⦿ https://orcid.org/0000-0003-0773-2100
Jincheng Tong ⦿ https://orcid.org/0000-0001-7762-1460
Thomas J Wood ⦿ https://orcid.org/0000-0002-5893-5664
Reza Younesi ⦿ https://orcid.org/0000-0003-2538-8104

References

[1] NEXGENNA—Sodium-ion Batteries (Available at: https://faraday.ac.uk/research/beyond-lithium-ion/sodium-ion-batteries/)
[2] Eftekhari A and Kim D-W 2018 Sodium-ion batteries: new opportunities beyond energy storage by lithium *J. Power Sources* **395** 336–48
[3] Perveen T, Siddiq M, Shahzad N, Ihsan R, Ahmad A and Shahzad M I 2020 Prospects in anode materials for sodium ion batteries—a review *Renew. Sustain. Energy Rev.* **119** 109549
[4] Hwang J-Y, Myung S-T and Sun Y-K 2017 Sodium-ion batteries: present and future *Chem. Soc. Rev.* **46** 3529–614
[5] Delmas C, Fouassier C and Hagenmuller P 1980 Structural classification and properties of the layered oxides *Physica* B **99** 81–85
[6] Liu Q, Hu Z, Chen M, Zou C, Jin H, Wang S, Chou S-L, Liu Y and Dou S-X 2020 The cathode choice for commercialization of sodium-ion batteries: layered transition metal oxides versus Prussian blue analogs *Adv. Funct. Mater.* **30** 1909530
[7] Vassilaras P, Ma X, Li X and Ceder G 2013 Electrochemical properties of monoclinic NaNiO₂ *J. Electrochem. Soc.* **160** A207–11
[8] Yabuuchi N, Yano M, Yoshida H, Kuze S and Komaba S 2013 Synthesis and electrode performance of O3-Type NaFeO₂-NaNi₁/₂Mn₁/₂O₂ solid solution for rechargeable sodium batteries *J. Electrochem. Soc.* **160** A3131–7
[9] Komaba S, Yabuuchi N, Nakayama T, Ogata A, Ishikawa T and Nakai I 2012 Study on the reversible electrode reaction of Na₁₋ₓNi₀.₅Mn₀.₅O₂ for a rechargeable sodium-ion battery *Inorg. Chem.* **51** 6211–20
[10] Kumakura S, Tahara Y, Kubota K, Chihara K and Komaba S 2016 Sodium and manganese stoichiometry of P2-Type Na₂/₃MnO₂ *Angew. Chem., Int. Ed.* **55** 12760–3
[11] D'Arienzo M, Ruffo R, Scotti R, Morazzoni F, Mari C M and Polizzi S 2012 Layered Na₀.₇₁CoO₂: a powerful candidate for viable and high performance Na-batteries *Phys. Chem. Chem. Phys.* **14** 5945–52
[12] Lu Z and Dahn J R 2001 *In situ* x-ray diffraction study of P2-Na₂/₃[Ni₁/₃Mn₂/₃]O₂ *J. Electrochem. Soc.* **148** A1225–9

[13] Li Z-Y, Gao R, Zhang J, Zhang X, Hu Z and Liu X 2016 New insights into designing high-rate performance cathode materials for sodium ion batteries by enlarging the slab-spacing of the Na-ion diffusion layer *J. Mater. Chem.* A **4** 3453–61

[14] Yoshida H, Yabuuchi N, Kubota K, Ikeuchi I, Garsuch A, Schulz-Dobrick M and Komaba S 2014 P2-type Na$_{2/3}$Ni$_{1/3}$Mn$_{2/3-x}$Ti$_x$O$_2$ as a new positive electrode for higher energy Na-ion batteries *Chem. Commun.* **50** 3677–80

[15] Barker J and Heap R 2019 O3/P2 mixed phase sodium-containing doped layered oxide materials *Patent WO 2019/197812*

[16] Assat G and Tarascon J-M 2018 Fundamental understanding and practical challenges of anionic redox activity in Li-ion batteries *Nat. Energy* **3** 373

[17] Maitra U *et al* 2018 Oxygen redox chemistry without excess alkali-metal ions in Na$_{2/3}$[Mg$_{0.28}$Mn$_{0.72}$]O$_2$ *Nat. Chem.* **10** 288

[18] Zheng W, Liu Q, Wang Z, Wua Z, Gu S, Cao L, Zhang K, Fransaer J and Lu Z 2020 Oxygen redox activity with small voltage hysteresis in Na$_{0.67}$Cu$_{0.28}$Mn$_{0.72}$O$_2$ for sodium-ion batteries *Energy Storage Mater.* **28** 300

[19] House R A *et al* 2020 Superstructure control of first-cycle voltage hysteresis in oxygen-redox cathodes *Nature* **577** 502

[20] Parant J-P, Olazcuaga R, Devalette M, Fouassier C and Hagenmuller P 1971 Sur quelques nouvelles phases de formule Na$_x$MnO$_2$ ($x \leqslant 1$) *J. Solid State Chem.* **3** 1

[21] House R A *et al* 2019 What triggers oxygen loss in oxygen redox cathode materials? *Chem. Mater.* **31** 3293

[22] Radin M D, Vinckeviciute J, Seshadri R and Van der Ven A 2019 Manganese oxidation as the origin of the anomalous capacity of Mn-containing Li-excess cathode materials *Nat. Energy* **4** 639

[23] Ma L A, Massel F, Naylor A J, Duda L-C and Younesi R 2019 Understanding charge compensation mechanisms in Na$_{0.56}$Mg$_{0.04}$Ni$_{0.19}$Mn$_{0.70}$O$_2$ *Commun. Chem.* **2** 125

[24] Mortemard De Boisse B, Nishimura S, Watanabe E, Lander L, Tsuchimoto A, Kikkawa J, Kobayashi E, Asakura D, Okubo M and Yamada A 2018 Highly reversible oxygen-redox chemistry at 4.1 V in Na$_{4/7-x}$[□$_{1/7}$Mn$_{6/7}$]O$_2$ (□: Mn vacancy) *Adv. Energy Mater.* **8** 1800409

[25] Wang P-F *et al* 2020 Both cationic and anionic redox chemistry in a P2-type sodium layered oxide *Nano Energy* **69** 104474

[26] Sharifi-Asl S, Lu J, Amine K and Shahbazian-Yassar R 2019 Oxygen release degradation in Li-ion battery cathode materials: mechanisms and mitigating approaches *Adv. Energy Mater.* **9** 1900551

[27] Chen S, Wen K, Fan J, Bando Y and Golberg D 2018 Progress and future prospects of high-voltage and high-safety electrolytes in advanced lithium batteries: from liquid to solid electrolytes *J. Mater. Chem.* A **6** 11631

[28] Barpanda P, Lander L, Nishimura S and Yamada A 2018 Polyanionic insertion materials for sodium-ion batteries *Adv. Energy Mater.* **8** 17030550–26

[29] Li H, Xu M, Zhang Z, Lai Y and Ma J 2020 Engineering of polyanion type cathode materials for sodium-ion batteries: toward higher energy/power density *Adv. Funct. Mater.* **30** 2000473-1–29

[30] Chotard J-N, Rousse G, David R, Mentré O, Courty M and Masquelier C 2015 Discovery of a sodium-ordered form of Na$_3$V$_2$(PO$_4$)$_3$ below ambient temperature *Chem. Mater.* **27** 5982–7

[31] Bianchini M, Brisset N, Fauth F, Weill F, Elkaim E, Suard E, Masquelier C and Croguennec L 2014 Na$_3$V$_2$(PO$_4$)$_2$F$_3$ revisited: a high-resolution diffraction study *Chem. Mater.* **26** 4238–47

[32] Bianchini M, Xiao P, Wang Y and Ceder G 2017 Additional sodium insertion into polyanionic cathodes for higher-energy Na-ion batteries *Adv. Energy Mater.* **7** 1700514-1–9

[33] Liang Z, Zhang X, Liu R, Ortiz G F, Zhong G, Xiang Y, Chen S, Mi J, Wu S and Yang Y 2020 New dimorphs of Na$_5$V(PO$_4$)$_2$F$_2$ as an ultrastable cathode material for sodium-ion batteries *ACS Appl. Energy Mater.* **3** 1181–9

[34] Kim M, Kim D, Lee W, Jang H M and Kang B 2018 New class of 3.7 V Fe-based positive electrode materials for Na-ion battery based on cation-disordered polyanion framework *Chem. Mater.* **30** 6346–52

[35] Plewa A, Kulka A, Hanc E, Zając W, Sun J, Lu L and Molenda J 2020 Facile aqueous synthesis of high performance Na$_2$FeM(SO$_4$)$_3$ (*M*=Fe, Mn, Ni) alluaudites for low cost Na-ion batteries *J. Mater. Chem.* A **8** 2728–40

[36] Song T, Yao W, Kiadkhunthod P, Zheng Y, Wu N, Zhou X, Tunmee S, Sattayaporn S and Tang Y 2020 A low-cost and environmentally friendly mixed polyanionic cathode for sodium-ion storage *Angew. Chem., Int. Ed.* **59** 740–5

[37] Mattei G S *et al* 2020 Enumeration as a tool for structure solution: a materials genomic approach to solving the cation-ordered structure of Na$_3$V$_2$(PO$_4$)$_2$F$_3$ *Chem. Mater.* **32** 8981–92

[38] Nguyen L H B, Iadecola A, Belin S, Olchowka J, Masquelier C, Carlier D and Croguennec L 2020 A combined operando synchrotron X-ray absorption spectroscopy and first-principles density functional theory study to unravel the vanadium redox paradox in the Na$_3$V$_2$(PO$_4$)$_2$F$_3$-Na$_3$V$_2$(PO$_4$)$_2$FO$_2$ compositions *J. Phys. Chem.* C **124** 23511–22

[39] Liu Q, Hu Z, Chen M, Zou C, Jin H, Wang S, Chou S-L, Liu Y and Dou S-X 2020 The cathode choice for commercialization of sodium-ion batteries: layered transition metal oxides versus Prussian blue analogs *Adv. Funct. Mater.* **30** 1909530

[40] You Y, Wu X-L, Yin Y-X and Guo Y-G 2014 High-quality Prussian blue crystals as superior cathode materials for room-temperature sodium-ion batteries *Energy Environ. Sci.* **7** 1643–7

[41] Wang L *et al* 2015 Rhombohedral Prussian white as cathode for rechargeable sodium-ion batteries *J. Am. Chem. Soc.* **137** 2548–54

[42] Li W-J, Han C, Cheng G, Chou S-L, Liu H-K and Dou S-X 2019 Chemical properties, structural properties, and energy storage applications of Prussian blue analogues *Small* **15** 1900470

[43] Shen L, Jiang Y, Liu Y, Ma J, Sun T and Zhu N 2020 High-stability monoclinic nickel hexacyanoferrate cathode materials for ultrafast aqueous sodium ion battery *Chem. Eng. J.* **388** 124228

[44] Rudola A, Du K and Balaya P 2017 Monoclinic sodium iron hexacyanoferrate cathode and non-flammable glyme-based electrolyte for inexpensive sodium-ion batteries *J. Electrochem. Soc.* **164** A1098

[45] You Y, Yao H-R, Xin S, Yin Y-X, Zuo T-T, Yang C-P, Guo Y-G, Cui Y, Wan L-J and Goodenough J B 2016 Subzero-temperature cathode for a sodium-ion battery *Adv. Mater.* **28** 7243–8

[46] Guo X, Wang Z, Deng Z, Li X, Wang B, Chen X and Ong S P 2019 Water contributes to higher energy density and cycling stability of Prussian blue analogue cathodes for aqueous sodium-ion batteries *Chem. Mater.* **31** 5933–42

[47] Ojwang D O, Häggström L, Ericsson T, Ångström J and Brant W R 2020 Influence of sodium content on the thermal behavior of low vacancy Prussian white cathode material *Dalton Trans.* **49** 3570–9

[48] Chen M, Zhang Z, Liu X, Li Y, Wang Y, Fan H, Liang X and Chen Q 2020 Prussian blue coated with reduced graphene oxide as high-performance cathode for lithium–sulfur batteries *RSC Adv.* **10** 31773–9

[49] Dehghani-Sanij A R, Tharumalingam E, Dusseault M B and Fraser R 2019 Study of energy storage systems and environmental challenges of batteries *Renew. Sustain. Energy Rev.* **104** 192–208

[50] Peters J F, Baumann M, Zimmermann B, Braun J and Weil M 2017 The environmental impact of Li-ion batteries and the role of key parameters—a review *Renew. Sustain. Energy Rev.* **67** 491–506

[51] Poizot P and Dolhem F 2011 Clean energy new deal for a sustainable world: from non-CO_2 generating energy sources to greener electrochemical storage devices *Energy Environ. Sci.* **4** 2003–19

[52] Poizot P, Gaubicher J, Renault S, Dubois L, Liang Y and Yao Y 2020 Opportunities and challenges for organic electrodes in electrochemical energy storage *Chem. Rev.* **120** 6490–557

[53] Tournier V *et al* 2020 An engineered PET depolymerase to break down and recycle plastic bottles *Nature* **580** 216–9

[54] Zhao Q, Lu Y and Chen J 2017 Advanced organic electrode materials for rechargeable sodium-ion batteries *Adv. Energy Mater.* **7** 1601792

[55] Rajagopalan R, Tang Y, Jia C, Ji X and Wang H 2020 Understanding the sodium storage mechanisms of organic electrodes in sodium ion batteries: issues and solutions *Energy Environ. Sci.* **13** 1568–92

[56] Deuchert K and Hünig S 1978 Multistage organic redox systems—a general structural principle *Angew. Chem., Int. Ed. Engl.* **17** 875–86

[57] Wang H, Yuan S, Ma D, Huang X, Meng F and Zhang X 2014 Tailored aromatic carbonyl derivative polyimides for high-power and long-cycle sodium-organic batteries *Adv. Energy Mater.* **4** 1301651

[58] Wu D, Zhang G, Lu D, Ma L, Xu Z, Xi X, Liu R, Liu P and Su Y 2018 Perylene diimide-diamine/carbon black composites as high performance lithium/sodium ion battery cathodes *J. Mater. Chem.* A **6** 13613–8

[59] Banda H, Damien D, Nagarajan K, Hariharan M and Shaijumon M M 2015 A polyimide based all-organic sodium ion battery *J. Mater. Chem.* A **3** 10453–8

[60] Lee M, Hong J, Lopez J, Sun Y, Feng D, Lim K, Chueh W C, Toney M F, Cui Y and Bao Z 2017 High-performance sodium–organic battery by realizing four-sodium storage in disodium rhodizonate *Nat. Energy* **2** 861–8

[61] Wang S, Wang L, Zhu Z, Hu Z, Zhao Q and Chen J 2014 All organic sodium-ion batteries with $Na_4C_8H_2O_6$ *Angew. Chem.* **126** 6002–6

[62] Song Z, Qian Y, Zhang T, Otani M and Zhou H 2015 Poly(benzoquinonyl sulfide) as a high-energy organic cathode for rechargeable Li and Na batteries *Adv. Sci.* **2** 1500124

[63] Kim J-K, Kim Y, Park S, Ko H and Kim Y 2016 Encapsulation of organic active materials in carbon nanotubes for application to high-electrochemical-performance sodium batteries *Energy Environ. Sci.* **9** 1264–9

[64] Kim H W, Kim H-J, Byeon H, Kim J, Yang J W, Kim Y and Kim J-K 2020 Binder-free organic cathode based on nitroxide radical polymer-functionalized carbon nanotubes and gel polymer electrolyte for high-performance sodium organic polymer batteries *J. Mater. Chem.* A **8** 17980–6

[65] Deng W, Liang X, Wu X, Qian J, Cao Y, Ai X, Feng J and Yang H 2013 A low cost, all-organic Na-ion battery based on polymeric cathode and anode *Sci. Rep.* **3** 2671

[66] Jouhara A, Dupré N, Gaillot A-C, Guyomard D, Dolhem F and Poizot P 2018 Raising the redox potential in carboxyphenolate-based positive organic materials via cation substitution *Nat. Commun.* **9** 4401

[67] Franklin R E 1951 Crystallite growth in graphitizing and non-graphitizing carbons *Proc. Royal Society of London Series A. Mathematical and Physical Sciences* **209** 196–218

[68] Stevens D A and Dahn J R 2001 *J. Electrochem. Soc.* **148** 803–11

[69] Franklin R E 1951 Crystallite growth in graphitizing and non-graphitizing carbons *Proc. R. Soc.* A **209** 196–218

[70] Au H *et al* 2020 *Energy Environ. Sci.* **13** 3469–79

[71] Roberts S and Kendrick E 2018 The re-emergence of sodium ion batteries: testing, processing, and manufacturability *Nanotechnol. Sci. Appl.* **11** 23–33

[72] Zhang B, Ghimbeu C M, Laberty C, Vix-Guterl C and Tarascon J-M 2016 *Adv. Energy Mater.* **6** 1501588

[73] Komaba S, Murata W, Ishikawa T, Yabuuchi N, Ozeki T, Nakayama T, Ogata A, Gotoh K and Fujiwara K 2011 *Adv. Funct. Mater.* **21** 3859–67

[74] Jafta C, Bridges C, Sun X G, Veith G, Paranthaman P and Dai S 2018 *Abstracts of Papers of the American Chemical Society* vol 256 p meeting abstract 524

[75] Gu M, Kushima A, Shao Y Y, Zhang J-G, Liu J, Browning N D, Li J and Wang C M 2013 *Nano Lett.* **13** 5203–11

[76] Weaving J S, Lim A, Millichamp J, Neville T P, Ledwoch D, Kendrick E, McMillan P F, Shearing P R, Howard C A and Brett D J L 2020 *ACS Appl. Energy Mater.* **3** 7474–84

[77] Stratford J M, Allan P K, Pecher O, Chater P A and Grey C P 2016 *Chem. Commun.* **52** 12430–3

[78] Gotoh K, Maeda M, Nagai A, Goto A, Tansho M, Hashi K, Shimizu T and Ishida H 2006 *J. Power Sources* **162** 1322–8

[79] Morita R, Gotoh K, Kubota K, Komaba S, Hashi K, Shimizu T and Ishida H 2019 *Carbon* **145** 712

[80] Bray J M *et al* 2020 *Nat. Commun.* **11** 2083

[81] Alcántara R, Ortiz G F, Lavela P, Tirado J L, Stoyanova R and Zhecheva E 2006 *Chem. Mater.* **18** 2293–301

[82] Le P M L *et al* 2020 *Adv. Funct. Mater.* **30** 2001151

[83] Eshetu G G, Diemant T, Hekmatfar M, Grugeon S, Behm R J, Laruelle S, Armand M and Passerini S 2019 *Nano Energy* **55** 327–40

[84] Zhang Z, Smith K, Jervis R, Shearing P R, Miller T S and Brett D J L 2020 *ACS Appl. Mater. Interfaces* **12** 35132–3514

[85] Qin Y P, Zhuang Q C, Shi Y L, Jiang L, Sun Z and Sun S G 2011 *Prog. Chem.* **23** 390–400

[86] Berkes B B, Jozwiuk A, Vracar M, Sommer H, Brezesinski T and Janek J 2015 *Anal. Chem.* **87** 5878–83

[87] Li J T, Fang J C, Su H and Sun S G 2011 *Prog. Chem.* **23** 349–56

[88] Sottmann J, Di Michiel M, Fjellvag H, Malavasi L, Margadonna S, Vajeeston P, Vaughan G B M and Wragg D S 2017 *Angew. Chem., Int. Ed.* **56** 11385–9

[89] Alptekin H, Au H, Jensen A C S, Olsson E, Goktas M, Headen T F, Adelhelm P, Cai Q, Drew A J and Titirici M 2020 Sodium storage mechanism investigations through structural changes in hard carbons *ACS Appl. Energy Mater.* **3** 9918–27

[90] Goktas M, Bolli C, Berg E J, Novák P, Pollok K, Langenhorst F, Roeder M V, Lenchuk O, Mollenhauer D and Adelhelm P 2018 *Adv. Energy Mater.* **8** 1702724

[91] Olsson E, Cottom J, Au H, Guo Z, Jensen A C S, Alptekin H, Drew A J, Titirici M-M and Cai Q 2020 *Adv. Funct. Mater.* **30** 1908209

[92] Bommier C, Ji X L and Greaney P A 2019 *Chem. Mater.* **31** 658–77

[93] Soto F A, Marzouk A, El-Mellouhi F and Balbuena P B 2018 *Chem. Mater.* **30** 3315–22

[94] Deringer V L, Merlet C, Hu Y C, Lee T H, Kattirtzi J A, Pecher O, Csanyi G, Elliott S R and Grey C P 2018 *Chem. Commun.* **54** 5988–91

[95] Xie F, Xu Z, Guo Z and Titirici M-M 2020 *Prog. Energy* **2** 042002

[96] Stevens D and Dahn J R 2000 *J. Electrochem. Soc.* **147** 1271–3

[97] Ding J *et al* 2013 *ACS Nano* **7** 11004–15

[98] Bommier C, Surta T W, Dolgos M and Ji X 2015 *Nano Lett.* **15** 5888–92

[99] Morikawa Y, Nishimura S-I, Hashimoto R-I, Ohnuma M and Yamada A 2020 *Adv. Energy Mater.* **10** 1903176

[100] Simone V, Boulineau A, De Geyer A, Rouchon D, Simonin L and Martinet S 2016 *J. Energy Chem.* **25** 761–8

[101] Li Y Q *et al* 2019 *Adv. Energy Mater.* **9** 1902852

[102] Forse A C, Merlet C, Allan P K, Humphreys E K, Griffin J M, Aslan M, Zeiger M, Presser V, Gogotsi Y and Grey C P 2015 *Chem. Mater.* **27** 6848–5727

[103] Wang J, Polleux J, Lim J and Dunn B 2007 Pseudocapacitive contributions to electrochemical energy storage in TiO_2 (anatase) nanoparticles *J. Phys. Chem.* **111** 14925–31

[104] Xu Y, Lotfabad E, Wang H, Farbod B, Xu Z, Kohandehghan A and Mitlin D 2013 Nanocrystalline anatase TiO_2: a new anode material for rechargeable sodium ion batteries *Chem. Commun.* **49** 8973–5

[105] Ohzuku T, Ueda A and Yamamoto N 1995 Zero-strain insertion material of Li $[Li_{1/3}Ti_{5/3}]O_4$ for rechargeable lithium cells *J. Electrochem. Soc.* **142** 1431–5

[106] Liang Z, Lin P, Shen H, Hong L and Quan C 2012 Spinel lithium titanate ($Li_4Ti_5O_{12}$) as novel anode material for room-temperature sodium-ion battery *Chin. Phys.* B **21** 028201

[107] Rudola A, Saravanan K, Devaraj S, Gong H and Balaya P 2013 $Na_2Ti_6O_{13}$: a potential anode for grid-storage sodium-ion batteries *Chem. Commun.* **49** 7451–3

[108] Cao K, Jiao L, Pang W K, Liu H, Zhou T, Guo Z, Wang Y and Yuan H 2016 $Na_2Ti_6O_{13}$ nanorods with dominant large interlayer spacing exposed facet for high-performance Na-ion batteries *Small* **12** 2991–7

[109] Senguttuvan P, Rousse G, Seznec V, Tarascon J and Palacín M 2011 $Na_2Ti_3O_7$: lowest voltage ever reported oxide insertion electrode for sodium ion batteries *Chem. Mater.* **23** 4109–11

[110] Cao Y, Ye Q, Wang F, Fan X, Hu L, Wang F, Zhai T and Li H 2020 A new triclinic phase $Na_2Ti_3O_7$ anode for sodium-ion battery *Adv. Funct. Mater.* **30** 2003733

[111] Wu C, Hua W, Zhang Z, Zhong B, Yang Z, Feng G, Xiang W, Wu Z and Guo X 2018 Design and synthesis of layered $Na_2Ti_3O_7$ and tunnel $Na_2Ti_6O_{13}$ hybrid structures with enhanced electrochemical behavior for sodium-ion batteries *Adv. Sci.* **5** 1800519

[112] Pan H, Lu X, Yu X, Hu Y, Li H, Yang X and Chen L 2013 Sodium storage and transport properties in layered $Na_2Ti_3O_7$ for room-temperature sodium-ion batteries *Adv. Energy Mater.* **3** 1186–94

[113] Marquez M, Zarrabeitia M, Martinez E, Barrio A, Rojo T and Cabanas M 2015 Composition and evolution of the solid-electrolyte interphase in $Na_2Ti_3O_7$ electrodes for Na-ion batteries: XPS and Auger parameter analysis *ACS Appl. Mater. Interfaces* **7** 7801–08

[114] Kulova T, Kudryashova Y, Kuz'mina A, Skundin A, Stenina I, Chekannikov A, Yaroslavtsev A and Libich J 2019 Study of degradation of $Na_2Ti_3O_7$-based electrode during cycling *J. Solid State Electrochem.* **23** 455–63

[115] Xu J, Ma C, Balasubramanian M and Meng Y S 2014 Understanding $Na_2Ti_3O_7$ as an ultra-low voltage anode material for a Na-ion battery *Chem. Commun.* **50** 12564–7

[116] Chen J, Zhou X, Mei C, Xu J and Wong C 2017 Electrochimica acta improving the sodiation performance of $Na_2Ti_3O_7$ through Nb-doping *Electrochim. Acta* **224** 446–51

[117] Xia J, Zhao H, Pang W, Yin Z, Zhou B, He G, Guo Z and Du Y 2018 Lanthanide doping induced electrochemical enhancement of $Na_2Ti_3O_7$ anodes for sodium-ion batteries *Chem. Sci.* **9** 3421–5

[118] Costa S, Choi Y, Fielding A, Naylor A, Griffin J, Sofer Z, Scanlon D and Ruiz N 2020 Surface engineering strategy using urea to improve the rate performance of $Na_2Ti_3O_7$ in Na-ion batteries *Chem. Eur. J.* **27** 3875–86

[119] Anwer S, Huang Y, Liu J, Liu J, Xu M, Wang Z, Chen R, Zhang J and Wu F 2017 Nature-inspired $Na_2Ti_3O_7$ nanosheets-formed three-dimensional microflowers architecture as a high-performance anode material for rechargeable sodium-ion batteries *ACS Appl. Mater. Interfaces* **9** 11669–77

[120] Chen Z, Lu L, Li N and Sun C 2019 $Na_2Ti_3O_7$ nanotubes as anode materials for sodium-ion batteries and self-powered systems *ChemElectroChem* **6** 3085–90

[121] Dong S, Shen L, Li H, Nie P, Zhu Y, Sheng Q and Zhang X 2015 Pseudocapacitive behaviours of $Na_2Ti_3O_7$ @CNT coaxial nanocables for high-performance sodium-ion capacitors *J. Mater. Chem. A* **3** 21277–83

[122] Chen S, Pang Y, Liang J and Ding S 2018 Red blood cell-like hollow carbon sphere anchored ultrathin $Na_2Ti_3O_7$ nanosheets as long cycling and high rate-performance anodes for sodium-ion batteries *J. Mater. Chem. A* **6** 13164–70

[123] Li L, Zheng Y, Zhang S, Yang J, Shao Z and Guo Z 2018 Recent progress on sodium ion batteries: potential high-performance anodes *Energy Environ. Sci.* **11** 2310–40

[124] Zhang L, Wei T, Jiang Z, Liu C, Jiang H, Chang J, Sheng L, Zhou Q, Yuan L and Fan Z 2018 Electrostatic interaction in electrospun nanofibers: double-layer carbon protection of $CoFe_2O_4$ nanosheets enabling ultralong-life and ultrahigh-rate lithium ion storage *Nano Energy* **48** 238–47

[125] Darwiche A, Marino C, Sougrati M T, Fraisse B, Stievano L and Monconduit L 2012 Better cycling performances of bulk Sb in Na-ion batteries compared to Li-ion systems: an unexpected electrochemical mechanism *J. Am. Chem. Soc.* **134** 20805–11

[126] Zhang H, Hasa I and Passerini S 2018 Beyond insertion for Na-ion batteries: nanostructured alloying and conversion anode materials *Adv. Energy Mater.* **8** 1702582

[127] Cabana J, Monconduit L, Larcher D and Palacín M R 2010 Beyond intercalation-based Li-ion batteries: the state of the art and challenges of electrode materials reacting through conversion reactions *Adv. Mater.* **22** E170–92

[128] Brennhagen A, Cavallo C, Wragg D, Sottmann J, Koposov A Y and Fjellvåg H 2021 Understanding the (de)sodiation mechanisms in Na-based batteries through operando x-ray methods *Batter Supercaps* **4** 1039–63

[129] Rodriguez J R, Aguirre S B and Pol V G 2019 Understanding sodium-ion battery anodes through operando spectroscopic techniques *Electrochim. Acta* **319** 791–800

[130] Zhu Y, Wen Y, Fan X, Gao T, Han F, Luo C, Liou S-C and Wang C 2015 Red phosphorus–single-walled carbon nanotube composite as a superior anode for sodium ion batteries *ACS Nano* **9** 3254–64

[131] Liu Y, Zhang N, Jiao L, Tao Z and Chen J 2015 Ultrasmall Sn nanoparticles embedded in carbon as high-performance anode for sodium-ion batteries *Adv. Funct. Mater.* **25** 214–20

[132] Loaiza L C, Monconduit L and Seznec V 2020 Si and Ge-based anode materials for Li-, Na-, and K-ion batteries: a perspective from structure to electrochemical mechanism *Small* **16** 1905260

[133] Sun J, Lee H-W, Pasta M, Yuan H, Zheng G, Sun Y, Li Y and Cui Y 2015 A phosphorene–graphene hybrid material as a high-capacity anode for sodium-ion batteries *Nat. Nanotechnol.* **10** 980–5

[134] Chen L, Fiore M, Wang J E, Ruffo R, Kim D-K and Longoni G 2018 Readiness level of sodium-ion battery technology: a materials review *Adv. Sus. Syst.* **2** 1700153

[135] Allan P K, Griffin J M, Darwiche A, Borkiewicz O J, Wiaderek K M, Chapman K W, Morris A J, Chupas P J, Monconduit L and Grey C P 2016 Tracking sodium-antimonide phase transformations in sodium-ion anodes: insights from operando pair distribution function analysis and solid-state NMR spectroscopy *J. Am. Chem. Soc.* **138** 2352–65

[136] Chang Y-M, Lin H-W, Li L-J and Chen H-Y 2020 Two-dimensional materials as anodes for sodium-ion batteries *Mater. Today Adv.* **6** 100054

[137] Eda G, Yamaguchi H, Voiry D, Fujita T, Chen M W and Chhowalla M 2011 Photoluminescence from chemically exfoliated MoS_2 *Nano Lett.* **11** 5111–6

[138] Acerce M, Voiry D and Chhowalla M 2015 Metallic 1T phase MoS_2 nanosheets as supercapacitor electrode materials *Nat. Nanotechnol.* **10** 313–8

[139] Geng X M, Jiao Y C, Han Y, Mukhopadhyay A, Yang L and Zhu H L 2017 Freestanding metallic 1T MoS_2 with dual ion diffusion paths as high rate anode for sodium-ion batteries *Adv. Funct. Mater.* **27** 1702998

[140] Zhang R, Qin Y, Liu P, Jia C K, Tang Y G and Wang H Y 2020 How does molybdenum disulfide store charge: a mini review *ChemSusChem* **13** 1354–65

[141] Wang X F, Shen X, Wang Z X, Yu R C and Chen L Q 2014 Atomic-scale clarification of structural transition of MoS_2 upon sodium intercalation *ACS Nano* **8** 11394–400

[142] Lacey S D, Wan J Y, Cresce A V, Russell S M, Dai J Q, Bao W Z, Xu K and Hu L B 2015 Atomic force microscopy studies on molybdenum disulfide flakes as sodium-ion anodes *Nano Lett.* **15** 1018–24

[143] Banis M N *et al* 2018 Revealing the charge/discharge mechanism of Na–O_2 cells by *in situ* soft x-ray absorption spectroscopy *Energy Environ. Sci.* **11** 2073–7

[144] Zhao Y, Goncharova L V, Lushington A, Sun Q, Yadegari H, Wang B Q, Xiao W, Li R Y and Sun X L 2017 Superior stable and long life sodium metal anodes achieved by atomic layer deposition *Adv. Mater.* **29** 1606663

[145] Liedel C 2020 Sustainable battery materials from biomass *ChemSusChem* **13** 2110–41

[146] Xu Y, Zhou M and Lei Y 2018 Organic materials for rechargeable sodium-ion batteries *Mater. Today* **21** 60–78

[147] Lu Y, Zhang Q, Li L, Niu Z and Chen J 2018 Design strategies toward enhancing the performance of organic electrode materials in metal-ion batteries *Chem* **4** 2786–813

[148] Desai A V, Morris R E and Armstrong A R 2020 Advances in organic anode materials for Na-/K-ion rechargeable batteries *ChemSusChem* **13** 4866–84

[149] Deng J, Luo W-B, Chou S-L, Liu H-K and Dou S-X 2018 Sodium-ion batteries: from academic research to practical commercialization *Adv. Energy Mater.* **8** 1701428

[150] Liu Y *et al* 2018 Activating aromatic rings as Na-ion storage sites to achieve high capacity *Chem* **4** 2463–78

[151] Lee S, Kwon J E, Hong J, Park S Y and Kang K 2019 The role of substituents in determining the redox potential of organic electrode materials in Li and Na rechargeable batteries: electronic effects vs. substituent-Li/Na ionic interaction *J. Mater. Chem.* A **7** 11438–43

[152] Ma C, Wu L, Jin Z, Zhao X-Y, Liu Y-S, Bai Y-L, Sun H, Wang K-X and Chen J-S 2018 Thiophene derivative as a high electrochemical active anode material for sodium-ion batteries: the effect of backbone sulfur *Chem. Mater.* **30** 8426–30

[153] Wan F, Wu X-L, Guo J-Z, Li J-Y, Zhang J-P, Niu L and Wang R-S 2015 Nanoeffects promote the electrochemical properties of organic $Na_2C_8H_4O_4$ as anode material for sodium-ion batteries *Nano Energy* **13** 450–7

[154] Haldar S, Kaleeswaran D, Rase D, Roy K, Ogale S and Vaidhyanathan R 2020 Tuning the electronic energy level of covalent organic frameworks for crafting high-rate Na-ion battery anode *Nanoscale Horiz.* **5** 1264–73

[155] Jain A, Shin Y and Persson K A 2016 Computational predictions of energy materials using density functional theory *Nat. Rev. Mater.* **1** 15004

[156] Mayo M and Morris A J 2017 Structure prediction of Li–Sn and Li–Sb intermetallics for lithium-ion batteries anodes *Chem. Mater.* **29** 5787–95

[157] Liu Y, Guo B, Zou X, Li Y and Shi S 2020 Machine learning assisted materials design and discovery for rechargeable batteries *Energy Storage Mater.* **31** 434–50

[158] Hinuma Y, Meng Y S and Ceder G 2008 Temperature-concentration phase diagram of P_2-Na_xCoO_2 from first-principles calculations *J. Phys. Rev.* B **77** 224111

[159] Sun Y, Guo S and Zhou H 2019 Adverse effects of interlayer-gliding in layered transition-metal oxides on electrochemical sodium-ion storage *Energy Environ. Sci.* **12** 825–40

[160] Schmidt T and Kümmel S 2016 The influence of one-electron self-interaction on d-electrons *Computation* **4** 33

[161] Dove M T and Fang H 2016 Negative thermal expansion and associated anomalous physical properties: review of the lattice dynamics theoretical foundation *Rep. Prog. Phys.* **79** 066503

[162] Davies D W, Butler K, Jackson A, Morris A, Frost J, Skelton J and Walsh A 2016 Computational screening of all stoichiometric inorganic materials *Chem* **1** 617–27

[163] Meutzner F *et al* 2018 Computational analysis and identification of battery materials *Phys. Sci. Rev.* **4** 1–32

[164] Zhao C *et al* 2020 Rational design of layered oxide materials for sodium-ion batteries *Science* **370** 708–11

[165] Ponrouch A, Monti D, Boschin A, Steen B, Johansson P and Palacín M R 2015 Non-aqueous electrolytes for sodium-ion batteries *J. Mater. Chem.* A **3** 22–42

[166] Lin Z, Xia Q, Wang W, Li W and Chou S 2019 Recent research progresses in ether- and ester-based electrolytes for sodium-ion batteries *InfoMat.* **1** 376–89

[167] Eshetu G G, Elia G A, Armand M, Forsyth M, Komaba S, Rojo T and Passerini S 2020 Electrolytes and interphases in sodium-based rechargeable batteries: recent advances and perspectives *Adv. Energy Mater.* **10** 2000093

[168] Bommier C and Ji X 2018 Electrolytes, SEI formation, and binders: a review of nonelectrode factors for sodium-ion battery anodes *Small* **14** 1703576

[169] Xu K 2014 Electrolytes and interphases in Li-ion batteries and beyond *Chem. Rev.* **114** 11503–618

[170] Chen J, Huang Z, Wang C, Porter S, Wang B, Lie W and Liu H K 2015 Sodium-difluoro(oxalato)borate (NaDFOB): a new electrolyte salt for Na-ion batteries *Chem. Commun.* **51** 9809–12

[171] Mogensen R, Colbin S, Menon A S, Björklund E and Younesi R 2020 Sodium bis(oxalato)borate in trimethyl phosphate: a fire-extinguishing, fluorine-free, and low-cost electrolyte for full-cell sodium-ion batteries *ACS Appl. Energy Mater.* **3** 4974–82

[172] Vidal-Abarca C, Lavela P, Tirado J L, Chadwick A V, Alfredsson M and Kelder E 2012 Improving the cyclability of sodium-ion cathodes by selection of electrolyte solvent *J. Power Sources* **197** 314–8

[173] Åvall G, Mindemark J, Brandell D and Johansson P 2018 Sodium-ion battery electrolytes: modeling and simulations *Adv. Energy Mater.* **8** 1703036

[174] Hope M A, Rinkel B L D, Gunnarsdóttir A B, Märker K, Menkin S, Paul S, Sergeyev I V and Grey C P 2020 Selective NMR observation of the SEI–metal interface by dynamic nuclear polarisation from lithium metal *Nat. Commun.* **11** 2224

[175] Ponrouch A, Dedryvère R, Monti D, Demet A E, Ateba Mba J M, Croguennec L, Masquelier C, Johansson P and Palacín M R 2013 Towards high energy density sodium ion batteries through electrolyte optimization *Energy Environ. Sci.* **6** 2361–9

[176] Westman K *et al* 2018 Diglyme based electrolytes for sodium-ion batteries *ACS Appl. Energy Mater.* **1** 2671–80

[177] Cometto C, Yan G, Mariyappan S and Tarascon J-M 2019 Means of using cyclic voltammetry to rapidly design a stable DMC-based electrolyte for Na-ion batteries *J. Electrochem. Soc.* **166** A3723–30

[178] (Available at: www.faradion.co.uk/) (Accessed 15 September 2020)

[179] Jónsson E and Johansson P 2012 Modern battery electrolytes: ion–ion interactions in Li^+/Na^+ conductors from DFT calculations *Phys. Chem. Chem. Phys.* **14** 10774–9

[180] Åvall G and Johansson P 2020 A novel approach to ligand-exchange rates applied to lithium-ion battery and sodium-ion battery electrolytes *J. Chem. Phys.* **152** 234104

[181] Monti D, Ponrouch A, Palacín M R and Johansson P 2016 Towards safer sodium-ion batteries via organic solvent/ionic liquid based hybrid electrolytes *J. Power Sources* **324** 712–21

[182] Monti D, Jónsson E, Boschin A, Palacín M R, Ponrouch A and Johansson P 2020 Towards standard electrolytes for sodium-ion batteries: physical properties, ion solvation and ion-pairing in alkyl carbonate solvents *Phys. Chem. Chem. Phys.* **22** 22768–77

[183] Huang J *et al* 2020 *Operando* decoding of chemical and thermal events in commercial Na(Li)-ion cells via optical sensors *Nat. Energy* **5** 674–83

[184] Yan G, Mariyappan S, Rousse G, Jacquet Q, Deschamps M, David R, Mirvaux B, Freeland J W and Tarascon J-M 2019 Higher energy and safer sodium ion batteries via an electrochemically made disordered $Na_3V_2(PO_4)_2F_3$ material *Nat. Commun.* **10** 585

[185] Vaalma C, Buchholz D, Weil M and Passerini S 2018 A cost and resource analysis of sodium-ion batteries *Nat. Rev. Mater.* **3** 18013

[186] Che H, Chen S, Xie Y, Wang H, Amine K, Liao X-Z and Ma Z-F 2017 Electrolyte design strategies and research progress for room-temperature sodium-ion batteries *Energy Environ. Sci.* **10** 1075–101

[187] Matsumoto K, Hwang J, Kaushik S, Chen C Y and Hagiwara R 2019 Advances in sodium secondary batteries utilizing ionic liquid electrolytes *Energy Environ. Sci.* **12** 3247–87

[188] Rakov D A, Chen F, Ferdousi S A, Li H, Pathirana T, Simonov A N, Howlett P C, Atkin R and Forsyth M 2020 Engineering high-energy-density sodium battery anodes for improved cycling with superconcentrated ionic-liquid electrolytes *Nat. Mater.* **19** 1096–101

[189] Jeong S, Hasa I and Passerini S 2019 Ionic liquid-based electrolytes for sodium-ion batteries: tuning properties to enhance the electrochemical performance of manganese-based layered oxide cathode *ACS Appl. Mater. Interfaces* **11** 22278–89

[190] Usui H, Domi Y, Fujiwara K, Shimizu M, Yamamoto T, Nohira T, Hagiwara R and Sakaguchi H 2017 Charge–discharge properties of a Sn_4P_3 negative electrode in ionic liquid electrolyte for Na-ion batteries *ACS Energy Lett.* **2** 1139–43

[191] Manohar C V, Mendes T C, Kar M, Wang D, Xiao C, Forsyth M, Mitra S and MacFarlane D R 2018 Ionic liquid electrolytes supporting high energy density in sodium-ion batteries based on sodium vanadium phosphate composites *Chem. Commun.* **54** 3500

[192] Wei S, Choudhury S, Xu J, Nath P, Tu Z and Archer L A 2017 Highly stable sodium batteries enabled by functional ionic polymer membranes *Adv. Mater.* **29** 1605512

[193] Peled E and Menkin S 2017 Review—SEI: past, present and future *J. Electrochem. Soc.* **164** A1703–19

[194] Moshkovich M, Gofer Y and Aurbach D 2001 Investigation of the electrochemical windows of aprotic alkali metal (Li, Na, K) salt solutions *J. Electrochem. Soc.* **148** E155

[195] Komaba S, Ishikawa T, Yabuuchi N, Murata W, Ito A and Ohsawa Y 2011 Fluorinated ethylene carbonate as electrolyte additive for rechargeable Na batteries *ACS Appl. Mater. Interfaces* **3** 4165–8

[196] Iermakova D I, Dugas R, Palacín M R and Ponrouch A 2015 On the comparative stability of Li and Na metal anode interfaces in conventional alkyl carbonate electrolytes *J. Electrochem. Soc.* **162** A7060–6

[197] Ma L A, Naylor A J, Nyholm L and Younesi R 2020 Strategies of mitigating dissolution of solid electrolyte interphases in sodium-ion batteries *Angew. Chem., Int. Ed.* **60** 4855–63

[198] Mogensen R, Brandell D and Younesi R 2016 Solubility of the solid electrolyte interphase (SEI) in sodium ion batteries *ACS Energy Lett.* **1** 1173–8

[199] Philippe B, Valvo M, Lindgren F, Rensmo H and Edström K 2014 Investigation of the electrode/electrolyte interface of Fe_2O_3 composite electrodes: Li vs Na batteries *Chem. Mater.* **26** 5028–41

[200] Chinnam P R and Wunder S L 2013 Self-assembled Janus-like multi-ionic lithium salts form nano-structured solid polymer electrolytes with high ionic conductivity and Li^+ ion transference number *J. Mater. Chem. A* **1** 1731–9

[201] Rao R P, Chen H M, Wong L L and Adams S 2017 $Na_{3+x}M_xP_{1-x}S_4$ ($M = Ge^{4+}$, Ti^{4+}, Sn^{4+}) enables high rate all-solid-state Na-ion batteries $Na_{2+2\delta}Fe_{2-\delta}(SO_4)_3|Na_{3+x}M_xP_{1-x}S_4|Na_2Ti_3O_7$ *J. Mater. Chem. A* **5** 3377–88

[202] Duchardt M, Ruschewitz U, Adams S, Dehnen S and Roling B 2018 Vacancy-controlled Na^+ superion conduction in $Na_{11}Sn_2PS_{12}$ *Angew. Chem., Int. Ed.* **57** 1351–5

[203] Zhang Z Z *et al* 2020 $Na_3Zr_2Si_2PO_{12}$: a stable Na^+-ion solid electrolyte for solid-state batteries *ACS Appl. Energy Mater.* **3** 7427–37

[204] He S N, Xu Y L, Chen Y J and Ma X N 2020 Enhanced ionic conductivity of an F^--assisted $Na_3Zr_2Si_2PO_{12}$ solid electrolyte for solid-state sodium batteries *J. Mater. Chem. A* **8** 12594–602

[205] Noi K, Suzuki K, Tanibata N, Hayashi A and Tatsumisago M 2018 Liquid-phase sintering of highly Na^+ ion conducting $Na_3Zr_2Si_2PO_{12}$ ceramics using Na_3BO_3 additive *J. Am. Ceram. Soc.* **101** 1255–65

[206] Zhang Z Z *et al* 2019 Correlated migration invokes higher Na^+-ion conductivity in NaSICON-type solid electrolytes *Adv. Energy Mater.* **9** 1902373

[207] Amores M, Baker P J, Cussen E J and Corr S A 2018 $Na_{1.5}La_{1.5}TeO_6$: Na^+ conduction in a novel Na-rich double perovskite *Chem. Commun.* **54** 10040–3

[208] Zhang Z Z *et al* 2017 A self-forming composite electrolyte for solid-state sodium battery with ultralong cycle life *Adv. Energy Mater.* **7** 1601196

[209] Cheng M, Qu T, Zi J, Yao Y, Liang F, Ma W, Yang B, Dai Y and Lei Y 2020 A hybrid solid electrolyte for solid-state sodium ion batteries with good cycle performance *Nanotechnology* **31** 425401

[210] Tchitchekova D S, Monti D, Johansson P, Bardé F, Randon-Vitanova A, Palacín M R and Ponrouch A 2017 On the reliability of half-cell tests for monovalent (Li^+, Na^+) and divalent (Mg^{2+}, Ca^{2+}) cation based batteries *J. Electrochem. Soc.* **164** A1384–92

[211] Dugas R, Forero-Saboya J D and Ponrouch A 2019 Methods and protocols for reliable electrochemical testing in post-Li batteries (Na, K, Mg, and Ca) *Chem. Mater.* **31** 8613–28

[212] Rudola A, Aurbach D and Balaya P 2014 A new phenomenon in sodium batteries: voltage step due to solvent interaction *Electrochem. Commun.* **46** 56–59

[213] Dugas R, Ponrouch A, Gachot G, David R, Palacin M R and Tarascon J M 2016 Na reactivity toward carbonate-based electrolytes: the effect of FEC as additive *J. Electrochem. Soc.* **163** A2333–9

[214] Lee S E and Tang M H 2019 Electroactive decomposition products cause erroneous intercalation signals in sodium-ion batteries *Electrochem. Commun.* **100** 70–73

[215] Kim Y-J, Lee H, Noh H, Lee J, Kim S, Ryou M-H, Lee Y M and Kim H-T 2017 Enhancing the cycling stability of sodium metal electrodes by building an inorganic–organic composite protective layer *ACS Appl. Mater. Interfaces* **9** 6000–6

[216] Luo W, Lin C-F, Zhao O, Noked M, Zhang Y, Rubloff G W and Hu L 2017 Ultrathin surface coating enables the stable sodium metal anode *Adv. Energy Mater.* **7** 1601526

[217] Schafzahl L, Hanzu I, Wilkening M and Freunberger S A 2017 An electrolyte for reversible cycling of sodium metal and intercalation compounds *ChemSusChem* **10** 401–8

[218] Lee J, Lee Y, Lee J, Lee S-M, Choi J-H, Kim H, Kwon M-S, Kang K, Lee K T and Choi N-S 2017 Ultraconcentrated sodium bis(fluorosulfonyl)imide-based electrolytes for high-performance sodium metal batteries *ACS Appl. Mater. Interfaces* **9** 3723–32

[219] Rupp R and Vlad A 2019 On the reliability of sodium metal anodes: the influence of neglected parameters *J. Electrochem. Soc.* **166** A3122–31

[220] Conder J and Villevieille C 2019 How reliable is the Na metal as a counter electrode in Na-ion half cells? *Chem. Commun.* **55** 1275–8

[221] Hwang J, Takeuchi K, Matsumoto K and Hagiwara R 2019 NASICON vs. Na metal: a new counter electrode to evaluate electrodes for Na secondary batteries *J. Mater. Chem.* A **7** 27057–65

[222] Lee S E and Tang M H 2019 Reliable reference electrodes for nonaqueous sodium-ion batteries *J. Electrochem. Soc.* **166** A3260–4

[223] Goonetilleke D, Pramudita J C, Hagan M, Al Bahri O K, Pang W K, Peterson V K, Groot J, Berg H and Sharma N 2017 *J. Power Sources* **343** 446–57

[224] Dolotko O, Senyshyn A, Mühlbauer M J, Nikolowski K and Ehrenberg H 2014 *J. Power Sources* **255** 197–203

[225] Sharma N, Yu D H, Zhu Y, Wu Y and Peterson V K 2017 *J. Power Sources* **342** 562–9

[226] Pang W K, Kalluri S, Peterson V K, Dou S X and Guo Z 2014 *Phys. Chem. Chem. Phys.* **16** 25377–85

[227] Somerville J W *et al* 2019 *Energy Environ. Sci.* **12** 2223–32

[228] Gutierrez A, Dose W M, Borkiewicz O, Guo F, Avdeev M, Kim S, Fister T T, Ren Y, Bareño J and Johnson C S 2018 *J. Phys. Chem.* C **122** 23251–60

[229] Tapia-Ruiz N, Dose W M, Sharma N, Chen H, Heath J, Somerville J W, Maitra U, Saiful Islam M and Bruce P G 2018 *Energy Environ. Sci.* **11** 1470–9

[230] Krogstad M J, Rosenkranz S, Wozniak J M, Jennings G, Ruff J P C, Vaughey J T and Osborn R 2020 *Nat. Mater.* **19** 63–68

[231] Weber T and Simonov A S 2012 *Z. Kristallogr.* **227** 238–47

[232] Pecher O, Carretero-González J, Griffith K J and Grey C P 2017 *Chem. Mater.* **29** 213–42

[233] Billaud J, Clément R J, Armstrong A R, Canales-Vázquez J, Rozier P, Grey C P and Bruce P G 2014 *J. Am. Chem. Soc.* **136** 17243–8

[234] Smiley D L and Goward G R 2016 *Chem. Mater.* **28** 7645–56

[235] Xiang Y *et al* 2020 *Nat. Nanotechnol.* **15** 883–90

[236] Samoson A 2019 *J. Magn. Reson.* **306** 167–72

[237] Kim J, Middlemiss D S, Chernova N A, Zhu B Y X, Masquelier C and Grey C P 2010 *J. Am. Chem. Soc.* **132** 16825–40

[238] Mondal A, Gaultois M W, Pell A J, Iannuzzi M, Grey C P, Hutter J and Kaupp M 2018 *J. Chem. Theory Comput.* **14** 377–94

[239] Rossini A J, Zagdoun A, Lelli M, Lesage A, Copéret C and Emsley L 1942–51 *Acc. Chem. Res.* **46**

[240] Jardón-Álvarez D, Reuveni G, Harchol A and Leskes M 2020 *J. Phys. Chem. Lett.* **11** 5439–45

[241] Harchol A, Reuveni G, Ri V, Thomas B, Carmieli R, Herber R H, Kim C and Leskes M 2020 *J. Phys. Chem.* C **124** 7082–90

[242] Liu Q *et al* 2020 *In situ* observation of sodium dendrite growth and concurrent mechanical property measurements using an environmental transmission electron microscopy–atomic force microscopy (ETEM-AFM) platform *ACS Energy Lett.* **5** 2546–59

[243] Li Z, Jiang K, Khan F, Goswami A, Liu J, Passian A and Thundat T 2019 Anomalous interfacial stress generation during sodium intercalation/extraction in MoS$_2$ thin-film anodes *Sci. Adv.* **5** eaav2820

[244] Choi J U, Voronina N, Sun Y-K and Myung S-T 2020 Recent progress and perspective of advanced high-energy Co-less Ni-rich cathodes for Li-ion batteries: yesterday, today, and tomorrow *Adv. Energy Mater.* **10** 2002027

[245] Chen Y, Niu Y, Lin C, Li J, Lin Y, Xu G, Palmer R E and Huang Z 2020 Insight into the intrinsic mechanism of improving electrochemical performance via constructing the preferred crystal orientation in lithium cobalt dioxide *Chem. Eng. J.* **399** 125708

[246] Liu T *et al* 2019 *In situ* quantification of interphasial chemistry in Li-ion battery *Nat. Nanotechnol.* **14** 50–56

[247] Seidl L, Bucher N, Chu E, Hartung S, Martens S, Schneider O and Stimming U 2017 Intercalation of solvated Na-ions into graphite *Energy Environ. Sci.* **10** 1631–42

[248] Shadike Z, Zhao E, Zhou Y-N, Yu X, Yang Y, Hu E, Bak S, Gu L and Yang X-Q 2018 Advanced characterization techniques for sodium-ion battery studies *Adv. Energy Mater.* **8** 1702588

[249] Inagaki K, Kolosov O V, Briggs G A D and Wright O B 2000 Waveguide ultrasonic force microscopy at 60 MHz *Appl. Phys. Lett.* **76** 1836–8

[250] Luria J, Kutes Y, Moore A, Zhang L, Stach E A and Huey B D 2016 Charge transport in CdTe solar cells revealed by conductive tomographic atomic force microscopy *Nat. Energy* **1** 16150

[251] Grier E J, Kolosov O, Petford-Long A K, Ward R C C, Wells M R and Hjorvarsson B 2000 Structural changes to epitaxial (0001) holmium layers during hydrogen loading *J. Phys. D: Appl. Phys.* **33** 894–900

[252] Yabuuchi N, Kubota K, Dahbi M and Komaba S 2014 Research development on sodium-ion batteries *Chem. Rev.* **114** 11636–82

[253] Bhandari A and Bhattacharya J 2017 Review—manganese dissolution from spinel cathode: few unanswered questions *J. Electrochem. Soc.* **164** A106–27

[254] Zhang D, Meng X-M, Zheng Y-M, Wang X-M, Xu S-D, Chen L and Liu S-B 2020 The critical role of titanium cation in the enhanced performance of P2-Na$_{0.5}$Ni$_{0.25}$Mn$_{0.60}$Ti$_{0.15}$O$_2$ cathode material for sodium-ion batteries *Phys. Chem. Chem. Phys.* **22** 19992–8

[255] Zhu L, Ding G, Xie L, Yang Q, Yang X and Cao X 2020 Facile preparation of NaV$_3$O$_8$/polytriphenylamine composites as cathode materials towards high-performance sodium storage *Int. J. Energy Res.* **44** 3215–23

[256] Liu T *et al* 2019 Correlation between manganese dissolution and dynamic phase stability in spinel-based lithium-ion battery *Nat. Commun.* **10** 4721

[257] Luo C, Langrock A, Fan X, Liang Y and Wang C 2017 P2-type transition metal oxides for high performance Na-ion battery cathodes *J. Mater. Chem.* A **5** 18214–20

[258] Tang Y, Zhang W, Xue L, Ding X, Wang T, Liu X, Liu J, Li X and Huang Y 2016 Polypyrrole-promoted superior cyclability and rate capability of NaxFe[Fe(CN)6] cathodes for sodium-ion batteries *J. Mater. Chem.* A **4** 6036–41

[259] You Y, Dolocan A, Li W and Manthiram A 2019 Understanding the air-exposure degradation chemistry at a nanoscale of layered oxide cathodes for sodium-ion batteries *Nano Lett.* **19** 182–8

[260] Lyu Y, Yu J, Wu J, Effat M B and Ciucci F 2019 Stabilizing Na-metal batteries with a manganese oxide cathode using a solid-state composite electrolyte *J. Power Sources* **416** 21–28

[261] Ranninger J, Wachs S J, Möller J, Mayrhofer K J J and Berkes B B 2020 On-line monitoring of dissolution processes in nonaqueous electrolytes—a case study with platinum *Electrochem. Commun.* **114** 106702

[262] Nikman S, Zhao D, Gonzalez-Perez V, Hoster H E and Mertens H F L 2021 Surface or bulkr Real-time manganese dissolution detection in a lithium-ion cathode *Electrochim. Acta* **386** 138373

[263] Lopes P P, Zorko M, Hawthorne K L, Connell J G, Ingram B J, Strmcnik D, Stamenkovic V R and Markovic N M 2018 Real-time monitoring of cation dissolution/deintercalation kinetics from transition-metal oxides in organic environments *J. Phys. Chem. Lett.* **9** 4935–40

[264] Chen J-S, Wang L-F, Fang B-J, Lee S-Y and Guo R-Z 2006 Rotating ring–disk electrode measurements on Mn dissolution and capacity losses of spinel electrodes in various organic electrolytes *J. Power Sources* **157** 515–21

[265] Zhao L, Chénard E, Çapraz Ö Ö, Sottos N R and White S R 2018 Direct detection of manganese ions in organic electrolyte by UV-vis spectroscopy *J. Electrochem. Soc.* **165** A345–8

[266] Delmas C 2018 Sodium and sodium-ion batteries: 50 years of research *Adv. Energy Mater.* **8** 1703137

[267] Chayambuka K, Mulder G, Danilov D L and Notten P H L 2020 From Li-ion batteries toward Na-ion chemistries: challenges and opportunities *Adv. Energy Mater.* **10** 2001310

[268] Harper G *et al* 2019 Recycling lithium-ion batteries from electric vehicles *Nature* **575** 75–86

[269] Pathan T S, Rashid M, Walker M, Widanage W D and Kendrick E 2019 Active formation of Li-ion batteries and its effect on cycle life *J. Phys. Energy* **1** 044003

[270] Kishore B, Chen L, Dancer C and Kendrick E 2020 Electrochemical formation protocols for maximising the life-time of a sodium ion battery *Chem. Commun.* **56** 12925–8

[271] Chen L, Kishore B, Walker M, Dancer C and Kendrick E 2020 Nanozeolite ZSM-5 electrolyte additive for long life sodium-ion batteries *Chem. Commun.* **56** 11609–12

[272] Ledwoch D, Robinson J B, Gastol D, Smith K, Shearing P R, Brett D J L and Kendrick E 2020 Hard carbon composite electrodes for sodium-ion batteries with nanozeolite and carbon black additives *Batter. Supercaps* **4** 163–72

[273] Chen C, Brosa Planella F, O'Regan K, Gastol D, Widanage W D and Kendrick E 2020 Development of experimental techniques for parameterization of multi-scale lithium-ion battery models *J. Electrochem. Soc.* **167** 080534

[274] The Faraday Institution 2019 *The Gigafactory Boom: The Demand for Battery Manufacturing in the UK* (available at: https://faraday.ac.uk/wp-content/uploads/2019/08/Faraday_Insights-2_FINAL.pdf)

[275] Jolly J 2020 UK's first car battery 'gigafactory' to be built by two startups *The Guardian* (available at: https://www.theguardian.com/business/2020/may/20/uk-first-car-battery-gigafactory-amte-power-britishvolt)

[276] Faradion 2020 Press release: faradion announces major partnership for developing sodium-ion batteries for commercial vehicles in India (available at: www.faradion.co.uk/faradion-announces-partnership-for-developing-sodium-ion-batteries-in-india/) (Accessed 3 August 2020)

[277] Bauer A, Song J, Vail S, Pan W, Barker J and Lu Y 2018 The scale-up and commercialization of nonaqueous Na-ion battery technologies *Adv. Energy Mater.* **8** 1702869

[278] Haselrieder W, Ivanov S, Tran H Y, Theil S, Froböse L, Westphal B, Wohlfahrt-Mehrens M and Kwade A 2014 Influence of formulation method and related processes on structural, electrical and electrochemical properties of LMS/NCA-blend electrodes *Prog. Solid State Chem.* **42** 157–74

[279] Wang P-F, You Y, Yin Y-X and Guo Y-G 2018 Layered oxide cathodes for sodium-ion batteries: phase transition, air stability, and performance *Adv. Energy Mater.* **8** 1701912

[280] Wang H, Liao X-Z, Yang Y, Yan X, He Y-S and Ma Z-F 2016 Large-scale synthesis of NaNi$_{1/3}$Fe$_{1/3}$Mn$_{1/3}$O$_2$ as high performance cathode materials for sodium ion batteries *J. Electrochem. Soc.* **163** A565–70

[281] Ludwig B, Zheng Z, Shou W, Wang Y and Pan H 2016 Solvent-free manufacturing of electrodes for lithium-ion batteries *Sci. Rep.* **6** 23150

[282] Schälicke G, Landwehr I, Dinter A, Pettinger K-H, Haselrieder W and Kwade A 2020 Solvent-free manufacturing of electrodes for lithium-ion batteries via electrostatic coating *Energy Technol.* **8** 1900309

[283] Samba A, Omar N, Gualous H, Capron O, Van Den Bossche P and Van Mierlo J 2014 Impact of tab location on large format lithium-ion pouch cell based on fully coupled tree-dimensional electrochemical-thermal modeling *Electrochim. Acta* **147** 319–29

[284] Rudola A *et al* 2021 Commercialisation of high energy density sodium-ion batteries: Faradion's journey and outlook *J. Mater. Chem.* A **9** 8279–302

[285] Broux T *et al* 2019 High rate performance for carbon-coated Na$_3$V$_2$(PO$_4$)$_2$F$_3$ in Na-ion batteries *Small Methods* **3** 1800215

[286] Rong X *et al* 2020 Na-ion batteries: from fundamental research to engineering exploration *Energy Storage Sci. Technol.* **9** 515–22

[287] Datasheet 2019 Natron energy blue tray 4000 *Distributed at the Battery Show* (*Novi, MI, 9–12 September*)

[288] (a) Datasheet. Toshiba rechargeable battery SCiB high power 2.9 Ah cell (available at: www.scib.jp/en/download/ToshibaRechargeableBattery-en.pdf) (Accessed 17 September 2020); (b) Datasheet Amaron Quanta 12V200Ah (available at: www.quanta.in/images/pdf/Quanta-SF-Brochure.pdf) (Accessed 17 September 2020); (c) Datasheet ENERpower Shandong goldencell electronics technology model HTCFR18650-1800mAh-3.2V (available at: https://enerpower.de/wp/wp-content/uploads/2019/07/Technical-Specifications-HTCFR18650-1800mAh-3.2V-EN.pdf) (Accessed 17 September 2020); (d) Datasheets A123 Nanophosphate® high power lithium ion cell ANR26650M1-B (available at: https://a123batteries.com/product_images/uploaded_images/26650.pdf, https://www.evlithium.com/A123-Battery/632.html, https://www.batteryspace.com/prod-specs/6610.pdf) (Accessed 17 September 2020); (e) Datasheet AA portable power Li-ion polymer battery 3.7V 10000 mAh PL-9059156 (available at: www.batteryspace.com/prod-specs/3.7V9059156.pdf) (Accessed 17 September 2020); (f) Datasheet Panasonic lithium ion NCR18650B (available at: www.batteryspace.com/prod-specs/NCR18650B.pdf) (Accessed 17 September 2020); (g) Datasheet LG Chem lithium ion INR21700 M50 18.20Wh (available at: http://queenbattery.com.cn/index.php?controller=attachment&id_attachment=111) (Accessed 17 September 2020)

[289] Reuning A *et al* 2019 Investigation of battery cells for prospective use in electric cars *PCIM Europe 2019; Int. Exhibition and Conf. for Power Electronics, Intelligent Motion, Renewable Energy and Energy Management* pp 1–7

[290] Jin T, Li H, Zhu K, Wang P-F, Liu P and Jiao L 2020 Polyanion-type cathode materials for sodium-ion batteries *Chem. Soc. Rev.* **49** 2342–77

[291] Henze V 2019 Battery pack prices fall as market ramps up with market average at $156/kWh in 2019 *BloombergNEF* (available at: https://about.bnef.com/blog/battery-pack-prices-fall-as-market-ramps-up-with-market-average-at-156-kwh-in-2019/?sf113554299=1) (Accessed 17 September 2020)

[292] Popp H, Zhang N, Jahn M, Arrinda M, Ritz S, Faber M, Sauer D U, Azais P and Cendoya I 2020 Ante-mortem-analyse sowie elektrische, thermische und Alterungstests von State-of-the-Art cylindrical lithium-ion cells *Elektrotech. Inf. Tech.* **137** 169–76

[293] (a) Datasheet Pylontech energy type cell PF25N (available at: http://en.pylontech.com.cn/service/download) (Accessed 17 September 2020); (b) Datasheet CATL LiFePO4 lithium battery 3.2V120Ah (available at: www.evlithium.com/CATL-Battery.html) (Accessed 17 September 2020); (c) Datasheet EVE energy LFP power battery LF280 (available at: www.dcmax.com.tw/LF280(3.2V280Ah).pdf) (Accessed 17 September 2020)

[294] 2019 Inventing the batteries of the future, research needs and future actions, batteries 2030+ roadmap, second draft (available at: https://battery2030.eu/digitalAssets/817/c_817144-l_1-k_battery-2030_roadmap-v2.1.pdf) (Accessed July 2020)

[295] Schnell J, Tietz F, Singer C, Hofer A, Billota N and Reinharta G 2019 Prospects of production technologies and manufacturing costs of oxide-based all-solid-state lithium batteries *Energy Environ. Sci.* **12** 1818–33

[296] Peters J F, Cruz A P and Weil M 2019 Exploring the economic potential of sodium-ion batteries *Batteries* **5** 10

[297] Barker J and Heap R J 2014 Doped nickelate compounds GB 250389A

[298] Sodium-ion battery (available at: https://en.wikipedia.org/wiki/Sodium-ion_battery) (Accessed June 2020)

[299] International Energy Agency 2019 *IEA World Energy Outlook 2019* (Paris: International Energy Agency)

[300] International Energy Agency 2020 Energy storage (available at: www.iea.org/reports/energy-storage) (Accessed August 2020)

[301] Barker J, Heap R J, Roche N, Tan C, Sayers R, Whitley J and Lui Y 2015 The commercialization of high energy density Na-ion battery technology *2nd Int. Symp. on Sodium Batteries* (*Phoenix, October*)

[302] Pfeifer K, Arnold S, Becherer J, Das C, Maibach J, Ehrenberg H and Dsoke S 2019 Can metallic sodium electrodes affect the electrochemistry of sodium-ion batteries? Reactivity issues and perspectives *ChemSusChem* **12** 3312–9